

The University of Michigan • Office of Research Administration
Ann Arbor, Michigan

EDGE-NOTCH SENSITIVITY OF
SHEET NICKEL-BASE SUPERALLOYS
AS INFLUENCED BY MAGNESIUM AND CARBON

by

Yancy E. Smith
James W. Freeman

Report 07674-1-F

August 1967

Final Report to:

The International Nickel Company, Inc.
New York, New York
Project 07674

TABLE OF CONTENTS

	Page
LIST OF TABLES	v
LIST OF FIGURES	vii
SUMMARY	ix
INTRODUCTION	1
BACKGROUND	2
EXPERIMENTAL PROCEDURE	4
Design of Experiment	4
Melting Stock	5
Melting Practice	6
Preliminary Hot Working	7
Final Conversion	7
Chemical Analysis	8
Evaluation of Material	8
As-Received Material	8
Solution Temperature Studies	9
X-Ray Diffraction Investigation	9
Preparation of Test Specimens	10
Heat Treatment	10
Specimen Design	10
Mechanical Testing	10
Tensile Tests	10
Creep-Rupture Tests	10
Evaluation of Tested Specimens	11
EXPERIMENTAL MATERIALS	11
Chemical Composition	12
Magnesium Content	12
Carbon Content	13
Zirconium Content	13
Gas Content	13
EFFECT OF MAGNESIUM ON CRACKING DURING PRODUCTION OF THE SHEET	13
MAGNESIUM ADDITIONS AND MICROSTRUCTURE	14
As-Cold-Worked Condition	15
As-Received S-Alloys	16
As-Received René 41 Alloy	16
Effect of Magnesium on Solution Temperatures	17
Carbide Solution for S-Alloy	17
Gamma Prime Solution	18
Checks on Solution Temperatures of S-Alloy	18
René 41 Alloy	19

TABLE OF CONTENTS

Effect of Magnesium on Grain Size	20
Effect of Magnesium on the Type of Carbide in High Carbon S-Alloy	20
Discussion of Microstructure and Magnesium	23
EFFECT OF MAGNESIUM ON RUPTURE PROPERTIES	
AT 1000°F	25
Selection of Heat Treatments	26
Short-Time Tensile Properties at 1000°F	27
Rupture Test Properties at 1000°F	29
Minimum Creep Rates During Rupture Tests	33
EXAMINATION OF SPECIMENS AFTER RUPTURE	
TESTING	34
Fracture Sequence	34
Microstructures of Rupture Test Specimens	37
Original Carbide Morphology	37
Microstructures of Fractured Specimens	39
Initial Gamma Prime Particles	42
Electron Microscopic Examination of Carbides	42
Inclusions in Magnesium-Treated Heats	43
GENERAL DISCUSSION	
Mechanism of Rupture	44
Reduction of Carbide Solution Temperatures by Magnesium	45
Influence of Degree of Carbide Solution on Tensile and Creep-Rupture Properties	47
Other Factors	49
CONCLUSIONS	
REFERENCES	
APPENDIX A - Quantitative Estimation from	
Diffraction Patterns	101

LIST OF TABLES

	Page
I. Chemical Compositions of Experimental Heats	55
II. Magnesium Analysis of Ingot and Sheet Material of Representative Heats	56
III. Reference Carbide Diffraction Patterns from ASTM Card File	57
IV. X-Ray Diffraction Patterns of Extracted Carbides from High Carbon S-Alloy with No Magnesium Addition	58
V. X-Ray Diffraction Patterns for High Carbon S-Alloy with Low Magnesium Addition	59
VI. X-Ray Diffraction Patterns for High Carbon S-Alloy with High Magnesium Addition	60
VII. Tensile Test Results - 1000°F	61
VIII. Creep-Rupture Properties - 1000°F, Low Carbon S-Alloy	62
IX. Creep-Rupture Properties - 1000°F, High Carbon S-Alloy	63
X. Creep-Rupture Properties - 1000°F, René 41	64

LIST OF FIGURES

	Page
1. Smooth Specimen Design.	65
2. Edge-Notched Specimen Design.	66
3. Range of Carbide Precipitation in As-Received Sheet.	67
4. Solution Treated Low Carbon S-Alloy--Two Hours, Water Quench, 250X.	68-69
5. Solution Treated Low Carbon S-Alloy--Ten Hours, Water Quench, 250X.	70-71
6. Solution Treated High Carbon S-Alloy--Two Hours, Water Quench, 250X.	72-73
7. Solution Treated High Carbon S-Alloy--Ten Hours, Water Quench, 250X.	74-75
8. Analyzed Magnesium Content versus Solution Temperature of Intergranular Carbides at Two Levels of Carbon.	76
9. Carbon Content versus Solution Temperature of Intergranular Carbides at Four Levels of Magnesium.	77
10. Solution Treated High Carbon S-Alloy with Pre-Heat Treatment. Two Hours 1900°F, Water Quench Plus Two Hours 1975°F, Water Quench, 250X.	78
11. Solution Treated High Carbon S-Alloy Specimens from Top of Ingots - Two Hours, 1975°F, Water Quench, 250X.	79
12. Solution Treated René 41. At Temperature One Hour, Water Quench, 100X.	80
13. Effect of Magnesium Content and Heat Treating Temperature on the Identity and Relative Quantities of Carbides in Specimens of High Carbon S-Alloy Quenched After One Hour at Temperature.	81
14. Fracture Toughness of Materials at 1000°F.	82

LIST OF FIGURES, continued

	Page
15. Stress-Rupture Life of Smooth and Edge-Notched Sheet Specimens of Low Carbon S-Alloy at 1000°F.	83
16. Stress-Rupture Life of Smooth and Edge-Notched Sheet Specimens of High Carbon S-Alloy at 1000°F.	84
17. Stress-Rupture Life of Smooth and Edge-Notched Sheet Specimens of René 41 at 1000°F.	85
18. Stress versus Minimum Creep Rate for S-Alloy and René 41 Sheet Specimens.	86
19. Extent of Intergranular Fracture Region of Smooth Specimens.	87
20. Extent of Intergranular Fracture Region of Notched Specimens.	88
21. Fracture Surfaces of Smooth and Notched Stress-Rupture Specimens, 3X.	89
22. Solution Treated and Aged Microstructures as Represented by Unstressed Section of Hot Tensile Specimens, 250X.	91
23. Deformed Areas Near Transgranular Regions of Fracture in Smooth Specimens.	92
24. Intergranular Fracture and Cracking in Smooth Specimens of S-Alloy.	93
25. An Example of Intergranular Cracking in a Smooth Rupture Specimen.	94
26. Intergranular Failure Initiation at Edge Notches.	95
27. Smooth Specimen Fractures of René 41.	96
28. Representative Electron Micrographs of Mechanical Test Specimens, 15,000X.	97
29. Electron Micrographs Showing Grain Boundaries and Prior Boundary Carbides.	98
30. Electron Micrographs of Stringers of a Phase Which Appeared Only in Magnesium-Containing Heats.	99

SUMMARY

A study of the possibility that magnesium would reduce the edge-notch sensitivity of nickel-base Ti+Al superalloy sheet under "creep-rupture" conditions at 1000°F was carried out. Laboratory vacuum melted heats of an experimental 20Cr-3.8Ti-1.2Al+B+Zr "S-alloy" and René 41 were used with aim residual Mg contents of 0, 0.02, 0.04, and 0.08 per cent. The materials used were solution treated, cold-rolled, and recrystallized during a final solution treatment. This is in contrast to most research on the creep-rupture properties of these alloys where hot-worked or cast materials are studied at higher temperatures.

In prior research for The International Nickel Company, Inc., it had been found that Mg improved ductility of the S-alloy barstock at 1200°F. It is thought that Mg is used in practice, and, it was considered possible that it might reduce the notch sensitivity of sheet.

The influence of varying carbon content was studied by using two series of S-alloy heats with approximate carbon contents of 0.03 and 0.07 per cent. The study included varied degrees of carbide solution through the differences in carbon content and the influence of Mg on the carbide solubility.

Prior research at the University for NASA had disclosed that for time periods longer than about 100 hours, edge-notched specimens of the nickel-base superalloys would rupture at 1000° and 1200°F under constant loads at surprisingly low stresses. This had been discovered in a research program planned to outline the possible upper temperature of usefulness of superalloys for supersonic transport airframes. The criterion used was the retention of notch strength after exposure under net section stresses of 40,000 psi. In some cases, the "rupture strengths" fell below 40,000 psi in less than 1000 hours. This would not only be a severe limitation on the alloys in SST applications, but it suggested that in other applications they might be subject to unrecognized stress concentration sensitivity at these relatively low temperatures.

The data from the present investigation did not prove whether or not Mg altered the edge-notch sensitivity in the 1000°F creep-rupture tests. Most

of the data suggested the possibility of a slight improvement in the long-time rupture strengths. Limited data at 1000°F on the 0.03 per cent carbon S-alloy suggested that Mg might be beneficial to N/S ratios in tensile tests. The 0.07 per cent carbon S-alloy and the René 41 had low N/S ratios at the highest Mg level.

The carbide solution temperatures were apparently reduced about 60°F by 0.020 to 0.06 per cent Mg in the S-alloy. Higher Mg raised the solution temperature of the high carbon S-alloy. Mg also increased the ratio of Cr_7C_3 to Cr_{23}C_6 for a given heat treatment. Apparently, Mg has a considerable effect on phase relationships. This suggests that it could have important effects in applications where carbide morphology is a problem, and that lesser amounts of Mg than were studied (even those which might be derived from MgO refractories) could be effective. The possible effects of Mg on carbide solution in René 41 with its predominantly high solution temperature M_6C carbides were not studied.

The heats with the largest Mg additions edge-cracked during initial hot working of the ingots. The data were inadequate to determine if Mg influenced subsequent hot working and cold working, or if it had any effects when added in smaller amounts.

Carbon content had far more effect than Mg on creep-rupture properties of S-alloy. The influence of undissolved versus dissolved carbides was not established by the experiments, although there were indications that both could be influencing properties.

As previously determined in research for NASA, rupture occurred first by the formation of intergranular cracks followed by abrupt transgranular fracture. The intergranular cracks are apparently formed by creep. The transgranular cracking occurred, presumably, when the intergranular cracks raised the stress high enough to cause transgranular fracture. This mechanism occurred in both smooth and notched specimens, with a higher stress required to initiate intergranular cracking in the smooth specimens for a given time for rupture. Speculation, perhaps undue, suggests that undissolved carbides at the sites of the grain boundaries which existed prior to recrystallization reduced fracture toughness and allowed transgranular fracture at

stresses comparatively lower than when carbides were dissolved. At the same time, undissolved carbides seemed to be associated with improved resistance to creep-rupture cracking.

The longer time creep-rupture strength and ductility of S-alloy increased with carbon content. René 41 with carbon contents similar to high carbon S-alloy was still stronger and more ductile. The rupture strengths up to breaks in the curves to lower strengths followed the same trends as the tensile strengths. Apparently, the transgranular "Fracture Toughness" could have a significant effect on rupture life, although the creep cracking, particularly initiation time, appeared to predominate as the rupture time increased.

The data were very limited. The results for Mg should be treated as possible trends which are sufficient to justify investigation into engineering alloy practice. It is entirely possible that Mg could be important in aspects other than those studied, particularly those involving producibility and costs. There are some data which suggest that the notch sensitivity could vary considerably with temperature and time and, therefore, the reported data for 1000°F might not be typical.

INTRODUCTION

An investigation was carried out to determine if magnesium treatment of nickel-base Ti+Al superalloys would reduce edge-notch sensitivity of thin sheet specimens under "creep-rupture conditions" at 1000°F. While Mg is reported to be extensively used in production, its role is not generally known. Prior research at the University sponsored by The International Nickel Company, Inc.,⁽¹⁾ had suggested that Mg could, in some cases, improve the rupture test ductility of round specimens at 1200°F. The data further suggested that beneficial effects from Mg might increase as the temperature was reduced. This ductility effect, together with the possibility that Mg might otherwise counteract embrittlement, was the reason for extending the research on Mg to the notch sensitivity problem of the thin sheet at the relatively low temperatures for superalloys.

Concurrent with the prior studies on the role of magnesium, research at the University of Michigan for NASA on supersonic transport materials^(2, 3) had disclosed that rupture of commercial nickel-base sheet alloy could occur in edge-notched specimens under constant loads in unexpectedly short times at 1000° and 1200°F, when the net section stress was at probable design stresses. The sensitivity was particularly severe at 1000°F. Inasmuch as the susceptibility to time dependent, abrupt crack propagation would limit the upper temperature of SST usefulness of such alloys, the possibility that Mg might reduce the problem was important. It should be recognized that the phenomenon being investigated differs from the usual short time tensile crack sensitivity test. In the problem studied, failure occurs at constant loads far lower than would be expected from tensile tests. The relationship between original net section stress and time to failure resembles that obtained on stress-rupture tests. Unless failure occurred during constant load exposure, the subsequent fracture toughness as measured by tensile tests usually remained virtually unchanged.

The experimental 20Cr-1.2Al-3.8Ti+Zr nickel-base alloy used by Schultz and Freeman for the prior research on Mg effects⁽¹⁾ was also used in this investigation. Comparative data were obtained for René 41 alloy. Experimental heats with 0.0, 0.02, 0.04, and 0.08 per cent aim residual Mg contents and processed to about 0.040-inch thick sheet were used. Varying degrees of carbide solution were included in the program by varying the carbon content and as a result of the Mg additions. In addition to the edge-notch sensitivity in rupture tests, limited tensile tests at 1000°F and possible microstructural effects of Mg were also studied.

BACKGROUND

Magnesium has long been used to counteract sulfur in nickel and certain nickel alloys to prevent embrittlement from the Ni-NiS eutectic, as first reported by Fleitman.⁽⁴⁾ The degree to which Mg is used in nickel-base superalloys is not known, but it is presumed to be common even though Mg is difficult to add with the usual vacuum melting methods for making the alloys. Furthermore, such alloys are generally low in sulfur due to the type of raw material used. Schultz had shown⁽⁵⁾ that elements normally present in such alloys in themselves counteract sulfur. However, even though sulfur in the alloys studied would be expected to be counteracted by other factors, Schultz did find some improvement in rupture-test ductility at 1200°F in the experimental 20Cr-1.2Al-3.8Ti+B+Zr alloy from additions of from 0.02 to 0.04 per cent Mg.⁽¹⁾ In the absence of B+Zr, Mg was not effective at 1200°F, or at 1500°F whether B+Zr was present or not. Larger amounts of Mg were detrimental to ductility at 1200°F.

The actual role of Mg in the Ti+Al superalloys is not known, or at least has not been published. Apparently, however, it is used fairly extensively in practice, and there is the possibility that counteracting obscure ductility-embrittlement effects might be a reason for doing so. The improved ductility found by Schultz at 1200°F supported this possibility. For these reasons, then, it was decided to determine if Mg could reduce the time

dependent edge-notch sensitivity of commercial sheet superalloys at the seemingly low temperatures for creep-rupture.

In addition, the research was planned to include a study of the structural features associated with magnesium. In making thin sheet, cold rolling is used. Consequently, in contrast to Schultz's research on barstock, heat treatments were applied to cold-reduced sheet. Two compositional variables were introduced. Based on Schultz's data on the experimental alloy, as well as numerous instances in commercial alloys, the effect of carbon on ductility and strength was included by using two levels of carbon content in the experimental alloy. The generality of the results was further extended by including the commercial alloy, René 41. Commercially produced René 41 had been studied extensively in the NASA program at the University of Michigan. Notches depressed the 1000-hour rupture strength of standard solution treated and aged material at 1000°F from 150,000 psi for unnotched specimens to 78,000 psi. Cold-worked and aged material was even more drastically reduced. Similar reductions in "rupture strength" had been obtained for Waspaloy and Inconel 718 alloys. All of these materials had been in the form of 0.025 inch thick sheet.

EXPERIMENTAL PROCEDURE

Design of Experiment

Twelve heats were made of the following aim compositions:

I. Low-Carbon S-Alloy*

$\frac{\% \text{ C}}{0.05}$	$\frac{\% \text{ Cr}}{20.0}$	$\frac{\% \text{ Ti}}{3.8}$	$\frac{\% \text{ Al}}{1.2}$	$\frac{\% \text{ B}}{0.0035}$	$\frac{\% \text{ Zr}}{0.045}$
-----------------------------	------------------------------	-----------------------------	-----------------------------	-------------------------------	-------------------------------

<u>Heat No.</u>	<u>% Mg</u>
1	No addition
3	0.02
5	0.04
7	0.08

II. High-Carbon S-Alloy

$\frac{\% \text{ C}}{0.10}$	$\frac{\% \text{ Cr}}{20.0}$	$\frac{\% \text{ Ti}}{3.8}$	$\frac{\% \text{ Al}}{1.2}$	$\frac{\% \text{ B}}{0.0035}$	$\frac{\% \text{ Zr}}{0.045}$
-----------------------------	------------------------------	-----------------------------	-----------------------------	-------------------------------	-------------------------------

<u>Heat No.</u>	<u>% Mg</u>
2	No addition
4	0.02
6	0.04
8	0.08

III. René 41 Alloy

$\frac{\% \text{ C}}{0.10}$	$\frac{\% \text{ Cr}}{19.0}$	$\frac{\% \text{ Co}}{11.0}$	$\frac{\% \text{ Mo}}{10.0}$	$\frac{\% \text{ Fe}}{2.5}$	$\frac{\% \text{ Ti}}{3.0}$	$\frac{\% \text{ Al}}{1.5}$	$\frac{\% \text{ B}}{0.0035}$	$\frac{\% \text{ Zr}}{0.045}$
-----------------------------	------------------------------	------------------------------	------------------------------	-----------------------------	-----------------------------	-----------------------------	-------------------------------	-------------------------------

<u>Heat No.</u>	<u>% Mg</u>
9	No addition
10	0.02
11	0.04
12	0.08

* "S-Alloy" is the term used in this report to indicate the experimental alloy used by Schultz to study the effect of Mg in barstock⁽¹⁾.

Melting Stock

Virgin melting materials were used to produce vacuum melted ingots.

The nickel used was Mond carbonyl nickel pellets for which a typical analysis is:

$\frac{\% \text{ C}}{0.013}$	$\frac{\% \text{ S}}{0.0030}$	$\frac{\% \text{ Pb}}{<0.001}$	$\frac{\% \text{ B}}{<0.001}$	$\frac{\% \text{ Si}}{<0.005}$	$\frac{\% \text{ Mn}}{<0.005}$	$\frac{\% \text{ Fe}}{0.011}$	$\frac{\% \text{ Co}}{<0.01}$
$\frac{\% \text{ Cu}}{<0.005}$	$\frac{\% \text{ P}}{0.002}$	$\frac{\% \text{ Mg}}{<0.005}$	$\frac{\% \text{ Al}}{<0.01}$	$\frac{\% \text{ Ti}}{<0.01}$	$\frac{\% \text{ Zr}}{<0.01}$		

Shieldalloy "VM" grade chromium was used which was analyzed as follows:

$\frac{\% \text{ Cr}}{99.50}$	$\frac{\% \text{ Fe}}{0.15}$	$\frac{\% \text{ Al}}{0.09}$	$\frac{\% \text{ Si}}{0.07}$	$\frac{\% \text{ C}}{0.04}$	$\frac{\% \text{ S}}{0.009}$
-------------------------------	------------------------------	------------------------------	------------------------------	-----------------------------	------------------------------

Titanium was added as sponge from Titanium Metals Corporation of America, Heat MD-115 which analyzed:

$\frac{\% \text{ Fe}}{0.05}$	$\frac{\% \text{ Mg}}{0.05}$	$\frac{\% \text{ Si}}{0.015}$	$\frac{\% \text{ Mn}}{0.003}$	$\frac{\% \text{ C}}{0.015}$
$\frac{\% \text{ Cl}}{0.10}$	$\frac{\% \text{ N}}{0.010}$	$\frac{\% \text{ O}}{0.08}$	$\frac{\% \text{ H}}{0.0025}$	$\frac{\% \text{ H}_2\text{O}}{0.025}$

The aluminum was 99.99 per cent pure aluminum ingot. Molybdenum metal was provided by The Climax Molybdenum Company and contained 0.017% C. Cobalt was obtained from Lot 216 of electrolytic cobalt from The International Nickel Company, Inc., and analyzed as follows:

$\frac{\% \text{ Co}}{99.62}$	$\frac{\% \text{ Ni}}{0.34}$	$\frac{\% \text{ Cu}}{0.005}$	$\frac{\% \text{ Fe}}{0.002}$	$\frac{\% \text{ Pb}}{0.00014}$	$\frac{\% \text{ C}}{0.02}$	$\frac{\% \text{ S}}{0.001}$
-------------------------------	------------------------------	-------------------------------	-------------------------------	---------------------------------	-----------------------------	------------------------------

Iron for the René 41 heats was Plast-Iron from the Glidden Company, which typically analyzes 99.9 per cent iron.

Magnesium was added as a nickel-magnesium alloy provided by The International Nickel Company, Inc., with the following composition:

$\frac{\% \text{ Mg}}{15.21}$	$\frac{\% \text{ Ni}}{81.1}$	$\frac{\% \text{ Si}}{0.22}$	$\frac{\% \text{ Cu}}{0.05}$
-------------------------------	------------------------------	------------------------------	------------------------------

Boron was added as nickel-boron from Union Carbide with the following composition:

$\frac{\% \text{ B}}{16.38}$	$\frac{\% \text{ Ni}}{77.25}$	$\frac{\% \text{ Fe}}{2.98}$	$\frac{\% \text{ Al}}{0.11}$	$\frac{\% \text{ Si}}{0.01}$	$\frac{\% \text{ C}}{0.44}$
------------------------------	-------------------------------	------------------------------	------------------------------	------------------------------	-----------------------------

Zirconium was added in the form of zirconium sponge. Carbon was added as powder obtained by machining spectroscopically pure graphite rod.

The crucibles used for all heats were 99 per cent fused alumina crucibles from the Norton Company. These are boron-free crucibles with the typical composition:

$\frac{\% \text{ Al}_2\text{O}_3}{99.01}$	$\frac{\% \text{ SiO}_2}{0.58}$	$\frac{\% \text{ Fe}_2\text{O}_3}{0.11}$	$\frac{\% \text{ Na}_2\text{O}_3}{0.17}$
---	---------------------------------	--	--

Melting Practice

The alloys were made as 4,800-gram (10.6-pound) heats in a vacuum melting furnace which was evacuated to 1-3 microns pressure before the power was turned on. Nickel, chromium and carbon were included in the initial melt down, with cobalt also being included in the René 41 heats. After melting this initial charge, other alloying materials were added at a slow rate while the power was held at the appropriate level to prevent solidification of the surface of the melt. The order of addition was Ti-Al for S-Alloy, and Mo-Fe-Ti-Al for René 41. Melting down the whole charge required 45 to 60 minutes. After the charge was melted down and any boil had subsided, the boron and zirconium addition was made. At this point in the process one of the two following procedures was followed depending on whether the heat was to contain magnesium:

1. No magnesium - Superheat was established and the heat was poured at less than 10 microns pressure and 2600°F for S-Alloy heats, and 2500°F for René 41 heats.
2. Magnesium - The furnace chamber was isolated from the vacuum pumping system and argon was bled into the tank to a pressure of one-half atmosphere. In the meantime, the melt was allowed to cool to near the freeze point on the surface. The nickel-magnesium addition was made under these conditions and then superheat was established in about three minutes. The heat was poured at the same temperature as for non-magnesium heats.

The argon used for back-filling was 99.995 per cent minimum purity with a maximum oxygen impurity of 10 ppm. It was passed over hot copper and titanium in the course of bleeding it into the tank.

The melts were poured into refractory hot-topped, 5 inch high by 2 1/4 inch diameter steel pipe molds which stood on a copper chill block.

Preliminary Hot Working

All ingots were radiographed to assure soundness. To prepare the ingots for strip rolling, it was necessary to reduce the thickness of the ingots so that they would fit in the small mill available and also to increase the width in order to obtain a sufficiently wide final strip. After removing all surface defects by grinding, the ingots were soaked for two hours at 2150°F and then squeezed in a 750-ton press to a thickness of 1 3/8 inches and a width of 2 3/4 inches, with only minor axial extension. The forged slabs were then cooled and the surfaces reconditioned by grinding. Specimens were cut from each end of the slabs at this stage for chemical analysis. The slabs were reheated to 2150°F and hot rolled in 5 per cent reductions to 0.9 inch in thickness. They were cooled and conditioned by grinding. The slabs were then shipped to the Eastern Stainless Steel Corporation for final hot and cold rolling.

Final Conversion

The slabs were preheated at 2150°F and hot rolled in small reductions to a thickness of about 0.280 inch using two or three passes per reheat. When this thickness was attained, they were cooled and cut into three sections each. The surface was reconditioned by grinding and the short pieces were numbered to maintain identity within each slab and then charged back into the furnace at 2150°F. These pieces were then hot rolled on down to about 0.045 to 0.050 inch in thickness using two passes per reheat and, finally, a single pass as the piece approached this final thickness.

The hot worked strip was charged back into the furnace for three minutes to dissolve the γ' , then water quenched and pickled to remove oxidation,

and then cut into smaller pieces for cold rolling. At this point, each of the original slabs had been cut into six pieces which were numbered 1 through 6 from the top of the original ingot. The pieces were cold reduced from 13 to 23 per cent in 10 to 30 passes to a final thickness of 0.036 to 0.042 inch. A typical cold rolling record was as follows (Heat 5):

<u>Piece</u>	<u>Number of Passes</u>	<u>t_i</u>	<u>t_f</u>	<u>% Reduction</u>	<u>L_i</u>	<u>L_f</u>
1	26	0.048	0.037	23	11 1/2	14 1/4
2	17	0.048	0.040	17	17 3/4	21
3	15	0.049	0.039	20	13 1/8	16 1/4
4	16	0.048	0.039	18	17 5/8	21
5	17	0.048	0.039	18	14 1/4	17 1/4
6	11	0.048	0.038	21	19 1/4	23 3/4

t_i = initial thickness

t_f = final thickness

L_i = initial length

L_f = final length

Chemical Analysis

The sections taken from both ends of the forged slabs were analyzed for major components as well as for minor additions and trace impurities by The Paul D. Merica Research Laboratory of the International Nickel Company, Inc. Also, specimens of some heats of the finished sheet material were analyzed for magnesium by the same laboratory.

Evaluation of Material

(1) As-Received Material. Metallographic specimens were polished on the surface lying in the plane of the sheet. They were polished consecutively on 60, 240, 400 and 600 grit paper, five micron and one micron diamond paste and, finally, on 0.1 micron alumina. Electrolytic "G" etch, which is

composed of 12 parts phosphoric acid, 41 parts nitric acid and 47 parts sulfuric acid by volume, was used to delineate both carbides and γ' precipitate.

(2) Solution Temperature Studies. In order to establish a solution treatment for the S-alloy material, specimens were taken from each heat to establish the dissolution characteristics of the intergranular carbides, including any possible heat-to-heat variations. Specimens were held at various temperatures for 30 and 60 minute periods and water quenched. The extent of intergranular carbide dissolution was evaluated by optical metallography. These initial specimens demonstrated that the temperature of essentially complete solution of intergranular carbides varied as a function of Mg content, and, therefore, a more comprehensive study of solution temperatures was conducted. Specimens from each heat were given both two and ten hour treatments at 25°F intervals over the complete carbide dissolution temperature range. All specimens were water quenched after heat treatment. Optical micrographs were taken of these structures.

A preliminary solution temperature study was also conducted on the René 41 material, although the heat treatment for the mechanical test specimens of this alloy was preselected to be the same as the standard commercial heat treatment so that the results could be compared with available test results on commercial material.

(3) X-Ray Diffraction Investigation. X-ray diffraction identification of extracted carbides was employed to obtain information which would explain the dependency of carbide solution temperature on the magnesium level. Carbides were extracted from solution treated specimens, when carbide solution was incomplete, as well as from solution treated and aged specimens using a solution of 10 per cent bromine in methanol. The carbides were separated by centrifuging, washed and dried, and then mixed together in a small, agate mortar for uniformity. A portion of the carbides was accumulated in the tip of a glass capillary tube to form a diffraction specimens. The X-ray diffraction patterns were obtained with 114.6 mm, Debye-Scherrer cameras using copper radiation and a nickel filter. In addition, an aluminum foil filter was used adjacent to the film in order to absorb the fluorescent radiation from

the titanium in the titanium carbonitride which is present in these alloys. In the interpretation of the patterns, shrinkage corrections were made in the determination of line positions, and relative line intensities were estimated visually.

Preparation of Test Specimens

(1) Heat Treatment. Specimen blanks of both alloys were solution treated in batches of ten in an argon atmosphere. They were air cooled quickly by dumping them on a metal plate and separating them so that no two were on top of each other. They were aged in an air atmosphere.

(2) Specimen Design. The dimensions of the smooth and notched specimens used are presented in Figures 1 and 2, respectively. They are not as wide as recommended by the ASTM., since the strip was not wide enough to make two full-width specimens.

Mechanical Testing

(1) Tensile Tests. Tensile tests were conducted on one smooth and one notched specimen from each heat in order to obtain data to guide the selection of stresses for creep-rupture testing. Specimens were pulled at a crosshead speed of 0.05 inch per minute, and the temperature was controlled in accordance with ASTM recommended procedures. Stress-strain relationships were determined with an optical extensometer system.

(2) Creep Rupture Tests. It was initially planned to obtain a stress-rupture curve at 1000°F for both smooth and notched specimens for each of the twelve heats of the material out to approximately 1000 hours. Based on data available on commercial René 41, the curves for the notched specimens were expected to break sharply downward at approximately 400 hours. In an attempt to complete testing in the time period of the contract, most of the tests were started concurrently. As data became available it became evident that the rupture curves for for notched specimens would not break down until considerably more than 1000 hours had elapsed. As a result, some of the notched specimens were tested for several thousands of hours. The curves

for the smooth specimens were not extended out this far because an increase in slope was not expected and the rupture times were within the expected range.

The creep-rupture tests were conducted in beam loaded machines in accordance with ASTM recommended procedures. Specimens were allowed a maximum of four hours to attain test temperature and temperature distribution before the load was applied. Rupture times were recorded automatically. Creep extension was measured by an optical extensometer system which has a sensitivity of five-millionths of an inch. Rupture ductility was determined in terms of both elongation and reduction of area.

Evaluation of Tested Specimens

Fractured tensile and creep-rupture specimens were reviewed with regard to the nature of the fracture surface and its relationship to the mechanism of failure. Optical micrographs of the fractures were made and compared with the visual observations of the fracture surfaces. Electron microscopy was used to determine whether deformation had altered the distribution of the γ' phase. All electron micrographs were of chromium shadowed single stage collodion replicas of the etched metal.

EXPERIMENTAL MATERIALS

The ingots were made by vacuum melting and adding Mg under a partial argon atmosphere, as described in the previous section. These were then hot pressed to slabs. At this point, samples were taken for chemical analysis. The slabs were hot rolled to sheet bar. The sheet bar was then hot rolled, solution treated, and cold reduced at the Eastern Stainless Steel Corporation. The final thickness was about 0.040-inch, this being the thinnest material the Eastern Stainless Steel Corporation would produce.

Chemical Composition

Chemical analyses were made on sections taken from the top and bottom of the ingots after they had been hot pressed to 1-3/8-inch slabs. The compositions indicated by these analyses (Table I) were, for the most part, within the range of variation expected for the type of melting practice employed. A few anomalous analyses were found, however, which do warrant further comment.

Magnesium Content

1. Magnesium was added with an expected recovery of 70 per cent. The results of chemical analysis indicated considerable variation from the expected recovery. The degree to which this represents varying losses, segregation, and/or analytical variability is not known. It seems unlikely, however, that Heat 10 actually had 0.03 per cent Mg when the aim content was 0.02 per cent. Likewise, the 0.05 per cent Mg of Heat 12 seems inexplicably low. The general agreement between the samples from the top and bottom of the ingot does not support segregation as an explanation of the variations.

2. The compositions given in Table I were determined on samples taken after the ingots had been hot pressed to 1-3/8-inch thick slabs; the experimental material was subsequently hot rolled, heat treated, and cold rolled to sheet. During this processing, the possibility of Mg loss existed. Re-analysis for Mg on the sheet material (Table II) gave results indicating the same trends in Mg content as were indicated by the original analyses (Table I), but at a slightly lower absolute level of Mg. It also suggested that the Mg of Heat 12 was actually higher than indicated by Table I. There was no definite indication that the final heat treatment of the cold-worked, as-received material had much affect on Mg content.

3. The data of Table II suggest some loss of Mg during processing. Yet, considering the difficulty of the analysis, the possibility does exist that the difference could be due to analyses being made in two batches at widely different times.

Carbon Content

The carbon contents of the S-alloy heats (Table I) were lower than expected. Thus, the "low carbon" series had carbon contents of the order of 0.02 per cent instead of the intended 0.05 per cent. The "high carbon" series ranged from about 0.05 to 0.08 per cent.

The René 41 heats came out closer to the expected contents, except that the amounts in Heats 11 and 12 were exceptionally high.

It is difficult to reproduce carbon contents much closer than were obtained within each of the three series of alloys. However, it is not possible to account for the low recovery of carbon in the S-alloy from any known experimental variable.

Zirconium Content

The results for the analyses for zirconium were puzzling for the S-alloy heats. Heat 1, when analyzed as a check on melting practice, came out as expected. The other seven heats had twice as much Zr, even though the addition was the same as Heat 1. The René 41 heats with the same addition of Zr had the expected percentage of Zr.

Gas Content

The analyses seemed to indicate that Mg resulted in lower oxygen contents than when no Mg was added. Otherwise, there did not appear to be a significant effect of Mg on gas contents. It should be recognized that vacuum melting could, in itself, reduce the gas contents to the point where any Mg effects that might be noted in higher gas content materials would not be evident.

EFFECT OF MAGNESIUM ON CRACKING DURING PRODUCTION OF THE SHEET

The possibility that Mg might influence the "hot workability" of the alloys was also considered. Since energy consumption during rolling or other

measures of "hot workability" were not experimentally measurable in the rolling operation, the only feature which served to reflect "hot workability" was cracking. Since no cracks developed in any of the Mg-free heats of the alloys, it was impossible to detect any improvement in "hot workability" that might be due to magnesium.

On the other hand, examination of the 1-3/8-inch slabs after hot pressing indicated that the slabs of each of the three materials with the largest Mg additions had developed hairline cracks along its edges, transverse to the flat surfaces. One crack was found in the René 41 slab (Heat 12) which was about 1/2-inch deep. It was cut out prior to subsequent working. No other cracking was noted and no further cracking occurred during hot rolling at the University. Cracking occurred during hot rolling at the Eastern Stainless Steel Corporation, but this was apparently due to temperature variations arising from handling difficulties. No effects attributable to Mg were noted during cold rolling.

From these data it would appear that the heats with an intended 0.08 per cent Mg content were more prone to crack during initial hot working than were the heats with smaller or no Mg additions. Previous work has also shown that the base materials (i. e., the alloys with no Mg additions) had good "hot workability". The data are not adequate to show if there was any improvement from the intermediate amounts of magnesium. Some of the data to be given later indicate that intermediate amounts of Mg can have an effect on other characteristics of the material which is different from the effect of the larger amounts of Mg. Schultz⁽¹⁾ also noticed that larger Mg additions (0.1 per cent) seemed to induce cracking during initial hot rolling.

MAGNESIUM ADDITIONS AND MICROSTRUCTURES

In planning the investigation, it was recognized that the final reduction of the experimental material should be cold finished in accordance with sheet production practice. The decision was also made to carry out the investigation on solution treated and aged materials. Enhancing tensile strength by cold working was eliminated on the basis of the NASA research which showed that the cold work would induce too much notch sensitivity for practical applications.

As-Cold-Worked Condition

The microstructures of the as-received, cold-worked materials were surveyed for initial uniformity. In addition to the need to know if magnesium was influencing microstructure, there were two reasons for this survey:

1. Six separate pieces were produced from each ingot. Therefore, the possibility existed that there could be significant differences between the pieces which might be reflected in the response to heat treatment.
2. The final heat treatment prior to cold working was 3 minutes at 2150°F followed by water quenching. Because of the rapid rate of the gamma prime reaction, this treatment resulted in complete solution of the gamma prime. However, this treatment subsequently proved to be rather critical in terms of the uniformity of carbide solution.

The microstructures of the S-alloy heats were carefully evaluated after solution treating over a range of temperatures. Initially, this was done to aid in the selection of a suitable solution treatment. When the results indicated an effect of magnesium on the temperature of solution of carbides*, (most evident as carbide particles in the grain boundaries), the solution temperature of carbides as a function of magnesium content was studied in detail. When it was found that Mg reduced the solution temperature of carbides, considerable research was done to discover the cause.

The heat treatment for René 41 had been preselected to be the same as that which was generally recommended for engineering applications. Accordingly, any effects of Mg on carbide solution temperatures were not studied.

*

The carbides referred to are those which go into solution and precipitate in accordance with thermal treatments, in contrast to Ti(C, N) which is generally distributed and does not change significantly during normal heat treatment.

As-Received S-Alloys

Photomicrographs of two of the six pieces of each material in the cold-reduced condition are shown in Figure 3. In this Figure, the number at the corner of each photomicrograph identifies which of the six pieces it illustrates. Presumably, the two show the extremes in carbide solution for each heat. The following comments are based on the studies which these photomicrographs summarize:

1. The undissolved carbides in the grain boundaries ranged from none to fairly extensive amounts.
2. There was just as much variation within each piece from individual heats as there was between pieces from the same heat.
3. The high carbon heats had somewhat more undissolved carbides than the low carbon heats.
4. The heats with the low and intermediate Mg additions, (Heats 3 and 5; 4 and 6) tended to have fewer carbides than those with no Mg (Heats 1 and 2), and with the largest Mg addition, particularly Heat 8.

Three minute heat treatments at 2150°F would be expected to be too short to cause complete solution of carbides, even though the types of carbides are known to have solution temperatures below 2150°F. It seems apparent that there was some variation in carbide precipitation prior to the final three minutes at 2150°F. Subsequent data suggest that the apparently more complete solution of carbides in the heats with 0.02 and 0.04 Mg additions could be due to the intermediate Mg additions lowering the solution temperature.

As-Received René 41 Alloy

The amount of undissolved carbide was more than for the S-alloy (Fig. 3), although some of the samples indicated fairly complete carbide

solution. There was as much variation between pieces from any one heat as there was between heats. No relationship to Mg additions was noted; or, more strictly speaking, the work done was inadequate to detect an effect of Mg on carbide solution if there was one.

René 41 is known to contain substantial amounts of M_6C carbide, which has a higher solution temperature than the carbides in S-alloy. Consequently, the evidence of more carbides in the René 41 was to be expected.

Effect of Magnesium on Solution Temperature

Because there had been no previous experience in heat treating S-alloy in the form of cold-reduced sheet, trial solution treatments were undertaken at several temperatures. It was expected that these would show the minimum temperature for solution of gamma prime and carbides (except the essentially insoluble $It(C, N)$ phases), and this temperature would be used for heat treating the sheet.

The René 41 sheet heat treatment was preselected to be one commonly used in practice. Solution temperatures were therefore studied only slightly.

Carbide Solution for S-Alloy

Increasing Mg contents were found to first reduce and then raise the temperatures at which intergranular carbides* disappeared from the S-alloy microstructure. This temperature was also higher, the higher the carbon content. Detailed examples of the microstructures as a function of solution treatment temperature are shown by Figs. 4 through 7. The structures after both 2 and 10 hours of heating are included. The similarity of the results suggests that equilibrium was achieved and showed the reproducibility of the observed effect. The temperatures at which carbides were no

* The largely insoluble, generally distributed $Ti(C, N)$ particles remained virtually unchanged during heat treatment and are not considered in this discussion.

longer visible in the structures are plotted as a function of the Mg contents in Figure 8, and as a function of carbon content in Figure 9. The curves in Figure 8 were established by adjusting the solution temperature (using the curves of Fig. 9) to 0.03 per cent carbon for the low carbon S-alloy, and to 0.07 per cent for the high carbon S-alloy. Therefore, the curves of Figure 8 show the best estimated temperatures of heating required for the prevention of carbide precipitation in the grain boundaries for carbon contents of 0.03 and 0.07 per cent.

The smallest addition of Mg used (0.02 per cent) reduced the carbide solution temperature about 60°F. At 0.04 per cent Mg, the solution temperature was about the same as that of the 0.02 per cent Mg heats; at the 0.06 per cent Mg level, the solution temperature was only slightly above this low value. However, at 0.075 per cent Mg, the temperature was back up to that of the heat for the 0.07 per cent carbon material with no Mg addition.

Gamma Prime Solution

In the micrographs presented in Figures 4 through 7, the gamma prime phase is visible as a general precipitate in the structure of the alloys heat treated at the lower temperatures. These microstructures suggest that Mg may have also lowered the gamma prime solution temperature slightly. The solution temperature for the gamma prime is, however, so sensitive to the Al+Ti content that the available information is neither proof nor disproof of an effect of Mg on the solution temperature of the gamma prime.

It should also be recognized that the low carbon S-alloy heat with no Mg addition (Heat 1) was somewhat higher in Al+Ti than the other three heats. This, in itself, may have resulted in a somewhat higher gamma prime solution temperature than the other heats with Mg added.

Checks on Solution Temperatures of S-Alloy

Because there was variation in the amount of carbides in the as-cold-worked materials (see Fig. 3), the possibility that it might be a factor in the observed carbide solution temperatures was checked. Samples were heated

first at 1900°F to precipitate and agglomerate carbides, and then at 1975°F to compare the solution effect with that shown by directly heating the cold-worked material. The results were the same (Fig. 10). In addition, samples were heated at 2150°F for complete solution of carbides and then reheated at 1975°F. During the reheating at 1975°F, carbides formed in the grain boundaries in those cases where they were present after direct heating of the cold-worked condition.

Therefore, these observations indicated that the curves of Figure 8 show near equilibrium carbide solution. Indications are that carbides precipitated or dissolved on heating at temperatures below the curves, according to whether or not the carbides were initially in solution or precipitated when the materials were received. Heating and cooling of the samples for the heat treatments used in establishing Figure 8 were sufficiently rapid to limit carbide precipitation and solution to the holding temperatures.

In the presentation of the data, the term "carbide solution temperature" has been used rather loosely. As judged by Figure 3, in most of the samples heated for the data presented in Figures 4 through 9, carbides actually precipitated when the temperature of heating was below the points in Figure 8.

The samples used for the data cited in Figures 4 through 10 were obtained on samples taken from material from near the center of the ingots. Samples of high carbon S-alloy taken from material from the tops of the ingots showed the same carbide versus heating temperature effects (Fig. 11). It seems unlikely that segregation was responsible for the observed effects of Mg on carbide solution temperature.

René 41 Alloy

The effect of Mg on carbide solution temperature was not investigated for René 41. A large proportion of the carbide in René 41 is M_6C with a higher solution temperature than the carbides in the S-alloy. Apparently, M_6C would gradually dissolve over an extended range of temperatures. Increasing the temperature of solution treatment for the low and high Mg heats

(Heats 10 and 12) from 1925°F to 2025°F did not result in nearly as much intergranular carbide solution (Fig. 12) as it did for S-alloy. Comparison with Figure 8 shows that all of the carbides would have been dissolved in the low magnesium heat of S-alloy at 2025°F, and would be nearly completely dissolved in the high magnesium heat. There would not have been the similarity of undissolved carbides present in both René 41 heats after treatment at 1925°F than in the S-alloys.

The microstructures of the René 41 alloy did show, for reasons which are not clear, more inclusions of what appear to be Ti(C, N) than did the S-alloy heats.

Effect of Magnesium on Grain Size

There were no readily evident effects of Mg on grain size; thus, this subject was not included. The data for materials subjected to creep-rupture tests in a later section of the report do show grain sizes after the heat treatment for rupture testing. The low carbon S-alloy had a larger grain size than the high carbon S-alloy. Any effects of magnesium, however, were minor. The René 41 alloy had a considerably finer grain size than the S-alloys. Again, however, there was no evident effect of magnesium.

Effect of Magnesium on the Type of Carbide in High Carbon S-Alloy

Because the effect of Mg addition on the carbide solution temperature was unexpected, and because considerable influence on mechanical properties is often attributed to carbides, this feature of the results seemed important. Accordingly, it seemed worthwhile to undertake research on the mechanism. It was decided to determine if the type of carbide was changed by Mg. Carbide extractions were made of samples of high carbon S-alloy heated one hour at temperatures of 1700°, 1900°, 1975°, 2000°, and 2150°F, and water

quenched. X-ray diffraction analyses of the extractions gave the data shown in Tables III through VI and summarized qualitatively in Figure 13. The investigation was limited to high carbon S-alloy because of time limitations and the probability that the qualitative results would be similar for the low carbon alloy.

In addition to as-quenched samples, samples which had been subsequently aged 16 hours at 1300°F were also included for some of the materials.

The one-hour heat treatment was used because this was the heat treatment finally selected for mechanical testing. The microstructures indicated that same degree of carbide solution previously described for two and ten hours of heating. The aging treatment was the same as the one used prior to mechanical testing.

The results of the X-ray analyses of the extracted carbides are, in Figure 13, necessarily expressed in terms of the relative amounts (see Appendix I) of the various carbides present, but cannot reflect the total amount of carbide in the specimens. Therefore, specimens heated close to the solution temperature may show high percentages of one type of carbide, although the total amount in the alloy may have been comparatively small due to nearly complete solution. With due recognition of these limitations of the data in Figure 13, then, the following effects of Mg on carbides are indicated:

1. Increasing Mg additions increased the percentage of Cr_7C_3 relative to the other carbides extracted from the alloy. No Cr_{23}C_6 was found in the high Mg heat except when it was aged at 1300°F. Apparently, $\text{Ti}(\text{C}, \text{N})$ did not change. All Mg-bearing heats had reduced ratios of Cr_{23}C_6 to Cr_7C_3 after aging at 1300°F in comparison to the Mg-free heat with all Cr_{23}C_6 .
2. Increasing the temperature of heat treatment increased the relative amount of Cr_7C_3 in the extractions. Reducing the temperature of heat treatment, particularly aging at 1300°F, increased the Cr_{23}C_6 .

3. Only Ti(C, N) was extracted from samples heat treated at 2150°F. Judging from the microstructures, this would have been true for heat treating at any temperature above 2050°F (see Fig. 2) for the no-Mg and high-Mg heats, and above 2000°F for the low and medium Mg heats. Reference to Figure 8 indicates that the amount of carbide in the 0.02 per cent Mg heat must have been very small after solution treatment at 1975° or 2000°F. Rechecks using microstructures had shown that there was very little difference in the degree of solution between most heats after being heated 1, 2, or 10 hours. It will later be shown that there were undissolved carbides visible in the creep-rupture specimens of this heat when treated at 1975°F. It is not certain if one hour was insufficient for complete solution, or if slight variations in the carbon or magnesium contents were sufficient to cause some variation in the temperatures for complete carbide solution.
4. The 1935°F solution treatment before aging the 0.02 per cent Mg alloy at 1300°F for extracting and identifying carbides, was a compromise to reduce the time-consuming determinations. By using 1935°F, the results appeared to be representative of solution treating at both 1900° and 1975°F. The results were also similar for 0.075 per cent Mg material aged at 1300°F for prior solution treatments at either 1975° or 2075°F. In fact, Figure 13 is a summary of far more extensive investigations in which the qualitative reviews of the diffraction patterns indicated that nothing further would be gained by quantitative measurements of the lines.

Discussion of Microstructures and Magnesium

The data indicate that only a small addition of Mg reduced the solution temperature for intergranular carbides in both high and low carbon S-alloy. While there were differences in composition among heats, they did not seem sufficient to cause the observed effects. This reduction in solution temperature was accompanied, in high carbon S-alloy, by an increase in the ratio of Cr_7C_3 to Cr_{23}C_6 carbides. There seems to be little doubt that Mg caused a similar change in the types of carbide in the low carbon S-alloy, even though no actual determinations were carried out.

It is acknowledged that there are severe limitations on the generality of the results. These limitations will be discussed later. It seems best to discuss first the unusual features in the data, assuming that they reflect effects of magnesium.

1. The heats with 0.02 per cent Mg had carbide solution temperatures as low as any of the heats with more Mg added. This suggests that considerably less Mg might also be effective in reducing carbide solution temperature. It also raises the interesting question of whether or not melting in a magnesia crucible alone could introduce enough Mg to produce a considerable alteration of the carbide reactions.

2. The data point out, to an unusual degree, that carbides can and do form at rather high temperatures. If the prior history prevented carbides from forming, they can precipitate at the temperatures of many of the commonly used "solution treatments".

3. Either or both Cr_{23}C_6 and Cr_7C_3 can be present in the type of alloy studied, as several investigators have shown.^(6, 7) The phases present are dependent upon specific compositions as well as on temperature and time of heat treatment. To explain the changes observed in solution temperature and type of carbide, it can be hypothesized that Mg changed the equilibrium and/or kinetic phase relationships of the alloy. For instance, the small amounts of Mg might have exerted sufficient influence on the thermodynamic

activity of some or all reacting components to shift phase equilibrium.

4. The metallographic observation of the degree of carbide solution would not differentiate between Cr_{23}C_6 and Cr_7C_3 . Therefore, the apparent constancy of undissolved carbides with 1, 2, and 10 hours of heating would not necessarily be evidence of equilibrium in phase relationships. Working with a similar alloy, Fell⁽⁶⁾ showed that time had marked effects on the relative amounts of Cr_{23}C_6 and Cr_7C_3 carbides. He also showed compositional effects on the kinetics of the reactions, as well as changes in the phase relations. Fell's data agree with the hypothesis and the general trends of this investigation.

5. The highest Mg-bearing, low carbon, S-alloy heat (Fig. 8) showed only a small increase from the minimum in carbide solution temperature. This could be due to the 0.06 per cent Mg in the heat being inadequate to shift the phase relationships to higher temperatures for the solution of carbides. The data available for the high carbon S-alloy also indicates that 0.06 per cent Mg would only slightly increase the solution temperature from the minimum. Apparently, then, more than 0.06 per cent Mg is needed for the marked increase in solution temperature from the minimum.

6. There are a number of limitations of the data presented in respect to the generality of the results. The most severe of these is that the data is restricted to a few small laboratory heats. It is not known if the effects would carry over to production heats. There were variations in composition between heats, particularly carbon content, although corrections were made in the presentation of the data. The inhomogeneities in microstructure were normal for alloys of the type investigated, and the methods used in evaluating the structures should have eliminated any significant effect of the inhomogeneities on the solution temperatures reported in Figure 8.

7. The reader is reminded that there were two special features of the investigation which are somewhat unusual:

- a. The Mg contents discussed are residual Mg remaining after this chemically-active element had completed reactions with other elements in the alloy.
- b. To a large extent, carbides precipitated rather than dissolved during the "solution treatments" below the solvus temperatures.

8. While the suggested mechanism of changes in the phase relationships by small amounts of Mg may be adequate to account for the observed changes in carbide solution temperatures, there are other effects of Mg which could be acting directly or indirectly. The oxygen contents of the heats (Table I) were reduced to very low values by Mg, a change which could have considerable effect on microstructure. The alloy is also subject to pronounced increase in creep-rupture strength from the small amounts of boron and zirconium added. A possible interaction between these elements and Mg which might influence carbides cannot be eliminated by available information.

9. Schultz reported⁽¹⁾ that Mg increased the number of particles of Ti(C, N) in S-alloy. This was not observed in the current research. The René 41 alloy, however, did appear to have more Ti(C, N) particles. However, the identification of the particles and/or the differences in conditions of making sheet and bar could be involved so that there are no real discrepancies.

EFFECT OF MAGNESIUM ON RUPTURE PROPERTIES AT 1000°F

The major objective of the investigation was to determine by mechanical testing if magnesium would reduce the edge-notch sensitivity of nickel-base, gamma-prime strengthened alloys in sheet form, at temperatures between about 800° and 1200°F. A test temperature of 1000°F was used. To accomplish this, it was necessary to select heat treatments for the S-alloys. Tensile tests were also conducted to guide selection of stresses for rupture tests.

Selection of Heat Treatments

Usually heat treatments for nickel-base, gamma prime alloys are established by extensive correlations between treatment conditions and creep rupture properties. In the case of the S-alloy, such data were not available for cold-reduced sheet at any temperature, and no test data were available for other forms at 1000°F. The original intent of the heat treatment studies previously described was to provide information on which to base a solution treatment for mechanical test specimens. It was considered that the temperature ought to be high enough to dissolve gamma prime. The need to dissolve carbides was less clear. Originally it was expected that the temperature would be high enough to dissolve carbides inasmuch as it was thought to be common practice to solution treat above the solution temperature for carbides, except for the high molybdenum alloys such as René 41.

The treatment finally selected for the S-alloy was one hour at 1975°F, air cool, plus an age of 16 hours at 1300°F. There were several reasons for selecting 1975°F. It was high enough to insure gamma prime solution. One hour, however, was necessary to obtain the carbide solution effects previously described. This would result in complete carbide solution in the low carbon heats with Mg added, but not in the heats with no Mg (Fig. 8). Varying, but incomplete, carbide solution would result in the high carbon S-alloy heats. Since carbides are generally credited with considerable effect on creep-rupture properties, it was hoped that the contrasting carbide solution effects would provide clarifying information.

The previous research on S-alloy had been done on barstock heated 8 hours at 1975°F and air cooled. It was considered that the far more intense heating and working of the sheet had introduced sufficient homogenization so that an 8-hour solution treatment was not necessary; thus, the time used was reduced to one hour. The aging treatment is the same one used on the barstock and closely simulates aging in engineering alloys. The heating and cooling rates for the solution treatment were slower than for the carbide solution studies. Presumably, therefore, carbide precipitation occurred during heating and cooling. Extensive carbide precipitation occurred during aging.

The same times and temperatures were used for René 41 as had been applied in the prior research evaluating this sheet for the SST: 0.5 hours at 1975°F, air cooled, plus 16 hours at 1400°F, air cooled. Air cooling rather than water quenching was used because no method was found of avoiding undue warpage of the specimen blanks as a result of water quenching. The René 41 sheet previously studied had been water quenched commercially under conditions which minimized warpage.

Short-Time Tensile Properties at 1000°F

No definite effect of magnesium was proved by the short-time tensile tests. There were, however, differences which suggested an effect of Mg, (Table VII and Fig. 14). These were:

1. The low carbon S-alloy heat with no Mg addition (Heat 1) had a lower notch tensile strength than the three heats with Mg added; it also had higher unnotched tensile and yield strengths with lower ductility. The consequence was a lower notched to smooth strength ratio (N/S ratio) without magnesium.
2. The high carbon S-alloy and the René 41 heats with the highest Mg addition (Heats 8 and 12, respectively) had low notch strengths and, consequently, comparatively low N/S ratios.
3. The René 41 heat without an Mg addition (Heat 9) had somewhat higher ductility than the heats with magnesium.
4. When viewed graphically (Fig. 14), there is a strong indication that Mg may be beneficial to fracture toughness at low carbon contents, and that more than 0.04 per cent Mg in the higher carbon alloys is detrimental.

Except for these cases, the apparently constant tensile properties, especially for the low carbon S-alloy, support the reality of the differences. The level

of shorter time rupture tests reported in the next section also supports the differences as characteristic of the heats, rather than simply data scatter. Because the differences between heats seem definite, there is a temptation to attribute the effects to magnesium. Yet, it is easily possible that some other factor could have been responsible.

In addition to the effect of magnesium, the following were noted:

1. The high carbon S-alloy had consistently higher strengths and lower ductility than the low carbon S-alloy. The higher strengths fit the generally expected pattern for increased carbon in these types of alloys. Only the Mg-free heat of low carbon S-alloy had the expected comparatively low ductility for low carbon content. Thus, the possibility of a beneficial effect of magnesium in the low carbon heats is further supported.
2. The fracture toughness of the low carbon S-alloy with Mg added was considerably higher than that of the high carbon S-alloy (Fig. 14), although at a lower strength level. For a given Mg content, the René 41 alloy had a lower notch toughness than the high carbon S-alloy, although tensile strengths were similar. It is not known to what degree the lower notch toughness of the René 41 alloy was due to other compositional differences.
3. The strength of the notched specimens of René 41 was low in comparison to their tensile strengths; this caused its fracture toughness to be lower than that of the S-alloy specimens.

During rupture tests, a few high-stressed specimens broke on loading at stresses below the short-time tensile strengths. Whether or not this was due to variations in tensile strength among specimens, or to testing conditions is uncertain. In other research at the University not yet published, marked variations in strength with strain rate have been observed for gamma

prime strengthened alloys. Also, the shorter time of heating at 1000°F prior to testing in the tensile tests might have caused some difference in strength. In general, however, this type of result leads to uncertainty with regard to the proof of Mg effects on tensile properties on the basis of the limited data in this report.

Rupture Test Properties at 1000°F

Possible effects of magnesium on rupture properties (Tables VIII, IX and X, and Figs. 15, 16, and 17) are somewhat complicated. The following observations can, however, be made:

1. The curves for the smooth specimens of low carbon S-alloy with Mg added (Fig. 15) turned down sooner and with more slope than the curve for the Mg-free heat. The result was considerably lower strength at long time periods for the heats with Mg added. In the longer-time tests on the Mg-free heat, notched specimens fractured through the loading pin holes, rather than the notches. Thus, the effect of Mg on notched, rupture strength at 1000°F was not well established. The assumption can be made, however, that Mg may have reduced stress concentration sensitivity at the probably lower temperatures at the loading pin holes, to the degree that fracture occurred there rather than in the gage section at the notches.* The data also suggest that the highest Mg heat had the best long-time strength. However, it will also be noted that the longest test on the intermediate Mg (0.04 per cent) heats also fractured in a pin hole. This leaves a rather strong question as to how effective Mg actually was in reducing the stress concentration sensitivity at the pin holes in comparison to some other unidentified variable.

2. The high carbon S-alloy exhibited no marked variations in rupture strength (Fig. 16) with varying Mg content.

3. Magnesium-bearing heats exhibited no marked difference in smooth specimen rupture strengths (Fig. 17) for René 41 alloy. The results

* There were experimental differences between Heat 1 and the other three heats which do not, however, seem to explain the pin hole fractures.

for the notched specimens are not as clear. The tendency is to assume some improvement in long-time properties of notched specimens to Mg additions, even though the intermediate Mg heat's longest test indicated low strength.

4. The René 41 material had higher, long-time notched strength than the material used for Reference 2. The unnotched specimen properties were, however, no different from those of Reference 2. The curves for the notched specimens did not break down as soon as those for Reference 2, and the slopes were less after the breaks. The prior data indicated that tests at stresses as low as 60,000 psi would be necessary to obtain rupture in about the desired maximum test time of about 1000 hours; and tests were started under 60,000 psi. When higher stress tests indicated that the rupture time of the 60,000 psi tests would be of the order of 10,000 hours, they were discontinued.

5. The Mg-bearing heats of low carbon S-alloy had higher elongation in the rupture tests than the Mg-free heat for time periods up to 100 to 200 hours. At longer time periods, there was little difference--all heats were low whether or not Mg had been added. The high carbon S-alloy may have had slightly higher ductility when Mg had been added. There was no noticeable effect in the René 41 alloy.

6. The major objective of the investigation was to determine if Mg would reduce the edge-notch sensitivity of nickel-base superalloys in sheet form, at the low end of the temperature range where creep occurs. The main concern was the marked increase in slope of the stress-rupture time curves at the longer times. The presentation of the results has emphasized this aspect of the data. However, it will be noted that the levels of strength prior to the increase in slope were generally similar to the short-time tensile strengths.

7. There were other results of the rupture tests not involving magnesium which should be noted.

- a. The stress-rupture time curves for smooth specimens of the S-alloys all underwent an increase in slope at the longer time periods. The curve for the Mg-free heat of

low carbon S-alloy simply did not curve as much as those with Mg. Accordingly, the curves for S-alloy have not been extrapolated to prolonged time periods. Curves rather than sharp breaks were drawn because the data seemed to be best represented this way and the slopes for long time periods had not been defined by the data. However, René 41 did not show the change in slope for curves for smooth specimens with one test out to 4500 hours.

- b. The level of rupture strengths of smooth specimens increased from low carbon S-alloy, to high carbon S-alloy, to René 41. This difference became greater with increased time for rupture. This was not nearly as marked for notched specimens, and did not become general until after the breaks in the stress-rupture time curves (longer than 100 hours). Even then, the main difference was the tendency for the René 41 alloy to have higher strength than the S-alloys.

8. Some general discussion of the results seems warranted at this point:

- a. In selecting the heat treatments for the S-alloy, carbide solution was to be an important variable, both from an effect of Mg on degree of solution and by carbon content itself. The comments on this aspect of the investigation will be deferred until after the presentation of the results of structural examination of the fractured specimens.
- b. The tendency for fracture to occur through the loading pin holes in the longer-time tests in low carbon S-alloy should not be ignored. It suggests that for some reason there was less resistance at long time periods to a comparatively mild stress concentration under the presumably lower temperature conditions at the pin holes, than at the sharp notches in the 1000° F gage length. It was found in the NASA research that

the degree of stress concentration can be relatively unimportant. This suggests that factors other than notch sharpness may be more important in the type of rupture being investigated. It is true that the loads on the pin holes were higher for notched than for unnotched specimens due to the larger net section of the latter. However, the pin loads on the longest duration, unnotched specimens were higher than those for the notched specimens which failed in the pin holes because of the differences in strength of the two types of specimens. Consequently, time may have been a factor. Some stress concentration effect must have occurred at the pin hole because the failure times were less than the shorter time, higher load tests indicated for the notched sections. Strengthening of the notch area cannot, therefore, be the answer.

- c. It should be noted that while magnesium may have reduced the tendency for pin hole fractures in long duration tests, it was not nearly as effective as raising the carbon content to that of the high carbon S-alloy.
- d. The reasons for the higher strength of the notched specimens of René 41 alloy used in this investigation in contrast to that of the specimens used for the NASA work are not known. However, unreported research for NASA has shown that increasing specimen thickness reduces the sensitivity to the edge notches. Presumably, therefore, at least part of the reason for the higher strengths in the current investigation is related to thickness--0.040-inch in the present investigation as opposed to 0.025-inch for the NASA research. The differences due to the use of small laboratory heats cannot, however, be ruled out.
- e. The tests were inadequate to prove or disprove whether small amounts of Mg tended to delay breaks in the curves

for notched specimens and to flatten out the curves when the larger amounts of magnesium were added, as the data suggest. If this should be the case, it could be quite important in applications involving prolonged service of the nickel-base superalloys. The suggestion that Mg might be damaging in low carbon alloys could also be important.

Minimum Creep Rates During Rupture Tests

The minimum creep rates during the rupture tests (Fig. 18, and Tables VII, IX, and X) indicate that the major difference in creep resistance measured in this way was due to the alloy, and not to the magnesium additions. With the possible exception of low carbon S-alloy, any effect of magnesium was minor in comparison to the differences between alloys.

The data for the Mg-free, low carbon S-alloy (Heat 1) had the same creep resistance as the high carbon S-alloy data, while the three Mg-bearing heats had lower creep resistance. This agrees with the higher rupture strength of the Mg-free heat at the longer time periods. The Al+Ti content reported for this heat (Table I) was higher than it was for the Mg heats, and might be the reason for the higher strength.

Careful examination of the data for the individual heats of each alloy shows that the general level of creep resistance between heats falls in about the same order as the rupture strengths. Unexpectedly, this is most evident in comparisons with the rupture tests on notched specimens. Subsequent data in the mechanism of fracture, however, will perhaps make this reasonable.

As in previous analyses of properties versus magnesium additions, the differences occurring when magnesium was added have not been sufficient to prove that they are real effects. However, it is evident from the creep data that the high creep resistance of the Mg-free, low carbon S-alloy in comparison to that of the heats with Mg additions was responsible for its correspondingly higher smooth rupture strength, irrespective of whether or not this higher creep resistance was due to the absence of magnesium. Secondly, the higher strengths of both the smooth and notched René 41 alloy in

the longer time rupture tests were due to higher creep strength. This was also true for the high carbon S-alloy in comparison to the low carbon S-alloy, except for the Mg-free heat.

EXAMINATION OF SPECIMENS AFTER RUPTURE TESTING

Visual and microscopic examination of the specimens after rupture testing was carried out to study any possible effect of magnesium on the mechanism of rupture and any effects of the degree of carbide solution. It included a limited electron microscope study of the structures.

Fracture Sequence

Rupture occurred by slow intergranular creep cracking leading to abrupt transgranular fracture when the cross sectional area had been sufficiently reduced for the applied load to exceed that required for rapid transgranular crack growth. This occurred in both notched and unnotched specimens. The creep cracking zones of the fractures were readily identifiable due to the discoloration by oxidation during this period of slow crack growth. This was measured and plotted as a function of rupture time (Figs. 19 and 20).

This sequence in the mechanisms of fracture leading to rupture was previously discovered in the research for NASA. Published studies of notch sensitivity under "creep rupture conditions" have been concerned almost entirely with higher temperatures, where the failure mechanism was almost always by creep-induced intergranular cracking. During recent years, however, there has been extensive study of crack sensitivity below the creep range where fracture occurs by transgranular cracking. Apparently, the specimens in this investigation fracture by a combination of the two mechanisms.

The factors controlling time for rupture, then, become mainly those which control the time required for the intergranular cracks to nucleate and grow to a size which will induce abrupt transgranular fracture. And, it follows that the sensitivity of the material to crack-induced transgranular fracture can be an important factor in the "rupture time".

Evidence supporting this dual nature of the failure mechanism is shown by Figures 19 and 20.

1. The percentage of intergranular fracture was less for the smooth than for the notched specimens. The stresses required to cause rupture in a given time were much higher for the smooth specimens. Consequently, once a creep crack formed, it did not have to grow nearly as much as in the notched specimen before abrupt transgranular fracture occurred as a result of the reduction in section by cracking raising the stress above the transgranular strength.
2. In both smooth and notched specimens, the percentage of intergranular cracking increased with time for rupture. The stresses were reduced to obtain the increase in rupture time. Consequently, more intergranular cracking was necessary before the stress was raised sufficiently to cause abrupt transgranular cracking.
3. The amount of cracking for a given time for rupture was generally less for René 41 than for the S-alloys. René 41 had a considerably higher creep-rupture strength, particularly at the longer time periods. Consequently, higher stresses were required for rupture in a given time. Therefore, less cracking occurred before the transgranular strength was exceeded. A similar difference was present, to some extent, between high and low carbon S-alloy.

These arguments for the sequence of events causing rupture are undoubtedly oversimplified. The data in this investigation do not make clear the

degree to which variation in tensile strength in the presence of the cracks, influenced the amount of cracking required to cause abrupt transgranular fracture. It is also not clear how much the rupture time was influenced by the crack length. For example, it is possible that the time governing the initiation of a creep crack could be the controlling factor, and creep crack growth could be relatively minor. Presumably, such factors do enter into rupture time to varying degrees, depending on the particular combinations of properties and test conditions. For instance, the tensile tests indicated that the René 41 alloy had somewhat low notched strength as compared to the S-alloys. This may have been part of the reason that René 41 had the smallest creep cracks at rupture.

The oversimplification carries over to the role of creep resistance and ductility in rupture tests. It seems probable that the higher creep resistance of René 41 and its high ductility in creep-rupture tests influenced the intergranular cracking process. Similarly, the low creep strength and low ductility of the low carbon S-alloy must have also influenced the creep-cracking process.

Finally, the cause for the increased slopes of the stress-rupture time curves was not established. Presumably, however, it must have been due in some way to the creep-cracking process. The NASA research indicated that stressed exposure did not appreciably affect the tensile strength of the smooth and notched specimens. It is therefore doubtful that time-dependent structural changes were involved.

The role of magnesium on the fracture sequences leading to rupture, if any, is not clear from the data. The most that can be said is that those differences between heats of each alloy, previously discussed as associated with Mg variations, were also reflected in the fracture sequences. For example, the lowest Mg heat of low carbon S-alloy (Heat 1), with its low tensile strength as a notched specimen, had comparatively less intergranular creep fracture than the other heats. Heat 3, with the low Mg addition and the lowest notched rupture strength, showed the most intergranular cracking. In the unnotched specimens of low carbon S-alloy, the lowest rupture strength

heats with low and intermediate Mg additions (Heats 3 and 5) tended to show less intergranular cracking for a given rupture time than the higher strength Heat 1 without Mg. Heat 7, with the largest Mg addition, seemed to be an exception. Similar observations could be made about the other heats.

The creep cracking was by no means uniform. It grew inward from the edges of smooth specimens. As is usual for creep cracking, there were a number of cracks spread out along the gage length, only one of which led to the abrupt transgranular fracture. The intergranular cracks which led to the complete rupture usually grew in from one edge (Fig. 21a). Notches served to localize the creep cracking to the base of the notch. In most cases, the crack causing rupture grew in from the notch on one edge, although there were cases where intergranular cracking grew in from both notches (Fig. 21b). It is not clear to what degree the variation in elongation of the smooth specimens was due to the relative amounts of creep and transgranular cracking.

The tendency for the cracks causing rupture to grow from one edge complicates the stress conditions. It is assumed that this resulted in a different stress concentration effect from the ideal, uniform crack growth from both edges. This could have had a considerable effect on the propagation of cracks and on rupture time, unless the crack initiation time was the controlling factor.

Microstructures of Rupture Test Specimens

Considerable effort was expended in studying the microstructures of the specimens before and after testing in an effort to obtain information relating structure to properties, with emphasis on the magnesium and carbide solution variables included in the investigation.

Original Carbide Morphology

All of the materials underwent recrystallization (Fig. 22) during solution heat treatment as a result of being cold worked. The grain sizes

indicated that the S-alloys, particularly the low carbon heats, underwent grain growth as well. The new grain boundaries of the S-alloy heats were outlined by carbides, especially those which precipitated during aging. Apparently, new grain boundaries in René 41 did not have sufficient carbide precipitated to be clearly outlined.

It is not certain from this investigation when carbides precipitated during solution treatment, and to what degree those which precipitated were located at the old grain boundaries rather than at the boundaries newly formed by recrystallization. Because the specimens were heated relatively slowly, it is possible that considerable carbide precipitation occurred by the time the specimens reached the recrystallization temperature. Generally, however, there seemed to be more undissolved carbides outlining the original grain boundaries of these specimens, than in the rapidly heated specimens used for the study of the effect of magnesium on solution temperatures of the S-alloys.

It will be noted that in low carbon S-alloy with no Mg (Heat 1) there were a considerable number of carbides within the new grains. Presumably, these are the undissolved carbides at 1975°F as predicted by Figure 8.

The other three heats of low carbon S-alloy had virtually no carbides within the grains, presumably because the solution temperature had been depressed below 1975°F by Mg, as indicated by Figure 8.

All of the high carbon S-alloy materials had a background of "ghost grain boundaries" as a result of undissolved carbides present at the sites of grain boundaries existing before recrystallization. The data of Figure 8 indicated that 1975°F should have completely dissolved carbides in the 0.02 per cent Mg Heat. Carbide solution was, however, incomplete in the test specimens. The reason for this was not determined.

The solution of carbides in René 41 alloy was far from complete. This was expected due to the predominance of the high solution temperature M_6C carbides. The incomplete solution resulted in an extensive outlining of the old grain boundaries by undissolved carbides. Considerable care is necessary to distinguish between the new, true grain boundaries formed by recrystallization and the old boundaries as outlined by the spheroidized,

undissolved carbides. Apparently, there was insufficient carbide solution carbide precipitation in the new boundaries dueing aging for them to stand out when etched.

Microstructures of Fractured Specimens

In the research for NASA it was determined that fracture occurred first by intergranular cracking, the surface of which darkened due to oxidation, and then transgranular fracture, the surface of which remained bright. This aspect of the microstructures has not been emphasized in this report.

Most of the smooth specimens showed evidence of extensive deformation throughout the gage length. (Figure 23 is an example of this type of deformation.) The stresses applied were generally above the yield strength, and general deformation was to be expected. The evidence of deformation in the notched specimens was limited to the region of the notch and the regions of transgranular fracture. For some reason, where the fracture was intercrystalline, even in smooth specimens, there was little or no evidence of plastic deformation (Figs. 24a and 24b). In contrast, Figures 24d and 24f show the marked deformation in the transgranular fractures of shorter-time, higher-stressed tests.

In the examination of the specimens, it was noted that there were frequently intergranular cracks adjacent to the main fracture, even when the fracture was transcrystalline. Figures 24e through 24g, and Figure 25 are examples of this. Figure 26 shows intergranular cracking as it has started at the notches. The usual intergranular cracks adjacent to the main crack are also evident. Again, it should be noted that the matrix was not deformed nearly as much as when the fractures were transcrystalline. Examples of primary transgranular fracture in René 41 alloy are shown in Figure 27 for unnotched specimens. The accompanying tendency for limited transgranular cracking, both from the edge and internally, is shown by Figures 27a, 27b, and 27d.

The deformation associated with transgranular fracture seems to indicate that it was ductile. In the smooth specimens, most of the tests were

well above the yield strengths, so that deformation of the grains was to be expected. In the notched specimens, all except the highest stress, shorter time tests were not loaded above the yield stress for the net section at the base of the notch. Therefore, the deformation could have been localized at the notch area by yielding ahead of the crack as it grew, and by general yielding as the stress increased with cracking. In longer tests, however, the net section stress was still below the yield strength when transgranular fracture occurred. This probably explains the comparatively high reduction of area for the elongation in the longer time, S-alloy specimens.

The intergranular cracking associated with the transgranular fracture is assumed to be evidence that there was little difference in the initiation of intergranular versus the transgranular cracking. Both could occur simultaneously. However, at the higher stresses, the transgranular cracks propagated more easily than the intergranular ones. It is usual to find numerous intergranular cracks adjacent to the main intergranular creep crack. It was therefore expected that such cracks would be found near the main intergranular cracks in the specimens examined. The information derived primarily from the NASA research, and substantiated by this investigation, indicates that the transgranular fracture occurred abruptly when the creep cracking raised the stress high enough for the crack to initiate transgranular fracture. This assumed that once a crack started in either a smooth or a notched specimen, the stress concentration would be similar because there would be sharp cracks in both cases. There was support for this concept in the NASA research. If specimens survived stressed exposure, there was not much change in short-time tensile properties. Apparently, the time after an intergranular crack was formed was comparatively short before abrupt transgranular fracture occurred, although it was long enough for the crack to oxidize. However, this aspect of the fracture mechanism could vary considerably depending on the test conditions and the properties of the alloys.

It should be noted that the metallographic examination did not clear up the cause of the unusual degree of notch sensitivity in the longer time tests (i. e. , the break in the stress-rupture time curves of the notched specimens

and the subsequently steeper slopes). In tests on notched specimens, it seems doubtful that the somewhat higher long-time strength of the René 41 alloy in comparison to the S-alloy was as much as might be expected on the basis of its higher ductility. The lower notched tensile strength of René 41 (see Table VII) could be involved by reducing the amount of cracking before abrupt transgranular fracture. It will be noted that René 41 also had higher ductility in tensile tests. The stresses based on the transgranular fracture area were also closer to the yield and notched tensile strengths than those of the S-alloy. It would appear that factors other than ductility as measured on smooth specimens or observed in the microstructures must be involved in the notch sensitivity of both short and long-time tests.

A number of aspects of these tests leave questions unanswered. The low long-time strengths of the notched specimens apparently involved the occurrence of transgranular fracture at lower stresses as the creep crack grew than the notched tensile test strengths. Therefore, it was not simply a matter of reduction of cross sectional area by creep cracking. In the majority of cases, the cracks started at only one edge and grew across to the other, with a consequent uncertainty of the stress relationships. There was nothing in the data to suggest that surface environmental effects, either during heat treatment or testing, were significant factors; yet these cannot be ruled out. In the NASA research, tests in vacuum units showed no change. In addition, the NASA research has not shown the loss of notched strength at long-time periods at temperatures so low that little or no creep occurred. Significant amounts of creep seem to be necessary for intergranular cracking.

The metallographic examinations were primarily concerned with the possible role of magnesium and carbide solution on fracture. No microstructural effects were observed which gave positive information on either variable.

In the previous discussion of microstructures before testing, it was noted that the grain size of high carbon S-alloy was smaller than low carbon S-alloy, and that René 41 had the smallest grain size. It seems quite probable that this entered into the fracture characteristics. The degree of intergranular cracking decreased with the grain size. In the usual case of

creep-rupture at higher temperatures, the larger grain sizes were more prone to crack intergranularly; this also seemed to be the case for this investigation. Again, however, grain size alone is inadequate to explain the results.

Initial Gamma Prime Particles

The specimens of the alloys as heat treated for rupture testing were examined by electron microscopy. The gamma prime particles were too small for exact comparisons of particle size (100 to 200 Å), but the general etching characteristics indicated no large variation (see Figure 28) between alloys or specimens as a result of compositional or inadvertent variations during heat treatment. The structures were generally those to be expected, although there could have been unresolved variations sufficient to have influenced properties somewhat.

The examination under the electron microscope did not show preferential precipitation or growth of gamma prime particles. The deformation observed by optical microscopic examination was not due to this cause, and was apparently visible as a result of staining from the etch.

Electron Microscopic Examination of Carbides

Previous discussions went to considerable lengths to show the variation in the solution and reprecipitation of carbides. Typical electron micrographs of carbide structures in specimens which had been tested are shown in Figure 29. Nearly continuous films of carbides were present in the grain boundaries of all materials. Apparently, the carbide films were thinner and more continuous, the less the degree of carbide solution prior to aging. For example, the film in the René 41 alloy (see Fig. 29c) was thin, but very continuous, because the degree of carbide solution was limited as a result of the incomplete solution of the M_6C carbides in the alloy at 1975°F.

Rows of globular carbides not associated with grain boundaries (see Figs. 29a and 29c) are examples of the carbides undissolved at the time of solution treatment, as previously discussed. Figure 29b is an example of complete carbide solution in the low carbon S-alloy heats with Mg since

there are no globular carbides. The rows of globular carbides in the other two electron micrographs are presumably located at the sites of grain boundaries which existed prior to recrystallization.

Inclusions in Magnesium-Treated Heats

There were some small, stringered inclusions in the heats to which magnesium had been added (see Fig. 30). Apparently they were malleable enough to roll out as stringers, probably during hot rolling. They also showed evidence of fragmentation, possibly during the cold reduction. These can also be seen by careful examination of Figures 4 through 7. They were not washed out by either cold or hot water, thus they were presumably not magnesium sulfide. There was no evidence to indicate that they had any role other than being inactive inclusions.

GENERAL DISCUSSION

The addition of magnesium to the sheet nickel-base superalloys investigated did not eliminate or drastically alter their sensitivity to sharp edge notches under creep-rupture conditions at 1000°F. There were some differences between Mg and Mg-free heats, however, which suggested that Mg might have some effect.

Magnesium appears to be harmful to long-time creep-rupture properties at 1000°F in low carbon S-alloy, particularly in smooth specimens. Fractures at the loading pin holes in some of the longer time tests clouded this observation for notched specimens. It might have been slightly beneficial in the high carbon S-alloy tests on notched specimens. Except for one test point, the data for René 41 also suggest that Mg was slightly beneficial in the tests on notched specimens. Magnesium apparently had no effect on long-time rupture strengths of unnotched specimens of high carbon S-alloy or René 41.

In tensile tests, Mg-bearing heats had improved N/S ratios and ductility for low carbon S-alloy. The heats of high carbon S-alloy and René 41 with the highest Mg addition had low N/S ratios. Magnesium may also

have reduced the ductility of René 41. The stress-rupture time curves for notched specimens followed the trends of the tensile tests up to the time they underwent an increase in slope.

Certainly the effects of Mg were much less than the differences between 0.03 and 0.07 per cent carbon in the S-alloy. The compositional differences between S-alloy and René 41, at least at the longer times, also overshadowed magnesium. Sheet thickness may have had more effect.

The implications of the data, assuming effects of magnesium, were discussed in detail as the data were presented. Further discussion would not be appropriate at this point. However, there were certain other results from the investigation which, together with, perhaps undue, speculation, lead to the certain hypothesis of interest.

Mechanism of Rupture

Both smooth and notched specimens first underwent slow intergranular cracking, followed by abrupt transgranular fracture. Prior research at the University for NASA showed that the intergranular cracking almost certainly occurred by creep. Higher stresses were required for rupture in a given time period for smooth than for notched specimens of a given alloy. There is evidence which suggests that the time for initiation of intergranular cracks was a major factor in the rupture time. Presumably, the stress concentration of the notch reduced this time for a given net section stress as compared to the smooth specimens.

However, it is not possible to ignore the certainty that variations in the amount of stress increase by cracking required to induce abrupt transgranular fracture, could be a considerable factor in the rupture time. Thus, the phenomena studied differs from the extensive studies reported in the literature for creep-rupture at higher temperatures, where the fractures have been almost entirely by intergranular creep cracking. This suggests that the fracture toughness of the matrix grains could be important in the notch sensitivity, of even the unnotched rupture properties at 1000°F. The main difference from

the usual tensile tests for fracture toughness is that the creep crack grows, reducing the cross section, until the fracture toughness is no longer sufficient to prevent abrupt transgranular fracture under the increasing stress at constant load.

Environmental effects cannot be ruled out as contributing to the notch sensitivity. However, the available information indicates that creep is necessary for the initial intergranular cracking, and tends to support creep alone as the major factor.

As the temperature is increased, the creep properties become increasingly predominant. At a sufficiently high temperature, somewhere above 1200°F for the type of alloys being studied, creep can completely control rupture time. Similarly, at a temperature low enough to suppress creep cracking, only the fracture toughness of the matrix controls failure, and time dependent rupture would disappear.

In the NASA work, it has been shown that at 1000°F on thin sheet, the rupture time is not particularly sensitive to the stress concentration factor of the notch. Presumably, this is due to creep providing a very sharp crack. The sharpness of the original notch is only important in so far as it controls the nucleation of the creep cracks and this is apparently not very sensitive to notch sharpness.

Reduction of Carbide Solution Temperatures by Magnesium

The microstructures showed that the addition of enough Mg to result in residual percentages of from 0.02 to about 0.06 lowered the carbide solution temperatures of the S-alloys about 60°F. The carbide solution temperature increased again with 0.075 per cent Mg in the high carbon S-alloy. Data were obtained which indicate that the magnesium suppressed the formation of Cr_{23}C_6 and promoted the formation of Cr_7C_3 . There were also data indicating that increasing the temperature of heat treatment promoted Cr_7C_3 formation.

An explanation of the decrease in carbide solution temperature was not obtained; it was hypothesized, however, that the equilibrium and/or kinetic phase relationships were changed by magnesium. It was suggested that a possible mechanism was a change in the thermodynamic activities of the components by small amounts of magnesium. It was also pointed out that the Mg probably reduced the oxygen content to very low levels, and this effect might be involved. Other factors, such as interaction with the potent boron+ zirconium addition, cannot be ruled out.

The smallest Mg addition resulted in as much reduction of the solution temperatures for carbides, as the intermediate additions did. Smaller additions of Mg could, therefore, be effective. This raises the question as to whether or not such small amounts of magnesium, as might be derived from reaction with magnesium refractories during melting or as used in "deoxidation", could influence carbide reactions.

A marked influence of carbides on properties is apparently a generally accepted problem in the engineering use of the alloys. Therefore, there is a possibility that Mg could be important in engineering practice by altering carbide reactions, particularly when such factors as heat, casting, and part size, conditions of processing, etc., differ from those used in this investigation and could have far more influence on properties than was evident in the small heats used.

It should also be noted that carbides precipitated in some of the samples of S-alloy during the "solution" heat treatments at 1975°F. This is based on the absence of carbides in a large proportion of the as-received material, the rapid heating to the solution temperature with little or no carbide precipitation, and on the presence of carbides in the grain boundaries after recrystallization.

It was unfortunate that there was no opportunity to determine if magnesium influenced carbide solution in the René 41 alloy, with its predominance of M_6C carbides.

Influence of Degree of Carbide Solution on Tensile and Creep-Rupture Properties

The choice of the 1975°F solution temperature for the S-alloys was based, in part, on the opportunity to vary the degree of carbide solution during the solution treatment. The use of both "low" and "high" carbon S-alloys had a similar effect. The results were discussed in detail in a previous section; they were certainly not conclusive. However, they do give rise to a certain speculative hypotheses of features which should be considered in future studies of the effects of carbide reactions.

In the tensile tests at 1000°F, those heats with presumably the least carbide solution tended to have the lowest N/S ratios in tensile tests. This was most noticeable in the René 41 alloy with its low N/S ratios when compared to the S-alloys. The low carbon S-alloy with no Mg and incomplete carbide solution had a low N/S ratio. The N/S ratios were lower for the high carbon S-alloy than for the low carbon S-alloy, with the highest Mg heat, with predominantly Cr_7C_3 carbides undissolved, being the lowest. The possibility therefore exists that carbides which remain undissolved, or precipitate at the solution temperature, can reduce the short-time, edge-notch sensitivity under tensile test conditions. For this to occur, the undissolved carbides would possibly need to be lined up within the grains at the sites of old grain boundaries because transgranular properties are mainly involved.

With a few exceptions, the data suggest that low matrix strength in materials with undissolved carbides, could have been involved in the results of the rupture tests. The relative amounts of intergranular cracking by creep before abrupt transgranular failure certainly decreased with decreased carbide solution. Apparently, the poor unnotched rupture properties of the low carbon S-alloy with Mg, in the longer time tests, was due to poor creep-rupture properties associated with low carbon content and complete carbide solution.

At the risk of further undue speculation, it is presumed that the amount of carbide in solution at the solution temperature, in itself had a pronounced effect on properties. However, it is not clear from this investigation

what this might be. Presumably, the characteristics of the carbide films in the grain boundaries influence creep cracking, and this can vary with the degree of carbide solution (and, presumably, carbon content). The carbon may also enter in the gamma prime, altering its effect.

The data showed that creep resistance (as measured by minimum creep rates) and rupture strengths of smooth specimens increased with carbon content. The only exception was the high strength of the Mg-free, low carbon S-alloy, which had a considerable proportion of undissolved carbides. The trend of the data, therefore, was towards increased rupture strength (and ductility) with undissolved carbides. René 41, with the least carbide solution, was the strongest and most ductile at a carbon level similar to the high carbon S-alloy. Presumably, the possibility exists that even though there were more undissolved carbides in high carbon S-alloy and René 41 than there were in low carbon S-alloy, there could have been more carbon in solution due to the higher carbon content. The high creep-rupture strength of the Mg-free, low carbon S-alloy heat and the René 41 seems to preclude this as an explanation. However, it is admitted that other compositional differences in the René 41 alloy could have been more influential than the carbon content.

Perhaps the joint effect of creep-rupture properties and transgranular properties upsets the commonly accepted roles and effects of carbides, as developed from high temperature studies of creep-rupture. In any event, there seems to be a general acceptance of the important effects of carbides. Consequently, any effects of magnesium on carbide solution could be important.

In this case, there is also another difference from most research on nickel-base superalloy, creep-rupture properties. The research was carried out on cold-worked material which recrystallized during the solution treatments. Most research on these alloys has been done on hot-worked (or cast) materials where recrystallization, if it occurred at all, would be far less pronounced.

Other Factors

The grain size decreased from low carbon S-alloy, to high carbon S-alloy, to René 41. Presumably, this was due to the increasing amounts of undissolved carbides. A definitive study was not made for the cause of this grain size effect, however. Apparently, the degree of carbide solution in the low carbon S-alloy without magnesium (Heat 1) was sufficient so that the remaining undissolved carbides were inadequate to prevent grain growth. This assumes that recrystallization occurred during heating to the solution temperature, and that the grain size was controlled by the subsequent grain growth at the solution temperature. The one-half hour solution treatment for René 41, compared to one hour for the S-alloy specimens, may also have contributed to its finer grain size.

It was noted that the intermediate Mg heats of high carbon S-alloy (Heats 4 and 6), with the lowest carbide solution temperatures for this alloy, also had somewhat larger grain sizes than the Mg-free and high Mg materials (Heats 2 and 8, respectively), with more undissolved carbides.

The role of grain size in relation to properties is not known. However, it presumably contributed to the comparatively high ductility of the other two materials in comparison to low carbon S-alloy in rupture tests. This would be especially true for René 41. If the amount of carbides and their morphology in grain boundaries are important to the creep cracking or the transgranular crack sensitivity, the interrelationships of amount of carbide in grain boundaries, the degree of carbide solution, and so forth, as previously discussed, would make grain size influential.

The fractures at the loading pin holes in the shoulders of the longer time tests on some of the low carbon S-alloy specimens, raises questions as to the generality of the results. Possibly the controlling factor or factors are temperature and time dependent. In the case of low carbon S-alloy, the failures occurred at lower stress concentrations, at the lower temperature of the pin holes, at the longer time periods, than at the higher stress concentrations of the notches at 1000°F. Research for NASA had indicated that

the notch sensitivity in the rupture tests could be surprisingly insensitive to the degree of stress concentration of the notch. It is not known whether the controlling factors are the creep-cracking initiation and/or growth, or the relationships of these to the fracture toughness. It could be that both vary with temperature and time.

One of the reasons for undertaking this investigation was Schultz's finding that Mg improved creep-rupture elongation and reduction of area at 1200°F in S-alloy round specimens. There was no corresponding improvement at 1500°F. Therefore, the possibility existed that magnesium might be beneficial at still lower temperatures than 1200°F, and thus might reduce notch sensitivity. Any improvement in ductility at 1000°F was limited to the shorter time tests. This, together with the notch sensitivity of the far more ductile René 41 with or without Mg, indicates that the longer time, creep-rupture ductility was not a major factor in the development of the notch sensitivity. It is possible that it was of some significance in shorter time tests. In fairness, it should be pointed out that Schultz's data were obtained at a higher temperature and on round specimens, which had not been cold worked prior to heat treatment. Any of these factors could have been more important than the ductility in controlling 1000°F properties of the sheet. It is worthy of note that the maximum ductility found by Schultz at 1200°F corresponded in Mg contents with the intermediate amounts found to give minimum carbide solution temperatures in this investigation. This seems to be more than a coincidence, and suggests that the observed effects were due to magnesium.

Schultz's research had indicated that other elements are rather effective in reducing deleterious effects of sulfur in the alloys studied. Consequently, it was not anticipated that this well known effectiveness of Mg in counteracting sulfur in other alloys would be involved in this investigation. In addition, the sulfur content of the alloys was very low. It would, perhaps, have been useful to have included some study of the effect of the magnesium at higher sulfur contents.

There did not appear to be any relationship between properties and the new inclusion which formed when Mg was added. The inclusions were

discontinuous and not associated with grain boundaries. They might have a noticeable effect at test conditions other than those used in this investigation.

CONCLUSIONS

Magnesium did not eliminate the sensitivity of thin sheet, nickel-base superalloys to edge notches in creep-rupture tests at 1000°F. There may have been a slight tendency for better long-time notched strengths. Low carbon S-alloy (0.03 per cent carbon) with Mg added had poorer smooth specimen, creep-rupture properties than the Mg-free alloy. Magnesium-bearing heats of low carbon S-alloy had somewhat higher N/S ratios and ductility in tensile tests at 1000°F. The heats of high carbon S-alloy (0.07 per cent carbon) and René 41 with the highest Mg content, also had somewhat low N/S ratios in tensile tests. All of the Mg-bearing heats of René 41 had slightly low ductility in tensile tests. However, it is by no means certain that the observed differences were due to magnesium rather than to other unidentified heat-to-heat differences. The residual Mg contents of the heats of each of the three alloys were approximately 0.02, 0.04 and 0.05 to 0.075 per cent.

A decrease of about 60°F in carbide solution temperatures was observed in S-alloy heats with up to 0.06 per cent magnesium. The magnesium-bearing heats also had increased ratios of Cr_7C_3 to $Cr_{23}C_6$ for "solution treatments" below the carbide solution temperature. If this effect of Mg on carbide solution temperatures and types of carbides should prove to be a general one, it could be important in engineering applications, where carbide morphology often has important effects on mechanical properties. The effect of Mg, if any, on carbide solubility in René 41, with its predominantly M_6C carbide, was not determined.

The highest magnesium additions induced susceptibility to edge cracking during initial ingot hot working. Too much magnesium can be damaging at this stage. The data were inadequate to show if magnesium affected hot or cold workability during subsequent working, or even if it might have been beneficial or harmful in smaller amounts.

As previously determined in the NASA research, the mechanism of rupture involved the development of intergranular creep cracks followed by abrupt transgranular fracture. This subject is discussed at some length in this report.

Part of the experimental work was designed to see if varying degrees of carbide solution (as controlled by carbon and magnesium contents) had significant effects on creep-rupture properties of S-alloy. Carbon content seemed, in general, to be more important than the degree of solution. The properties were, however, better at the higher carbon level with the accompanying larger amounts of undissolved carbides. The data did suggest that undissolved carbides may have promoted transgranular fracture; that is, they may have reduced the "fracture toughness" at 1000°F of the type existing in the alloys studied. This included René 41. Although not well established, the results also suggested that undissolved carbides were in some way associated with higher creep-rupture properties.

Admittedly, there are many limitations to the results. Comparisons with other research on creep-rupture notch sensitivity should recognize that cold-worked and recrystallized material was studied, in contrast to the usual use of hot-worked or cast materials, as well as studying creep-rupture at higher temperatures. Also, the sensitivity to notches and the factors affecting it may vary with temperature and time, so that this investigation, using 1000°F, may not have given general results. The suggestion that Mg (even in amounts considerably less than the smallest studied) could have pronounced effects on carbides seems to be important enough to warrant further consideration. The same could be true for the data on N/S ratios at both long and short times, even though the effects seemed small in this investigation. In addition, considerable useful information can be derived from other aspects of the test results outside of the effects related to Mg. However, most important is the recognition that Mg could be influential in other areas, such as producability and fabricability factors involving costs, even though they did not have large effects in the notch problem.

REFERENCES

1. Schultz, J. W., and Freeman, J. W., "The Influence of Magnesium on the Creep-Rupture Properties of a Ni-Cr-Ti-Al Alloy," University of Michigan Report 02947-6-P, April 1965.
2. Cullen, T. M., and Freeman, J. W., "The Mechanical Properties at 800°, 1000° and 1200°F of Two Superalloys Under Consideration for Use in the Supersonic Transport," NASA CR-92, September, 1964.
3. Cullen, T. M., and Freeman, J. W., "The Mechanical Properties of Inconel 718 Sheet Alloy at 800°, 1000° and 1200°F," NASA CR-268, July, 1965.
4. Bieber, C. G., and Decker, R. F., "The Melting of Malleable Nickel and Nickel Alloys," Trans. AIME, 221, p 629-636
5. Schultz, J. W., and Freeman, J. W., "The Influence of Sulfur on the Creep-Rupture Properties and Hot Working Characteristics of Several Experimental Nickel Base Alloys," University of Michigan Report 02947-5-F, December, 1964.
6. Fell, E. A., "The Effect of Thermal Treatment on the Constitution of 80-20 Nickel-Chromium Alloys Hardened with Ti and Al," Metallurgia, p 157-166, April, 1961.
7. Beech, J., and Warrington, D. H., "M₇C₃ to M₂₃C₆ Transformation in Chromium Containing Alloys," JISI, p 460-468, May, 1966.
8. Wood, D. R., and Cook, R. M., "Effects of Trace Contents of Impurity Elements on the Creep-Rupture Properties of Nickel-Base Alloys," Metallurgia, p 109-117, March, 1963.

TABLE I
Chemical Compositions of Experimental Heats

Heat No.	Notes	Mg	C	Cr	Co	Mo	Ti	Al(d)	Fe	B	Zr	S	O	N	H
<u>Low Carbon S-Alloy</u>															
Aim			0.05	20.0			3.80	1.20		0.0035	0.045	<0.007			
1 Top	a	<0.01	0.034	20.17	----	----	3.90	1.41	0.2	0.0026	0.044	0.0034	56	8	1.7
1 Bottom	a	<0.01	0.034	20.14	----	----	3.90	1.39	0.1	0.0017	0.040	0.0027	11	11	1.4
3 Top	b,c	0.02	0.027	19.6	----	----	3.68	1.25	---	0.003	0.07	0.0061	7	18	2.4
3 Bottom	b,c	0.02	0.020	19.6	----	----	3.68	1.29	---	0.002	0.08	0.0052	<5	17	1.8
5 Top	b,c	0.03	0.023	19.5	----	----	3.70	1.26	---	0.003	0.09	0.0066	<5	5	1.3
5 Bottom	b,c	0.03	0.029	20.0	----	----	3.70	1.29	---	0.003	0.10	0.0040	<5	11	1.1
7 Top	b,c	0.06	0.037	19.5	----	----	3.70	1.25	---	0.004	0.08	0.002	11	25	1.8
7 Bottom	b,c	0.06	0.037	19.4	----	----	3.62	1.29	---	0.004	0.07	0.002	<5	22	2.7
<u>High Carbon S-Alloy</u>															
Aim			0.10	20.0			3.8	1.20		0.0035	0.045	<0.007			
2 Top	b,c	<0.01	0.067	19.4	----	----	3.90	1.35	---	0.003	0.08	0.011	22	10	2.5
2 Bottom	b,c	<0.01	0.069	19.9	----	----	3.90	1.40	---	0.003	0.08	0.0052	27	7	2.9
4 Top	b,c	0.02	0.057	19.3	----	----	3.72	1.28	---	0.004	0.08	0.0068	<5	6	1.3
4 Bottom	b,c	0.02	0.051	19.3	----	----	3.72	1.32	---	0.003	0.07	0.0055	<5	5	1.3
6 Top	b,c	0.04	0.075	19.7	----	----	3.82	1.32	---	0.003	0.08	0.0046	<5	13	1.9
6 Bottom	b,c	0.04	0.072	19.6	----	----	3.82	1.36	---	0.003	0.08	0.0048	<5	16	2.2
8 Top	b,c	0.07	0.080	19.4	----	----	3.72	1.25	---	0.003	0.08	0.0026	5	15	2.0
8 Bottom	b,c	0.08	0.080	19.0	----	----	3.72	1.28	---	0.003	0.08	0.0026	<5	16	1.6
<u>René 41</u>															
Aim			0.10	19.0	11.0	10.0	3.0 ^(e)	1.5	2.5	0.0035	0.045	<0.007			
9 Top	b	<0.01	0.090	18.1	10.4	10.5	2.45	1.53	2.44	0.002	0.05	0.0028	12	<5	2.1
9 Bottom	b	<0.01	0.086	18.0	10.4	10.8	2.45	1.55	2.40	0.003	0.05	0.0030	5	19	2.8
10 Top	b	0.03	0.093	18.5	10.6	11.3	2.55	1.60	2.38	0.003	0.05	0.0052	12	<5	1.9
10 Bottom	b	0.03	0.093	18.5	10.7	11.0	2.50	1.66	2.39	0.004	0.05	0.0036	<5	13	2.8
11 Top	b	0.04	0.13	18.4	10.5	11.1	2.38	1.53	2.40	0.003	0.05	0.0063	<5	6	0.9
11 Bottom	b	0.04	0.13	18.4	10.5	11.0	2.38	1.57	2.34	0.003	0.04	0.002	<5	12	1.8
12 Top	b	0.05	0.13	18.2	10.5	10.8	2.42	1.48	2.39	0.003	0.05	0.0034	6	15	1.8
12 Bottom	b	0.05	0.13	18.0	10.4	10.5	2.42	1.55	2.37	0.003	0.05	0.0027	<5	20	1.4

(a) 0.004 Cu, 0.02 Mn, 0.01 Si; Ag, Zn, Sn, Ca, Be, Bi, As, Pb, Sb, Hg, Co not detected.
 (b) Ag, As, Bi, Cd, Pb, Sn, Zn not detected.
 (c) Zr analyses too high because 0.045% Zr was added in all cases.
 (d) All aluminum analyses of S-Alloy appear to be slightly higher than the actual aluminum content.
 (e) Good high temperature properties, combined with the lack of a likely means for losing Ti from René 41, suggests that these analyses are low.
 Note: Samples for chemical analyses taken from each end of the hot pressed, 1 3/8" wide, 1" thick slab from each ingot.

TABLE II

Magnesium Analysis of Ingot and Sheet Material
of Representative Heats

<u>Alloy</u>	<u>Heat No.</u>	<u>Original Mg Analysis of Ingots, %</u>	<u>Mg Analysis of Sheet, %</u>	<u>Condition of Sheet Specimen</u>
Low Carbon S-Alloy	3	0.02	0.01	Solution treated and aged
	7	0.06	0.04	Solution treated and aged
High Carbon S-Alloy	2	0.02	0.01	As cold worked
	8	0.075	0.06	As cold worked
René 41	9	0.03	0.02	As cold worked
	12	0.05	0.06	As cold worked

TABLE III

Reference Carbide Diffraction Patterns from ASTM Card File

TiC		Cr_{23}C_6		Cr_7C_3	
Card No. 6-0614		Card No. 9-122		Card No. 11-550	
<u>d</u>	<u>I</u>	<u>d</u>	<u>I</u>	<u>d</u>	<u>I</u>
* 2.580	80	3.21	25	2.68	20
* 2.179	100	3.07	25	2.35	20
* 1.535	50	2.66	50	* 2.28	70
1.311	30	2.44	25	2.22	50
1.255	10	* 2.38	100	2.14	50
1.086	5	2.17	100	* 2.12	70
0.997	5	2.05	100	2.04	100
0.971	30	* 1.88	75	2.02	50
0.884	30	1.80	100	1.96	70
0.833	30	* 1.77	50	1.90	50
		1.68	25	1.84	60
		1.62	25	1.81	70
		* 1.60	50	1.78	50
		1.49	25	* 1.75	70
		1.48	25	1.71	60
		1.38	25	1.62	60
		1.34	25	1.51	50
		1.33	50	1.44	70
		1.29	75+25	* 1.35	80
		1.25	125+75	1.33	50
		1.23	100	1.32	30
		1.22	25	1.29	30
		1.19	75	1.28	60
		1.17	75	1.27	30
				1.26	70
				1.24	20
				1.227	60
				1.215	60
				1.21	80
				1.194	50
				1.188	100
				1.174	70
				1.170	100

* These lines were used to estimate the relative amounts of the individual carbides in accordance with Appendix A.

TABLE V

X-Ray Diffraction Patterns for High Carbon S-Alloy with Low Magnesium Addition

1700°F, W. Q.		1900°F, W. Q.		1975°F, W. Q.		2000°F, W. Q.		1935°F, W. Q. Age 1300°F	
<u>d</u>	<u>I</u>	<u>d</u>	<u>I</u>	<u>d</u>	<u>I</u>	<u>d</u>	<u>I</u>	<u>d</u>	<u>I</u>
						3.65	13		
						2.668	15	2.644	4
2.486	45	2.480	15	2.477	50	2.492	100	2.471	6
						2.408	10		
2.374	15	2.378	10	2.370	10			2.363	18
2.294	15	2.289	10	2.287	25	2.297	12	2.284	8
2.156	50	2.150	25	2.147	60	2.155	80	2.159	18
2.117	35	2.118	25	2.116	60	2.125	14	2.113	8
						2.094	12		
2.042	100	2.043	100	2.040	100	2.045	50	2.04	100
				1.904	3				
1.879	10	1.879	10	1.876	3			1.873	15
1.846	4	1.847	6	1.844	10				
1.813	10	1.813	10	1.811	20	1.815	12		
1.796	12	1.792	12					1.792	13
1.771	8	1.768	6	1.775	3			1.764	10
1.751	6	1.750	8	1.749	16	1.753	10		
						1.672	15		
1.622	4							1.618	6
1.605	4							1.608	8
1.524	35	1.522	15	1.521	35	1.524	50	1.522	8
1.504	12	1.505	8	1.503	17	1.503	12		
						1.478	15		
				1.439	8	1.438	10		
1.352	8	1.355	6	1.351	12				
1.330	8			1.331	6			1.331	8
1.301	15			1.298	20	1.300	30		
<u>Phase</u>	<u>%</u>	<u>%</u>		<u>%</u>		<u>%</u>		<u>%</u>	
Ti(C, N)	35	20		40		65		17	
Cr ₂₃ C ₆	25	25		10				58	
Cr ₇ C ₃	40	55		50		35		25	

TABLE VI
X-Ray Diffraction Patterns for High Carbon S-Alloy with High Magnesium Addition

Phase	1700°F, W. Q.		1900°F, W. Q.		1935°F, W. Q.		1975°F, W. Q.		2000°F, W. Q.		2025°F, W. Q.		2150°F, W. Q.		1975°F, W. Q. Age 1300°F		2025°F, W. Q. Age 1300°F	
	d	I	d	I	d	I	d	I	d	I	d	I	d	I	d	I	d	I
Ti(C, N)	2.485	25	2.476	25	2.486	40	2.493	25	2.494	50	2.483	60	2.486	90	2.483	30	2.476	25
	2.290	25	2.283	30	2.287	40	2.293	35	2.296	30	2.289	25			2.290	40	2.282	20
	2.153	15	2.149	25	2.152	30	2.155	20	2.157	40	2.153	60	2.154	100	2.158	35	2.146	35
	2.115	30	2.115	30	2.118	40	2.118	30	2.124	40	2.114	25			2.118	40	2.113	35
Cr ₂₃ C ₆	2.041	100	2.041	100	2.043	100	2.045	100	2.047	100	2.042	100			2.046	100	2.038	100
	1.899	6	1.899	6	1.900	4			1.903	4							1.893	4
	1.846	4	1.844	18	1.842	10	1.845	15	1.849	10	1.845	6			1.846	8	1.842	10
	1.811	15	1.803	6	1.812	30	1.814	22	1.817	30	1.813	20			1.814	20	1.808	15
Cr ₇ C ₃	1.750	15	1.748	18	1.749	20	1.751	22	1.755	15	1.750	10			1.755	18	1.747	14
									1.674	4								
									1.615	4								
	1.520	18	1.523	25	1.523	20	1.525	25	1.526	30	1.523	30	1.525	60	1.526	15	1.522	30
1.444	6	1.440	12	1.441	6	1.437	10	1.439	12							1.438	10	
1.349	8	1.350	15	1.350	10	1.351	12	1.352	12	1.350	8			1.353	12	1.349	12	
1.301	10	1.301	18	1.300	12	1.298	15	1.303	15	1.298	20	1.300	35			1.326	6	
																	1.300	14
	%		%		%		%		%		%		%		%		%	%
	14		20		25		17		28		37		100		25		25	25
	86		80		75		83		72		63				15		15	15
															60		60	60

TABLE VII

Tensile Test Results - 1000°F

Heat No.	% Mg	% C	Notch TS, psi	Smooth TS, psi	N/S Notch Ratio	YS, psi	$\frac{YS}{TS} \times 100$	Elong.	R.A.
1	<0.01	0.034	127,000	160,000	0.79	127,200	79	11.0	21.2
Low Carbon S-Alloy 3	0.02	0.024	141,000	155,000	0.92	116,200	75	27.5	32.5
5	0.03	0.026	142,000	155,000	0.92	116,000	75	25.0	31.9
7	0.06	0.037	146,000	157,000	0.94	118,600	76	23.5	30.4
2	<0.01	0.068	150,000	177,000	0.86	134,000	76	17.5	27.0
High Carbon S-Alloy 4	0.02	0.054	148,000	169,000	0.87	125,000	74	19.5	30.3
6	0.04	0.074	154,000	177,000	0.86	130,000	73	17.5	17.9
8	0.075	0.080	131,000	168,000	0.78	128,000	76	17.5	26.0
9	<0.01	0.088	137,000	173,000	0.79	123,500	71	32.0	33.1
10	0.03	0.093	138,000	180,000	0.76	131,000	73	22.5	22.7
René 41 11	0.04	0.13	130,000	166,000	0.78	121,500	73	24.0	28.8
12	0.05	0.13	124,000	182,000	0.67	131,600	73	22.0	23.1

TABLE VIII
 Creep-Rupture Properties - 1000°F
 Low Carbon S-Alloy

Heat No.	% Mg	% C	Type of Specimen	Stress, ksi	Min. Creep Rate, %/hr	Rupture Time hr	Elong., %	R. A. %	Remarks		
1	<0.01	0.034	Smooth	153	-----	Loading	---	----	Pinhole		
				140	-----	14.6	3.0	10.8			
				140	3.09×10^{-3}	192.9	3.0	10.5			
				133	8.33×10^{-4}	443.1	1.5	9.3			
			Notch	110		19.2					
				100		151.0					
				70		879.3+					Pinhole
				50		1607.0+					Pinhole
3	0.02	0.024	Smooth	148	-----	Loading	29.5	32.9			
				143	2.77×10^{-2}	25.6	15.5	21.0			
				135	1.00×10^{-2}	55.0	10.5	13.8			
				115	1.29×10^{-3}	298.8	2.0	11.7			
			Notch	125		21.8					
				100		106.5					
				70		473.1					
				50		1346.2					
5	0.03	0.026	Smooth	148	1.98×10^{-2}	23.4	17.0	17.4			
				130	9.55×10^{-3}	44.5	8.5	17.3			
				140	1.04×10^{-2}	50.7	11.5	14.8			
				115	1.43×10^{-4}	423.0	1.5	11.9			
			Notch	126		47.5					
				100		112.4					
				70		193.3					
				50		2927.6+					Pinhole
7	0.06	0.037	Smooth	149	2.00×10^{-2}	38.9	13.0	17.4			
				137	5.90×10^{-3}	125.7	7.0	15.4			
				130	2.68×10^{-3}	170.6	7.5	16.2			
				110	9.23×10^{-5}	623.8	1.5	9.7			
			Notch	130		24.1					
				120		59.7					
				90		248.0					
				60		3977.4					

"Pinhole" = Fractured through loading pinhole rather than notch in gage section.

TABLE IX
Creep-Rupture Properties - 1000°F
High Carbon S-Alloy

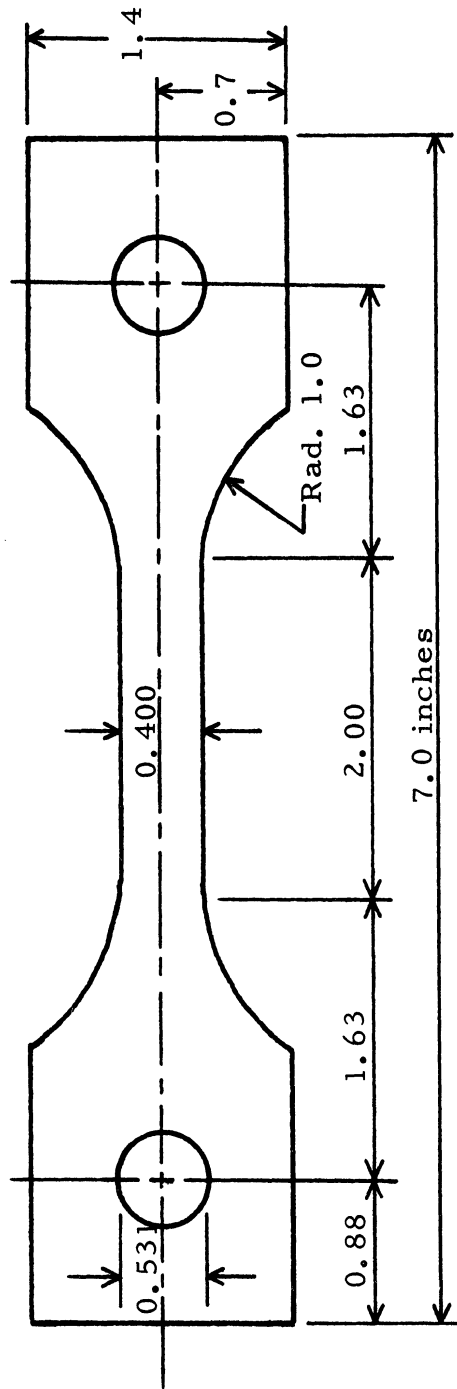
Heat No.	% Mg	% C	Type of Specimen	Stress, ksi	Min. Creep Rate, %/hr	Rupture Time, hr	Elong., %	R. A., %		
2	<0.01	0.068	Smooth	169	1.17×10^{-1}	13.2	13.0	17.6		
				157	2.94×10^{-2}	56.5	6.5	12.5		
				147	3.96×10^{-3}	254.1	3.5	10.7		
				137	1.71×10^{-3}	640.2	2.0	8.3		
			Notch	135		Loading				
				100		53.5				
				70		1165.1				
				80		5880 I. P.				
4	0.02	0.054	Smooth	162	7.92×10^{-2}	19.1	15.0	17.4		
				157		20.3	16.0	17.5		
				151	1.33×10^{-2}	100.2	8.0	13.9		
				144	4.65×10^{-3}	248.1	4.5	12.6		
			Notch	130		69.3				
				100		217.7				
				70		1563.9				
				80		5880 I. P.				
6	0.04	0.074	Smooth	165	4.92×10^{-2}	44.2	11.0	26.5		
				157		86.6	6.5	13.6		
				145	2.61×10^{-3}	288.5	2.5	16.9		
				135	1.22×10^{-3}	572.7	3.0	6.3		
			Notch	135		8.3				
				100		394.1				
				70		1952.2				
				80		5880 I. P.				
8	0.075	0.080	Smooth	160	8.33×10^{-2}	18.2	11.5	16.7		
				148	1.17×10^{-2}	92.4	7.0	13.9		
				144	4.65×10^{-3}	140.9	4.5	12.6		
				130	7.14×10^{-4}	1016.7	3.0	8.7		
			Notch	115		11.1				
				100		185.7				
				75		923.1				
				80		5880 I. P.				

I. P. = In Progress July 31, 1967.

TABLE X
Creep-Rupture Properties - 1000°F
Rend 41

Heat No.	% Mg	% C	Type of Specimen	Stress, ksi	Min. Creep Rate, %/hr	Rupture Time, hr	Elong., %	R. A., %
9	<0.01	0.088	Smooth	168	-----	Loading	24.5	29.0
				161	1.72×10^{-2}	67.3	25.0	20.5
				165	1.50×10^{-2}	85.3	19.5	18.3
				157	3.54×10^{-3}	244.2	15.0	16.0
				153	6.95×10^{-4}	646.1	11.5	12.3
			Notch	120		302.5		
				80		3843.3		
10	0.03	0.093	Smooth	170	-----	Loading		
				168		408.4	13.0	17.2
				160	8.39×10^{-4}	658.7	9.5	13.9
			Notch	120		800.7		
				128		905.9		
				80		6264.9		
11	0.04	0.13	Smooth	158	5.88×10^{-3}	102.8	16.5	19.4
				150	6.37×10^{-4}	1519.5	9.0	9.3
			Notch	120		215.0		
				112		375.3		
				80		1659.7		
12	0.05	0.13	Smooth	175	6.67×10^{-2}	15.4	21.5	24.3
				162	2.23×10^{-2}	405.8	12.0	15.9
				150	1.25×10^{-4}	4460 +	(Discontinued)	
			Notch	112		336.1		
				106		510.4		
				80		7392 I. P.		

I. P. = In Progress July 31, 1967.



Thickness approximately 0.040 inch

Figure 1. Smooth Specimen Design.

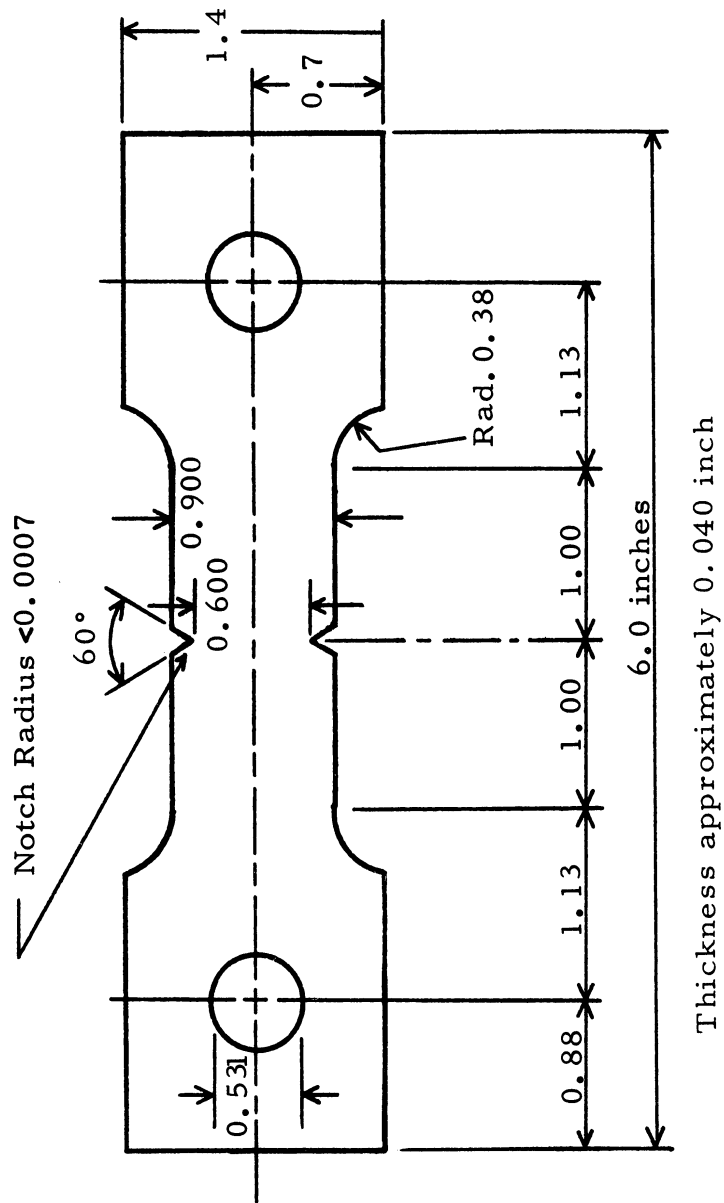


Figure 2. Edge-Notched Specimen Design.

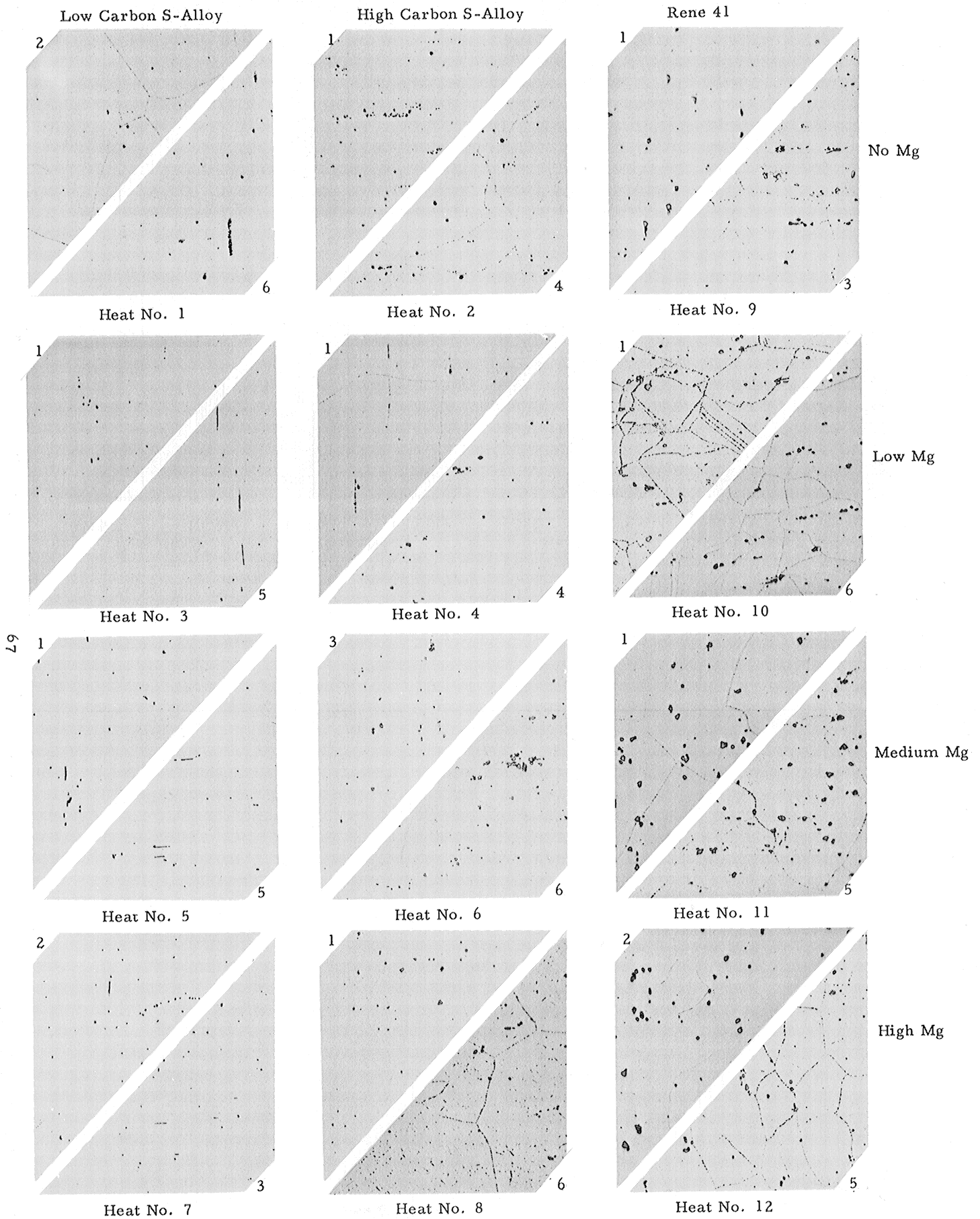
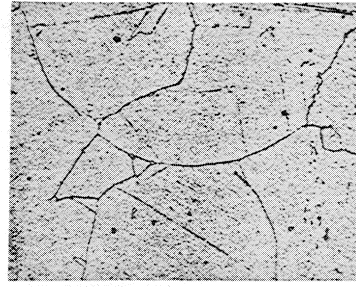


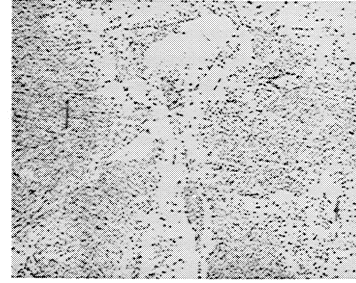
Figure 3. Range of Carbide Precipitation in As-Received Sheet. (Note: the numbers of the pieces used from each of the heats are indicated in the corners). 250X.

Heat No. 1
No Mg
.034%C



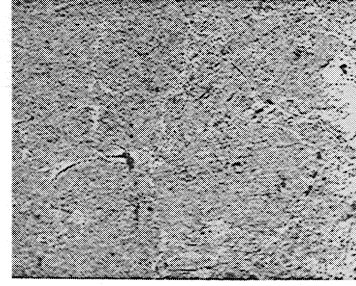
a.

Heat No. 3
.024%C
.02%Mg



b.

Heat No. 5
.026%C
.03%Mg



c.

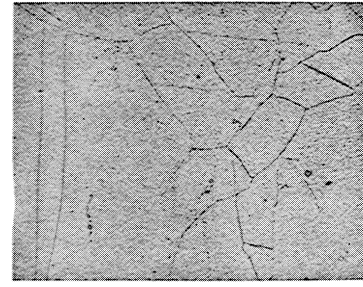
Heat No. 7
.037%C
.06%Mg



d.

1875°F S. T.

1900°F S. T.



e.



f.



g.



h.

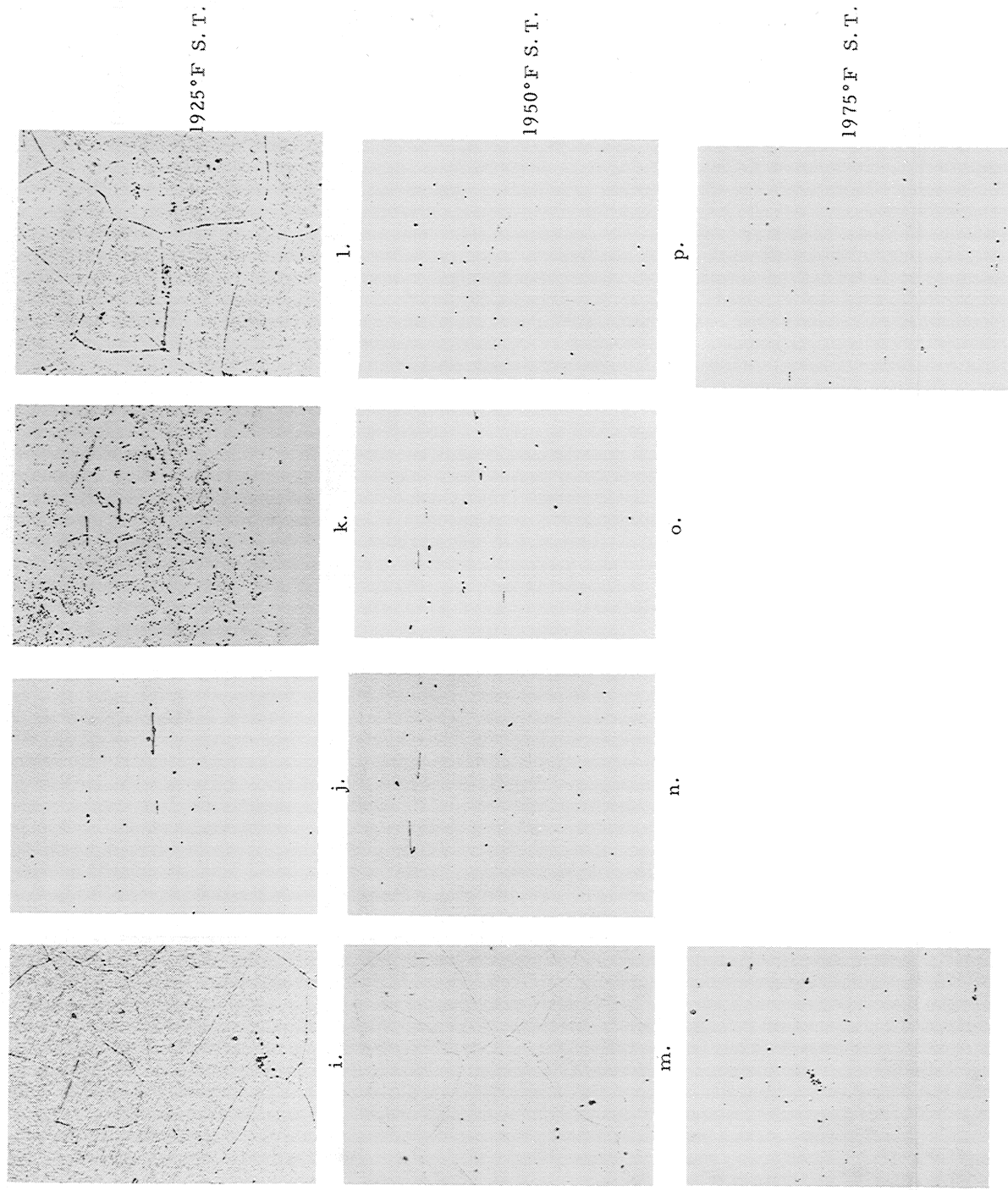


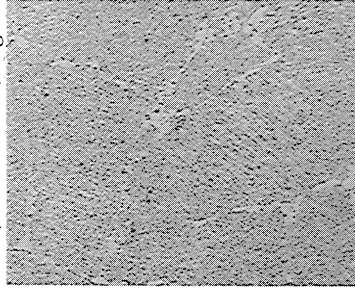
Figure 4. Solution Treated Low Carbon S-Alloy--Two Hours, Water Quench, 250X.

Heat No. 1
.034%C
.No Mg



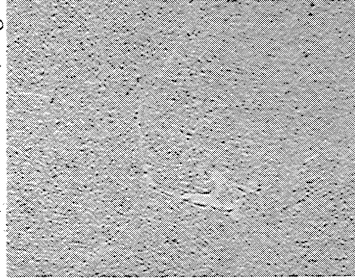
a.

Heat No. 3
.024%C
.02%Mg



b.

Heat No. 5
.026%C
.03%Mg



c.

Heat No. 7
.037%C
.06%Mg



d.

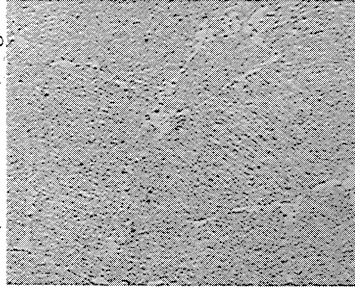
1875°F S. T.

Heat No. 1
.034%C
.No Mg



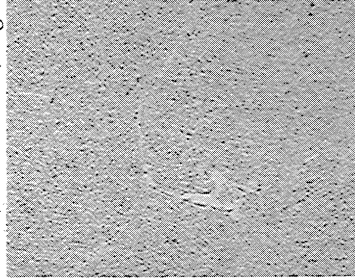
e.

Heat No. 3
.024%C
.02%Mg



f.

Heat No. 5
.026%C
.03%Mg



g.

Heat No. 7
.037%C
.06%Mg

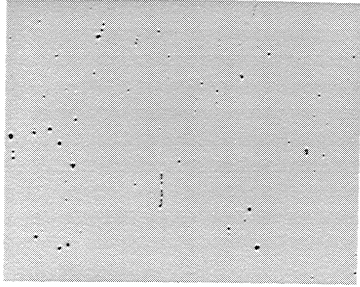


h.

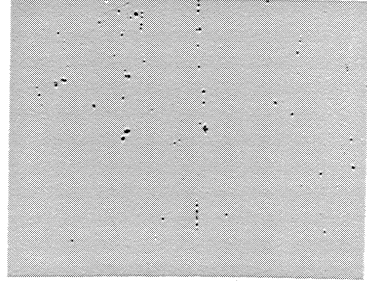
1900°F S. T.



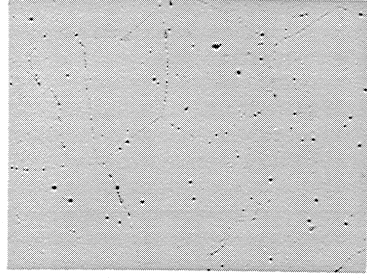
i.



j.

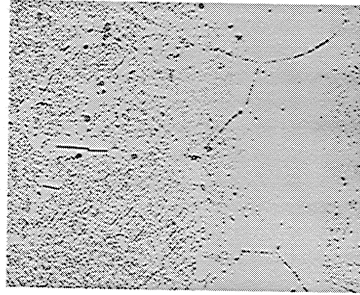


k.

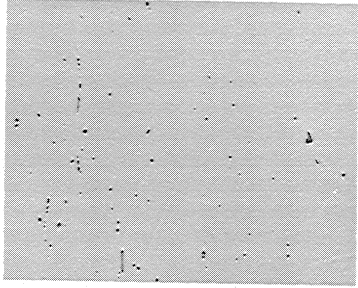


l.

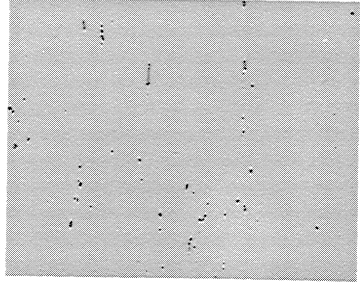
1925° F S. T.



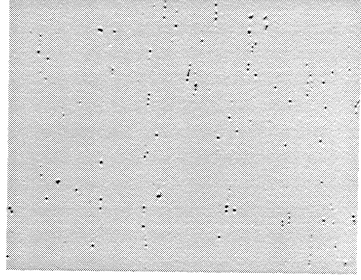
m.



n.

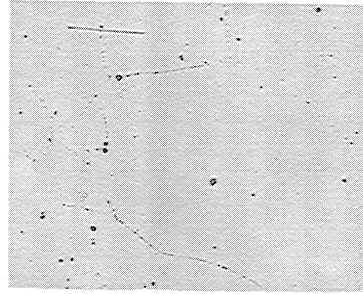


o.

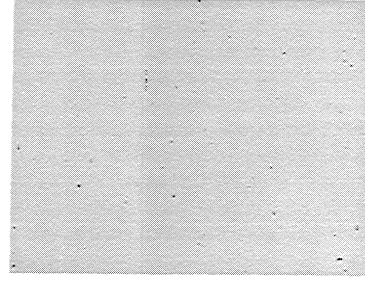


p.

1950° F S. T.



q.



r.

1975° F S. T.

Figure 5. Solution Treated Low Carbon S-Alloy--Ten Hours, Water Quench, 250X.

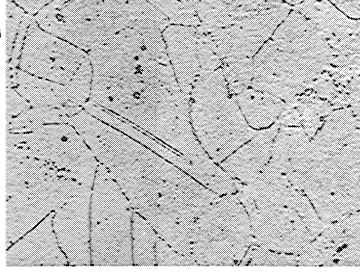
Heat No. 2
No Mg
.068%C



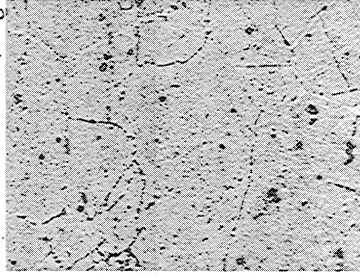
Heat No. 4
.054%C
.02% Mg



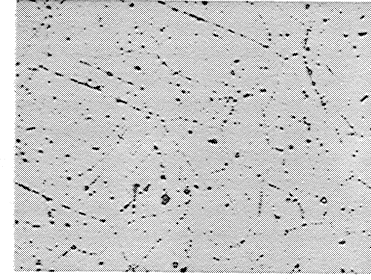
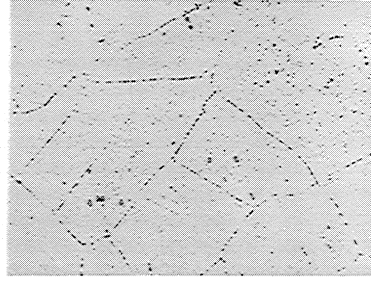
Heat No. 6
.074%C
.04%Mg



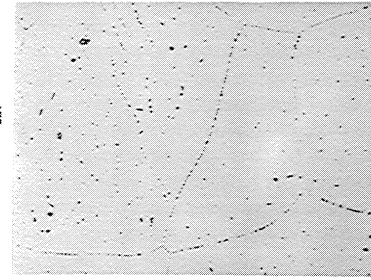
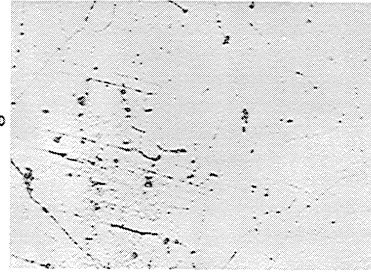
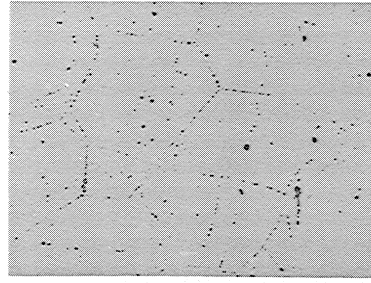
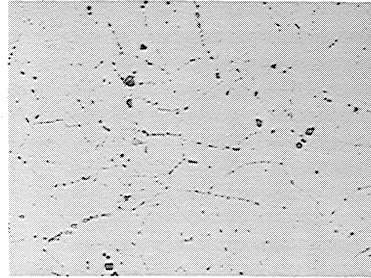
Heat No. 8
.080%C
.075%Mg



1900°F S.T.



1925°F S.T.



1950°F S.T.

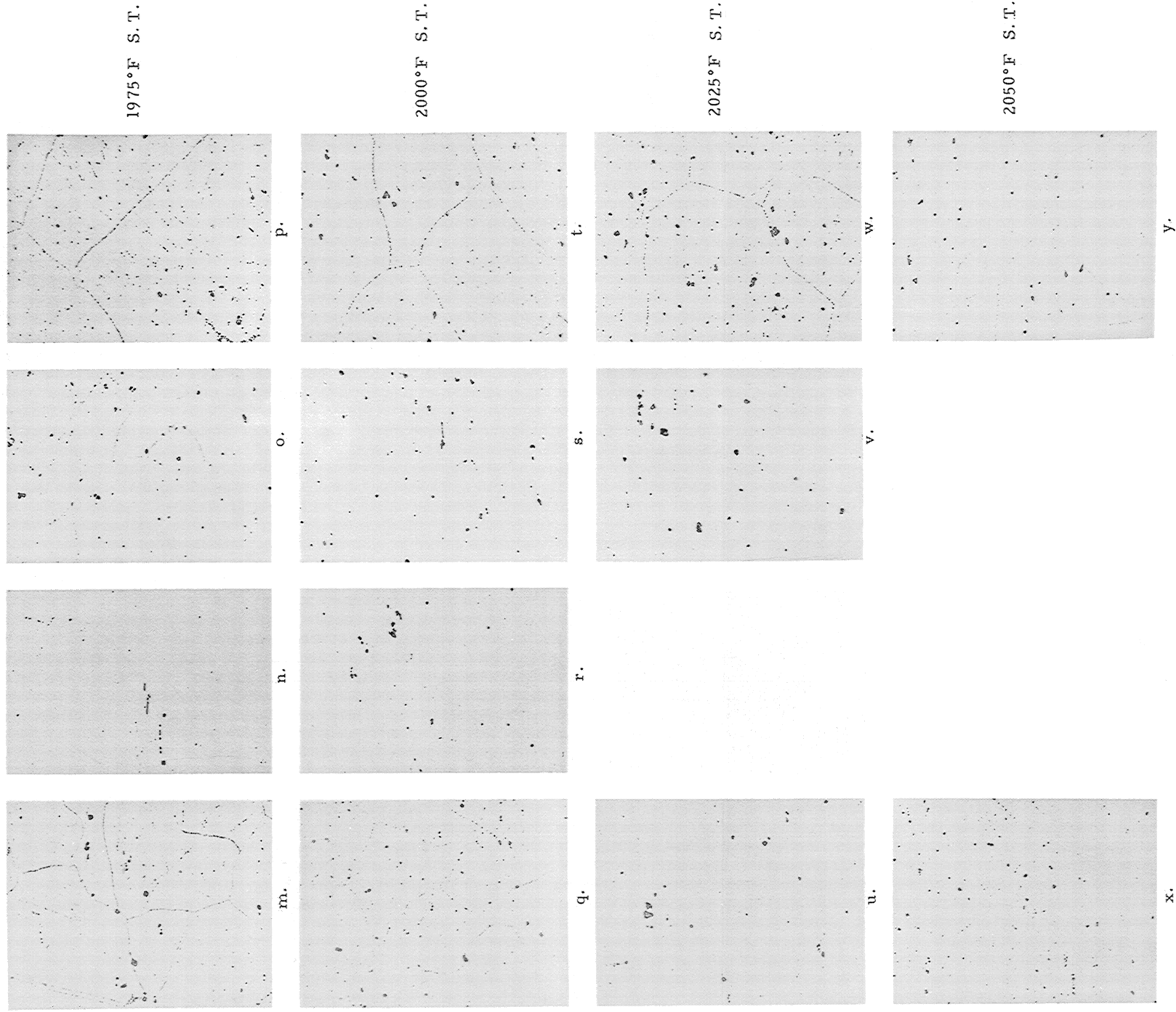
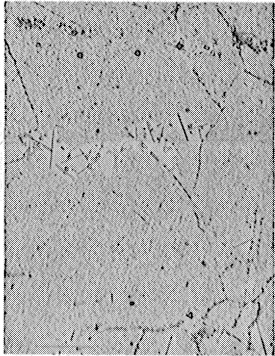


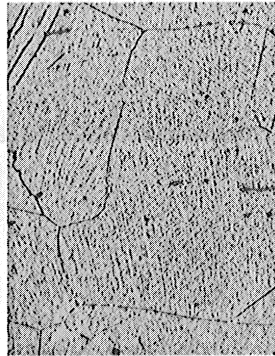
Figure 6. Solution Treated High Carbon S-Alloy--Two Hours, Water Quench, 250X.

Heat No. 2
.068%C No Mg



a.

Heat No. 4
.054%C .02%Mg



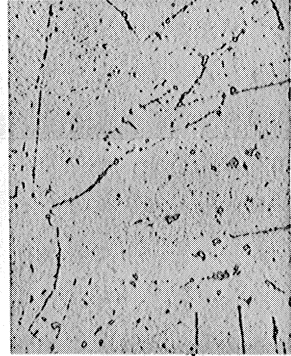
b.

Heat No. 6
.074%C .04%Mg



c.

Heat No. 8
.080%C .075%Mg

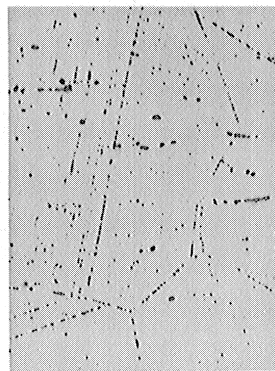


d.

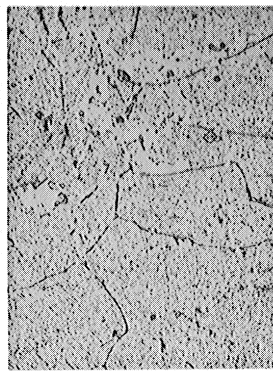
1900°F S. T.



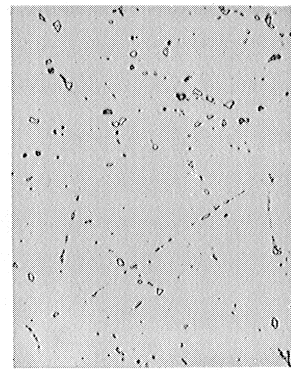
e.



f.

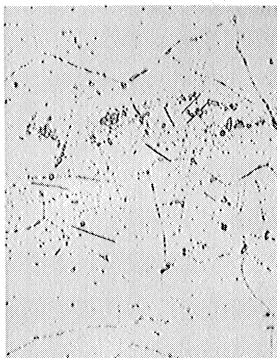


g.

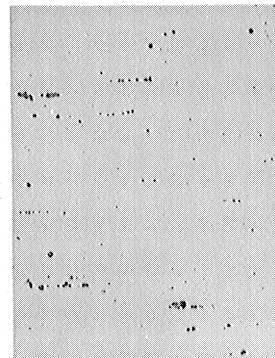


h.

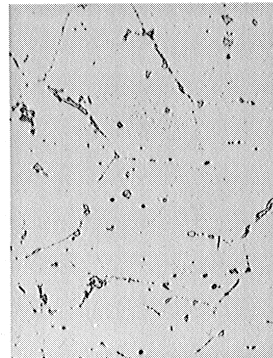
1925°F S. T.



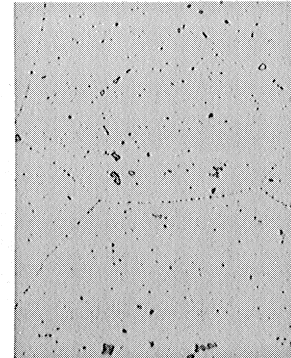
i.



j.



k.



l.

1950°F S. T.

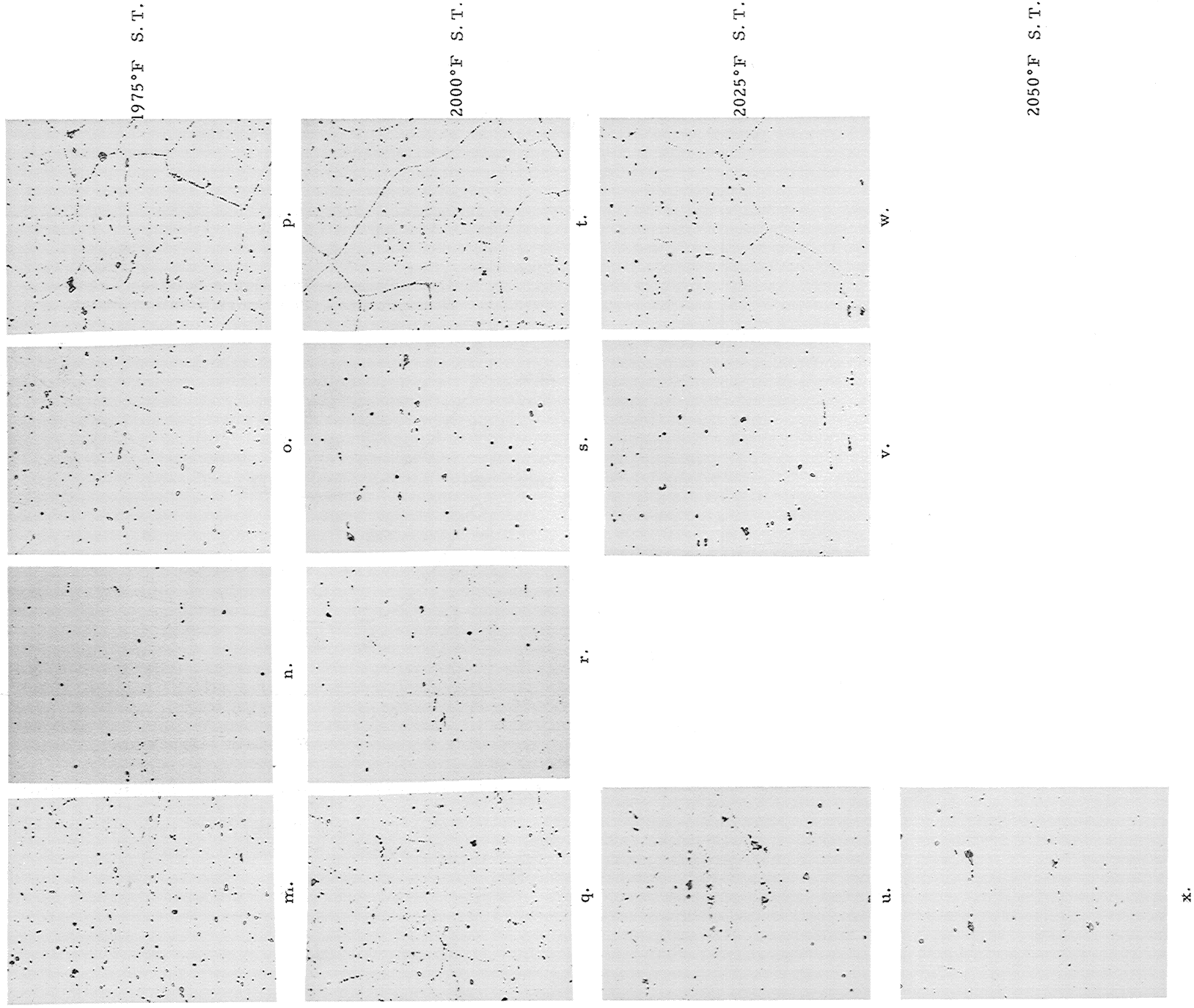


Figure 7. Solution Treated High Carbon S-Alloy--Ten Hours, Water Quench, 250X.

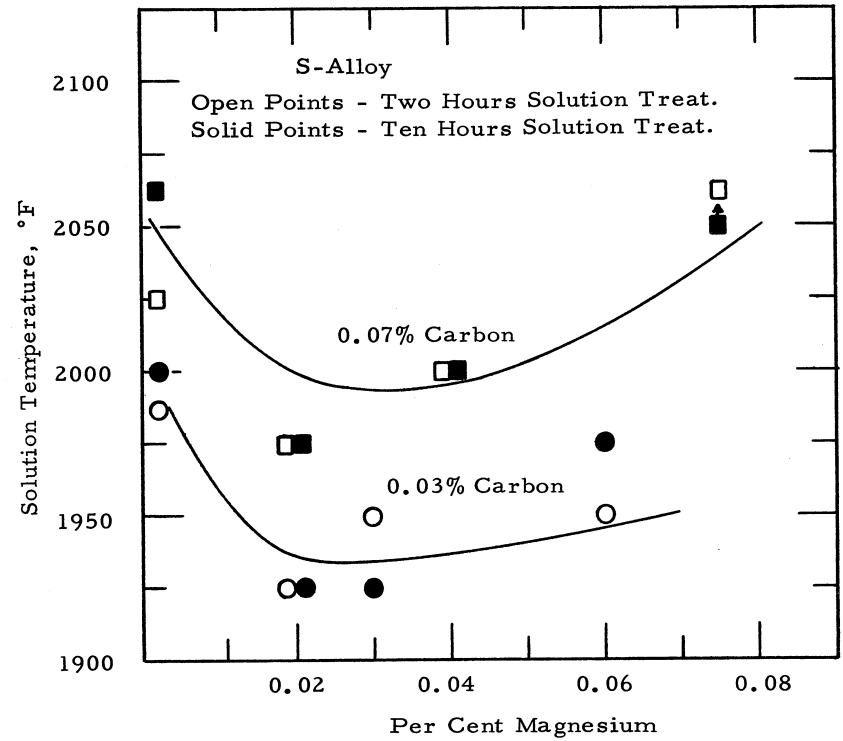


Figure 8. Analyzed Magnesium Content versus Solution Temperature of Intergranular Carbides at Two Levels of Carbon. (Curves are adjusted for variations in carbon content.)

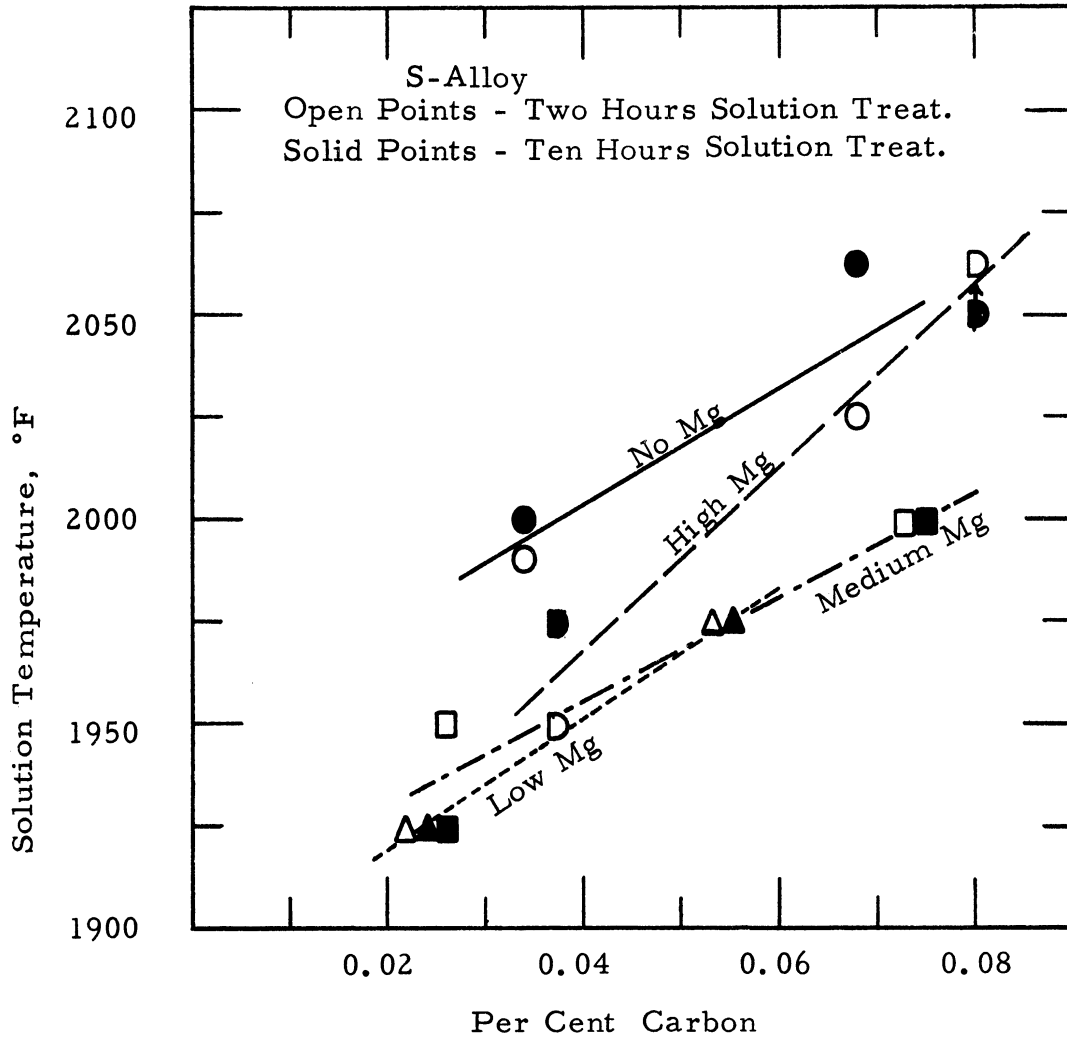


Figure 9. Carbon Content versus Solution Temperature of Intergranular Carbides at Four Levels of Magnesium.

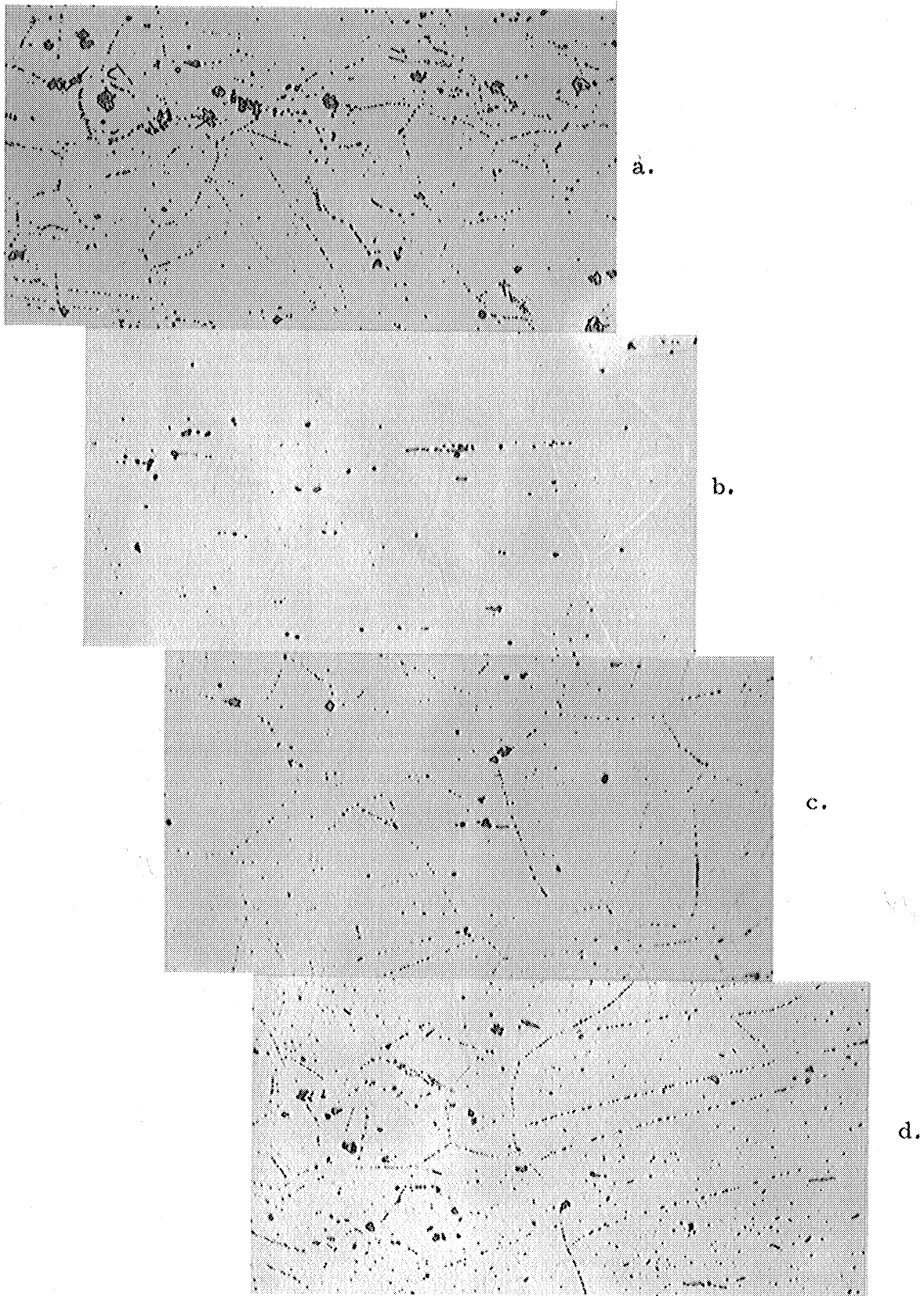


Figure 10. Solution Treated High Carbon S-Alloy with Pre-Heat Treatment, Two Hours 1900°F, Water Quench Plus Two Hours 1975°F, Water Quench, 250X. a) Heat No. 2; b) Heat No. 4; c) Heat No. 6; d) Heat No. 8.

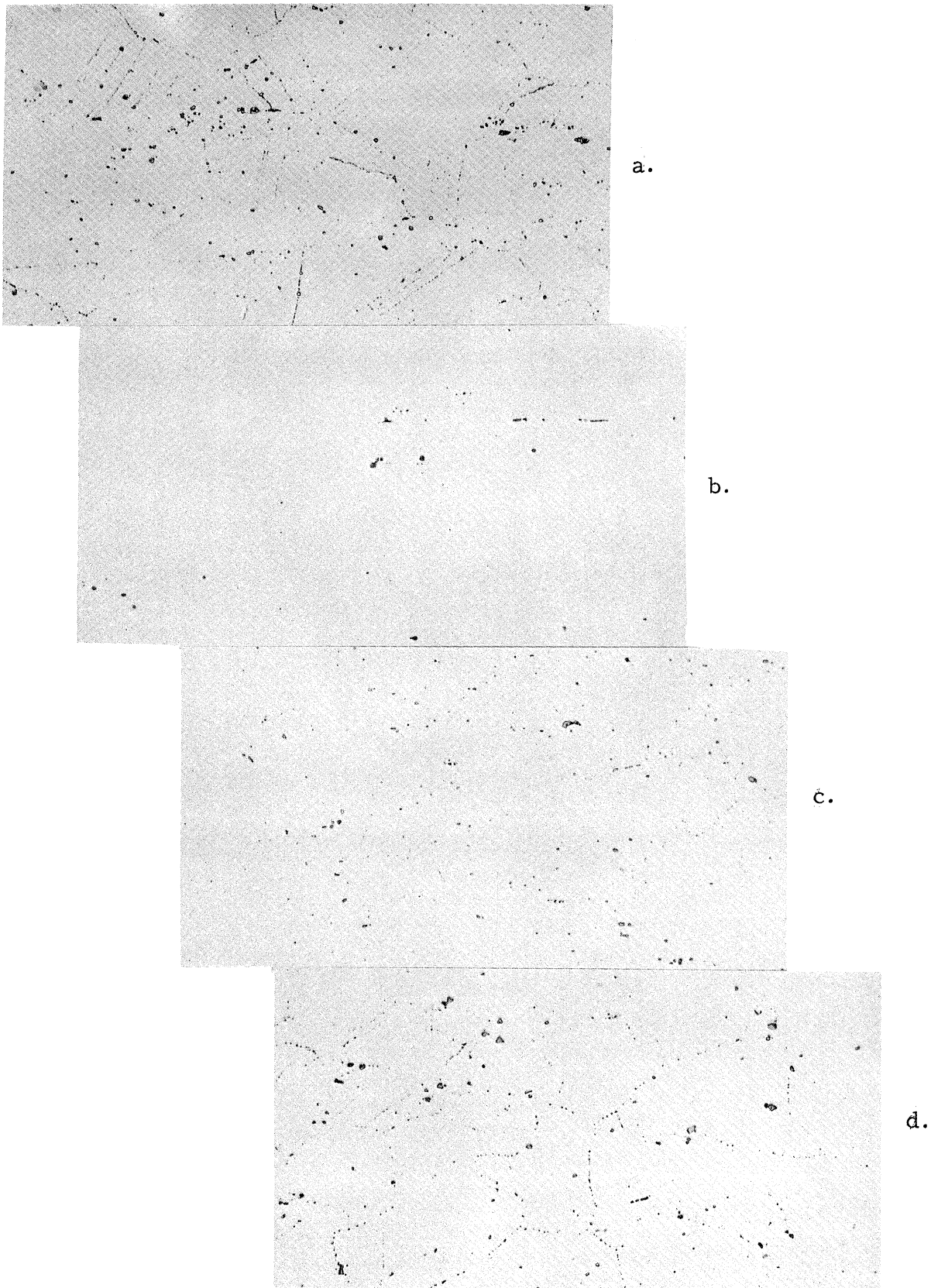
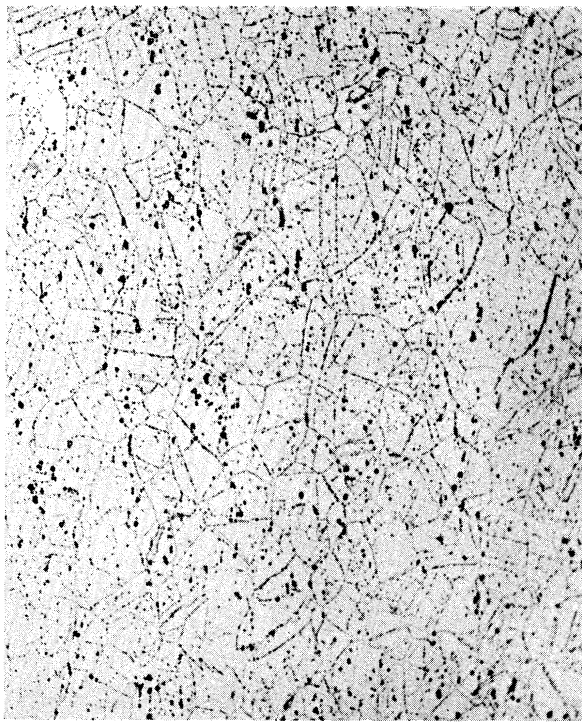
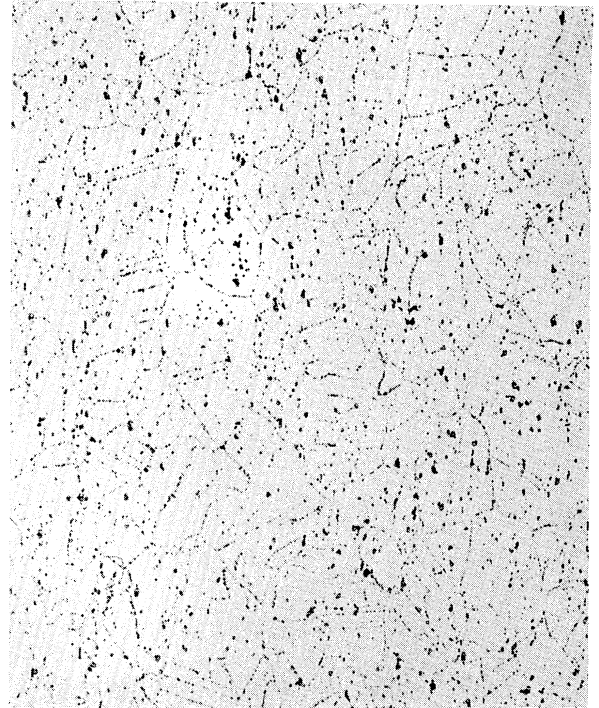


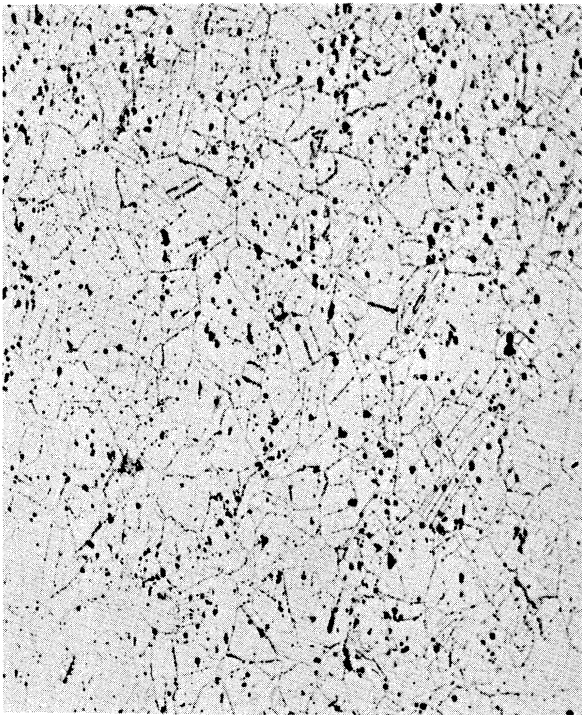
Figure 11. Solution Treated High Carbon S-Alloy Specimens from Top of Ingots - Two Hours, 1975°F, Water Quench, 250X.
a) Heat No. 2; b) Heat No. 4; c) Heat No. 6; d) Heat No. 8.



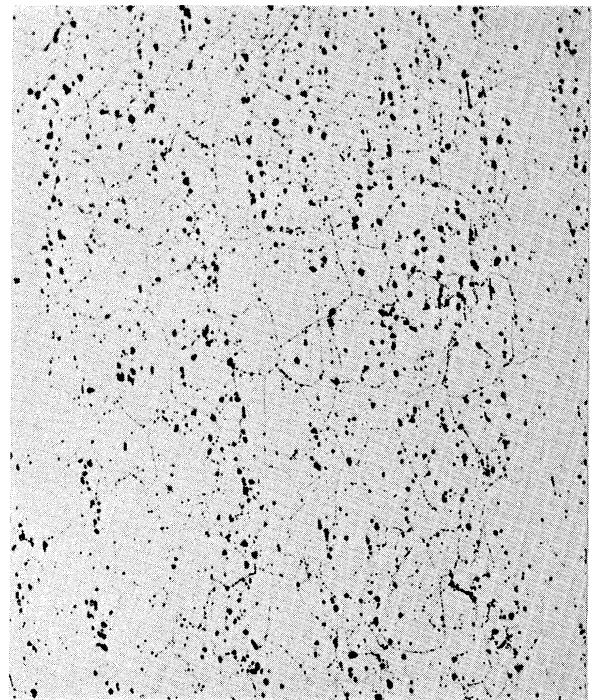
a.



b.



c.



d.

Figure 12. Solution Treated René 41. At Temperature One Hour, Water Quench, 100X. a) Heat No. 10, 1925°F; b) Heat No. 10, 2025°F; c) Heat No. 12, 1925°F; d) Heat No. 12, 2025°F.

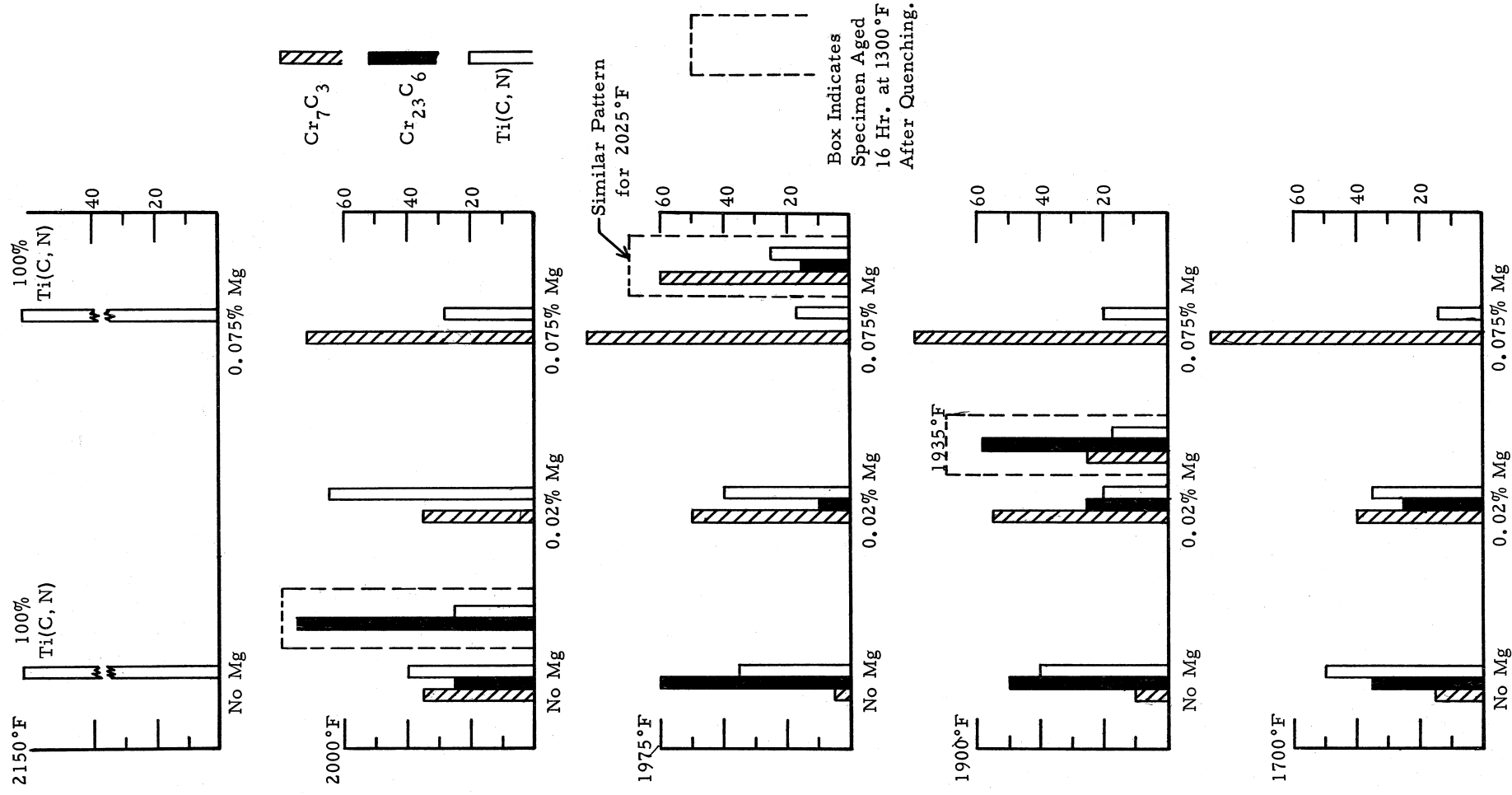


Figure 13. Effect of Magnesium Content and Heat Treating Temperature on the Identity and Relative Quantities of Carbides in Specimens of High Carbon S-Alloy Quenched After One Hour at Temperature.*
 *The relative quantities of carbide phases were estimated from x-ray powder patterns of extracted carbides.

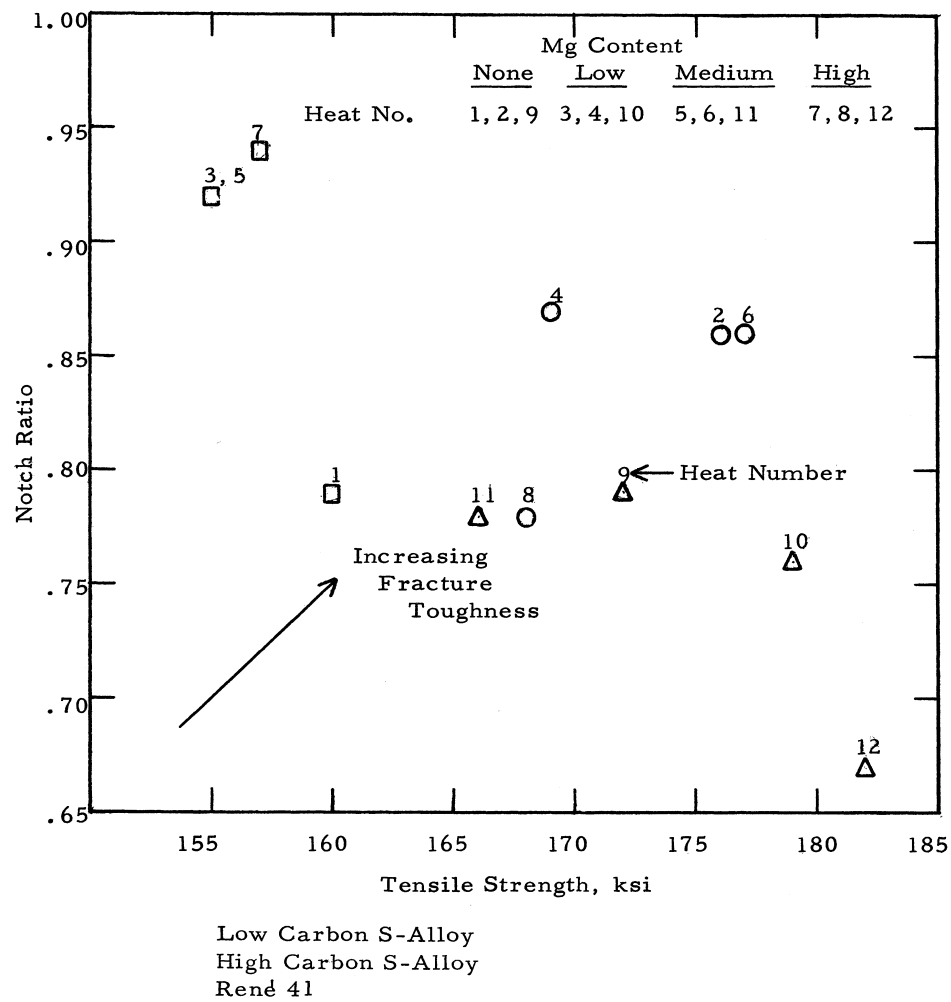


Figure 14. Fracture Toughness of Materials at 1000°F.

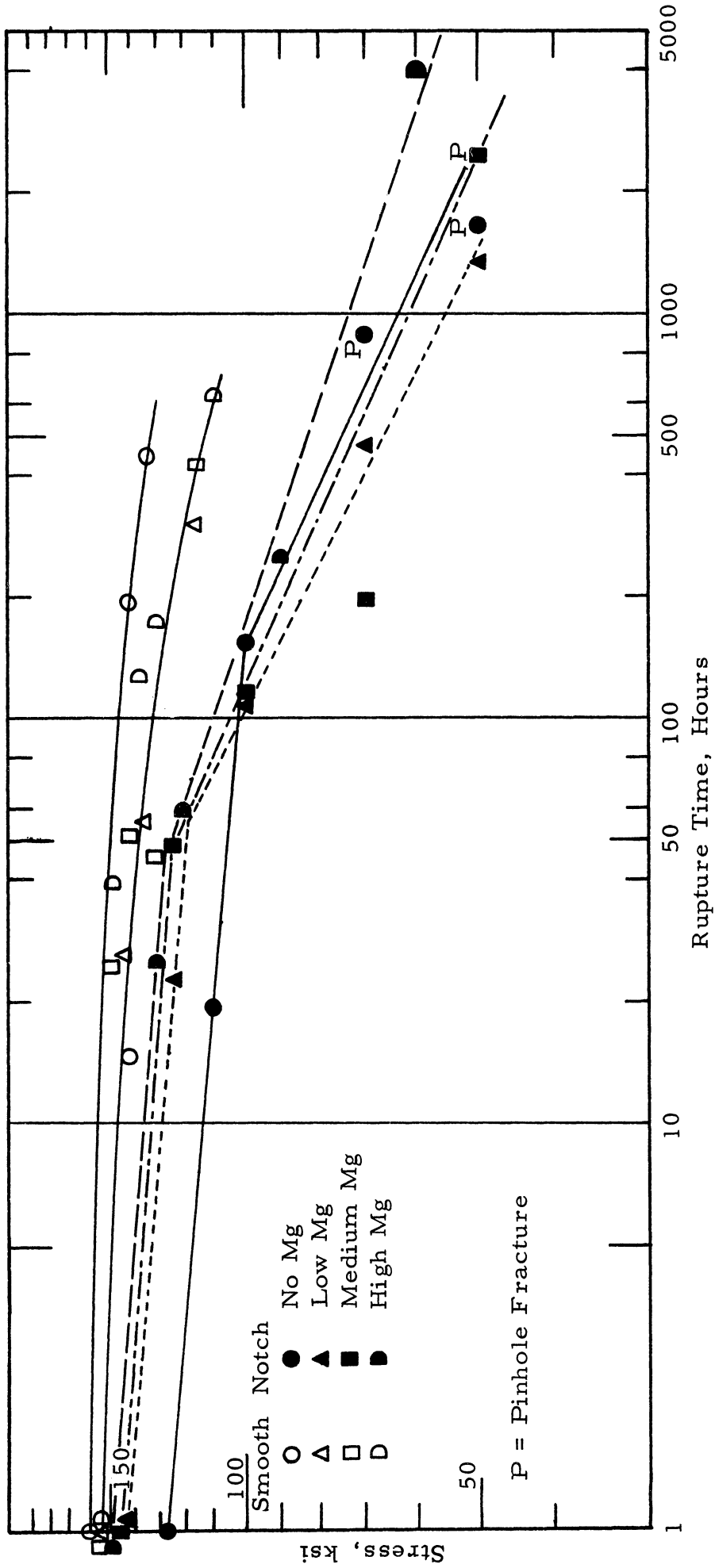


Figure 15. Stress-Rupture Life of Smooth and Edge-Notched Sheet Specimens of Low Carbon S-Alloy at 1000°F.

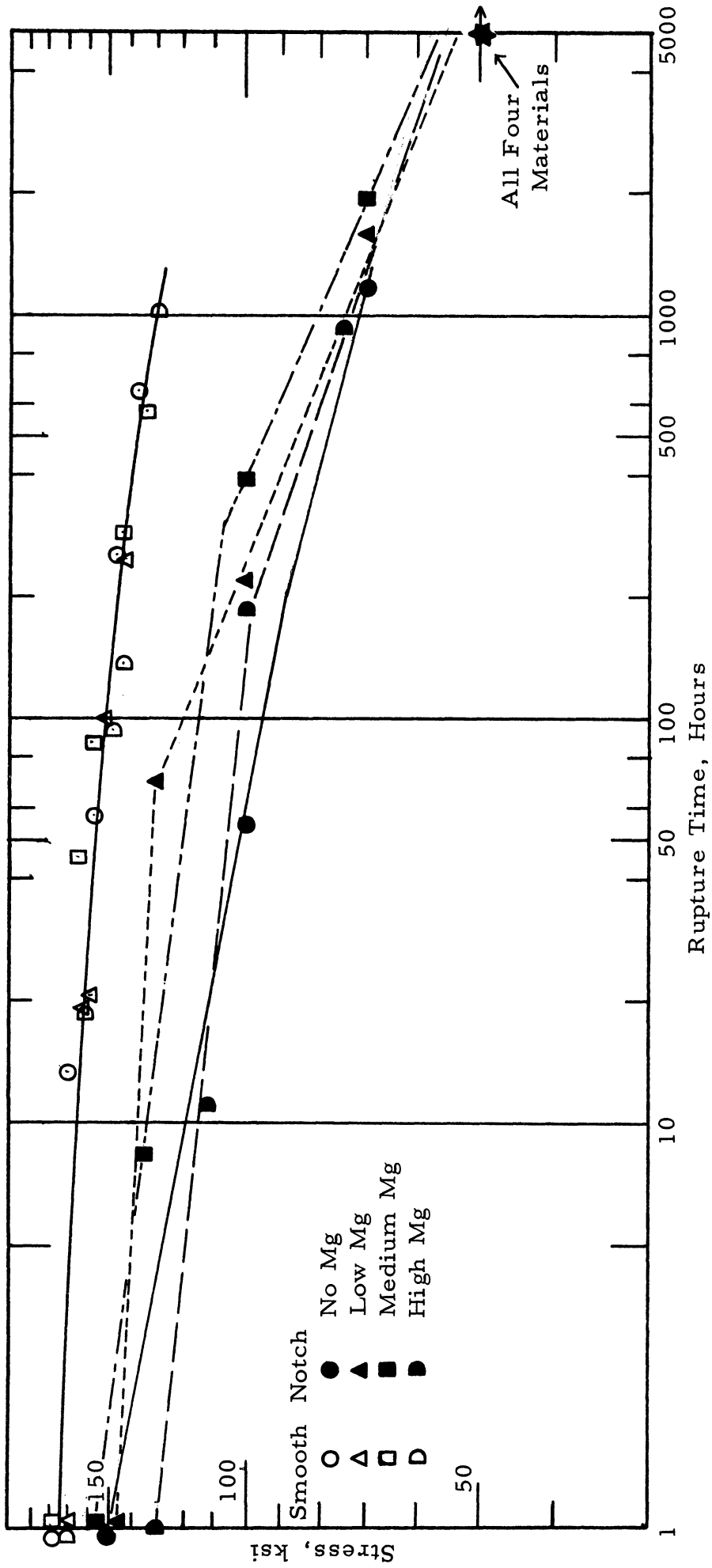


Figure 16. Stress-Rupture Life of Smooth and Edge-Notched Sheet Specimens of High Carbon S-Alloy at 1000°F.

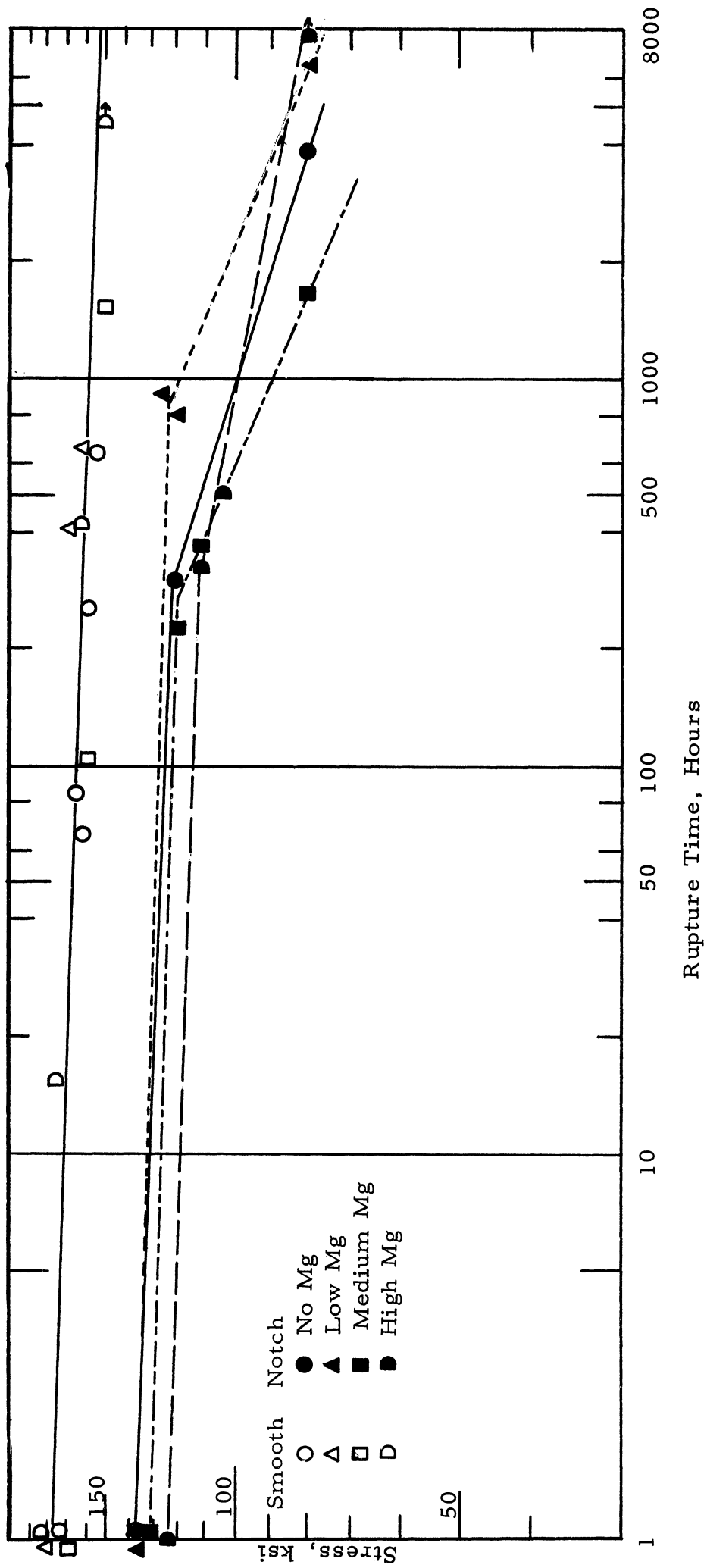


Figure 17. Stress-Rupture Life of Smooth and Edge-Notched Sheet Specimens of Rene' 41 at 1000°F.

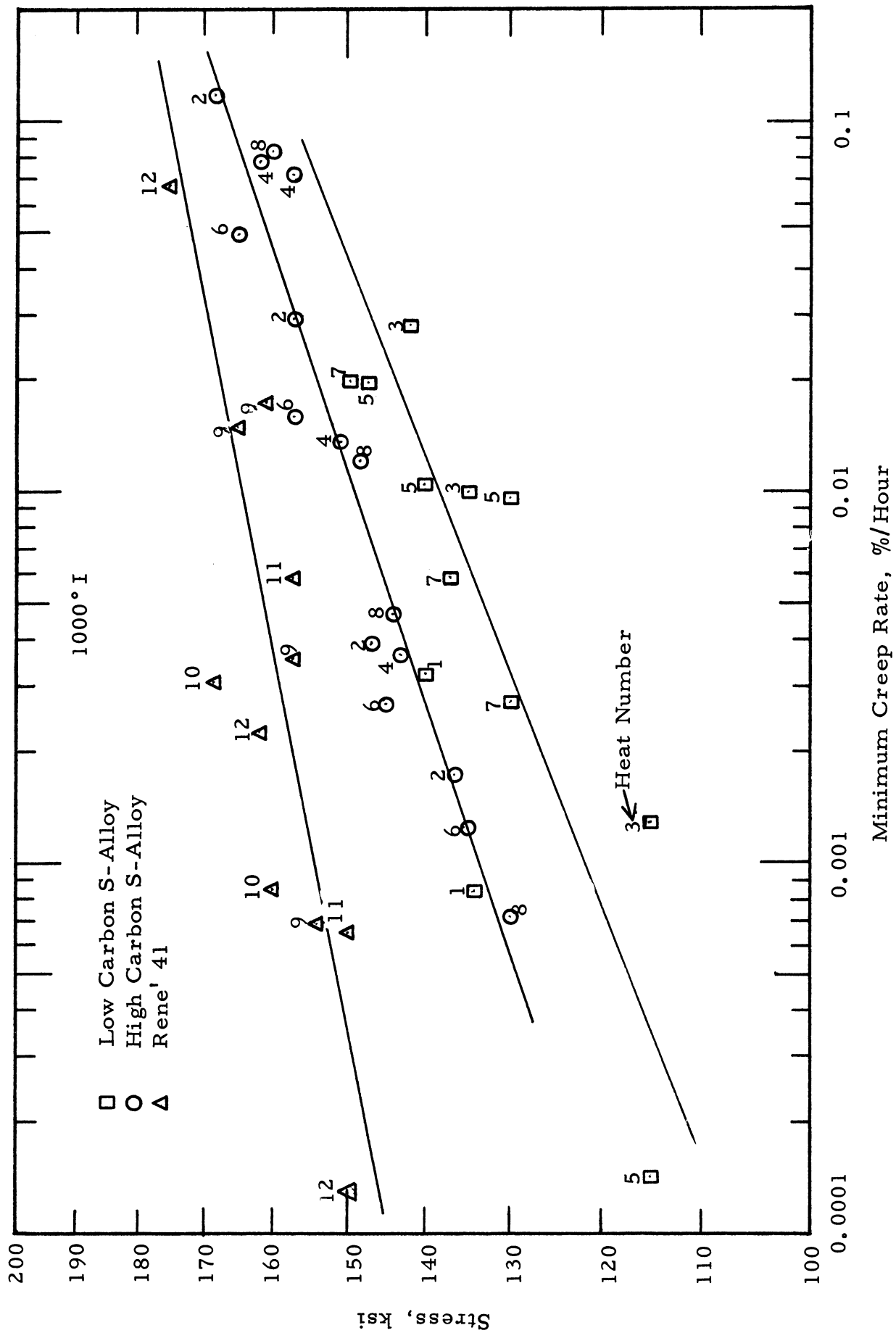


Figure 18. Stress vs. Minimum Creep Rate for S-Alloy and Rene' 41 Sheet Specimens.

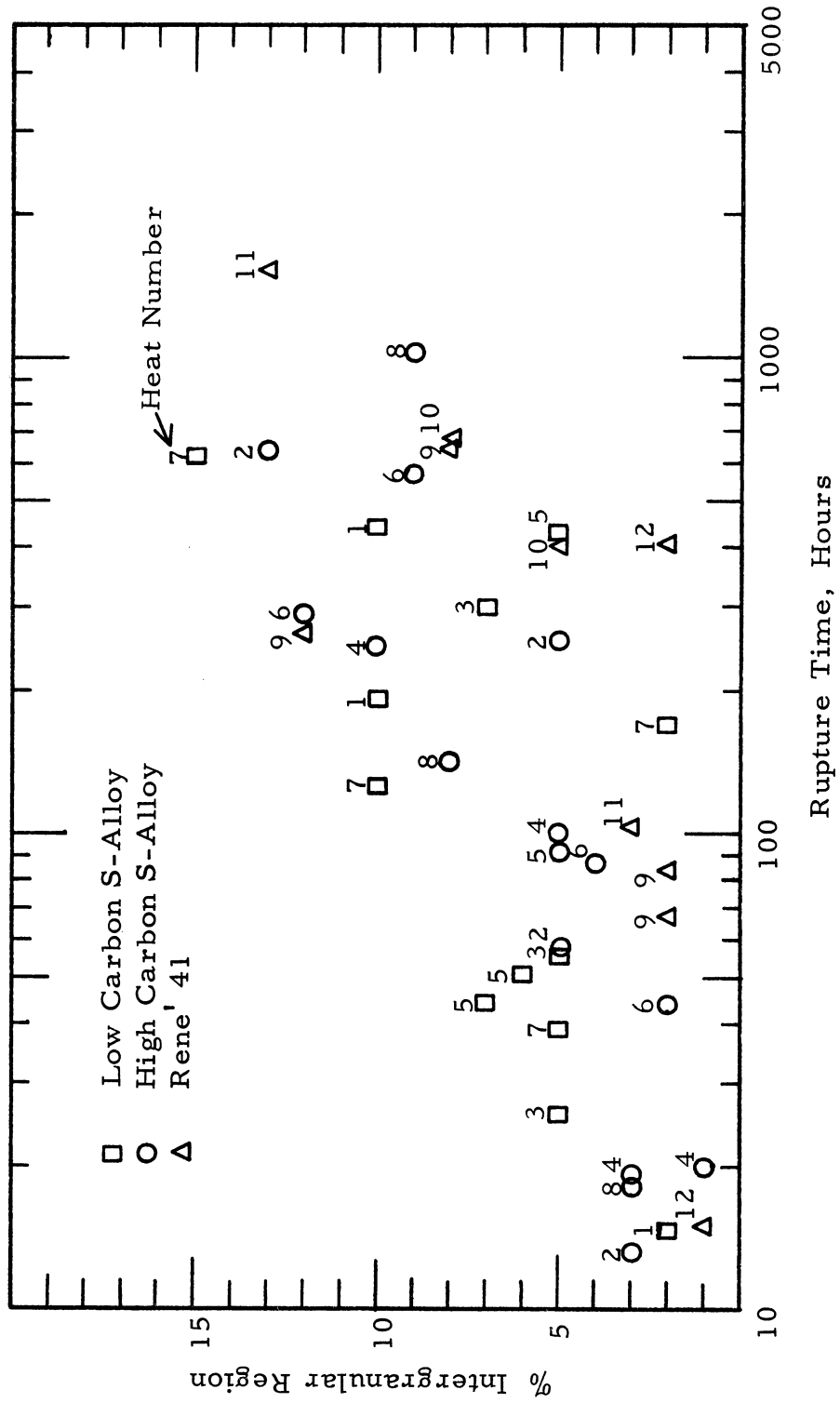


Figure 19. Extent of Intergranular Fracture Region of Smooth Specimens.

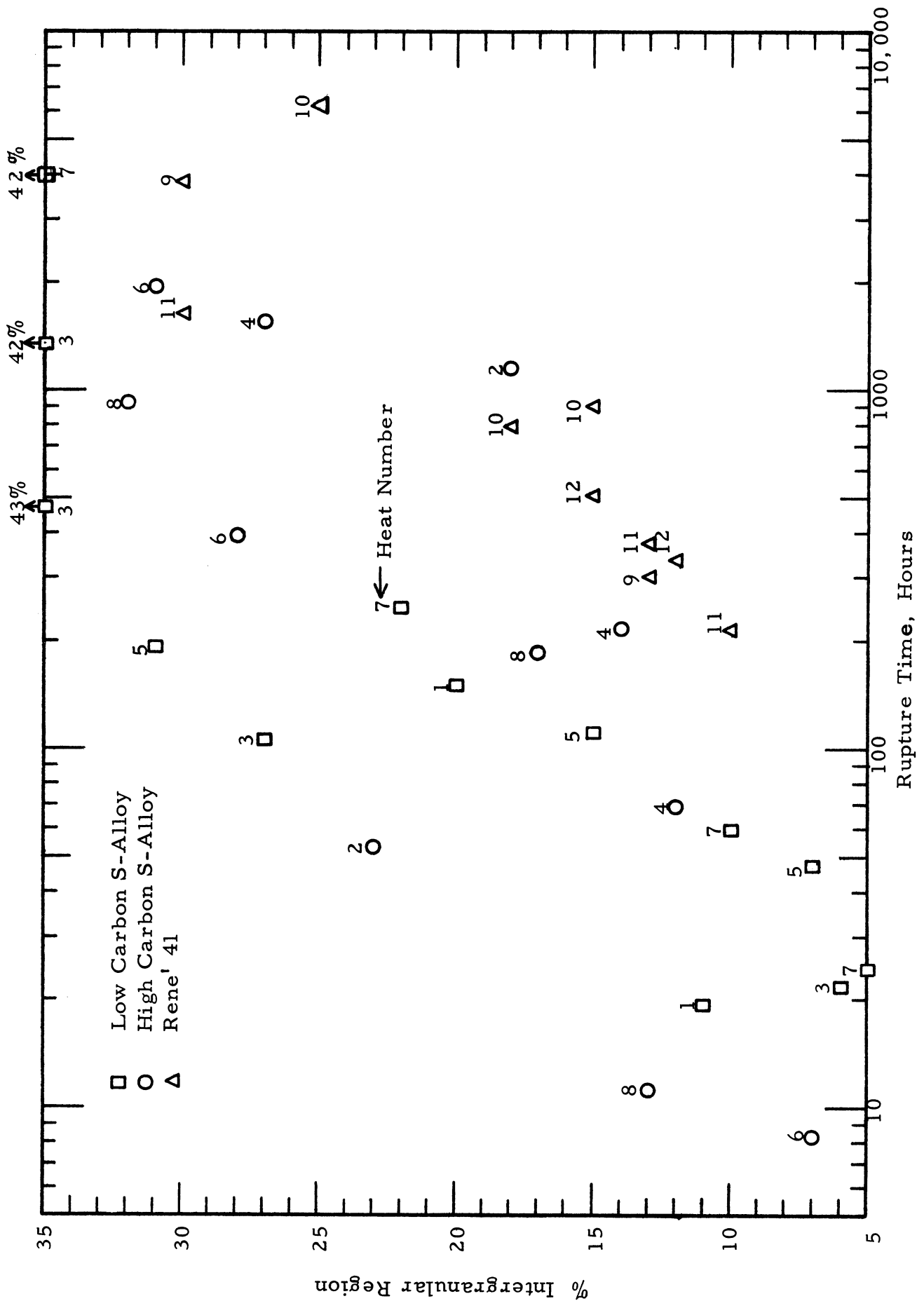


Figure 20. Extent of Intergranular Fracture Region of Notched Specimens.

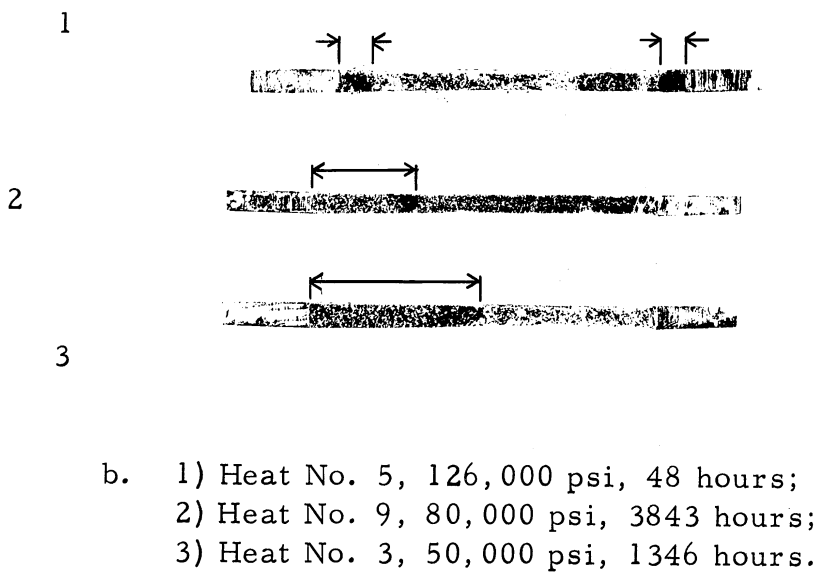
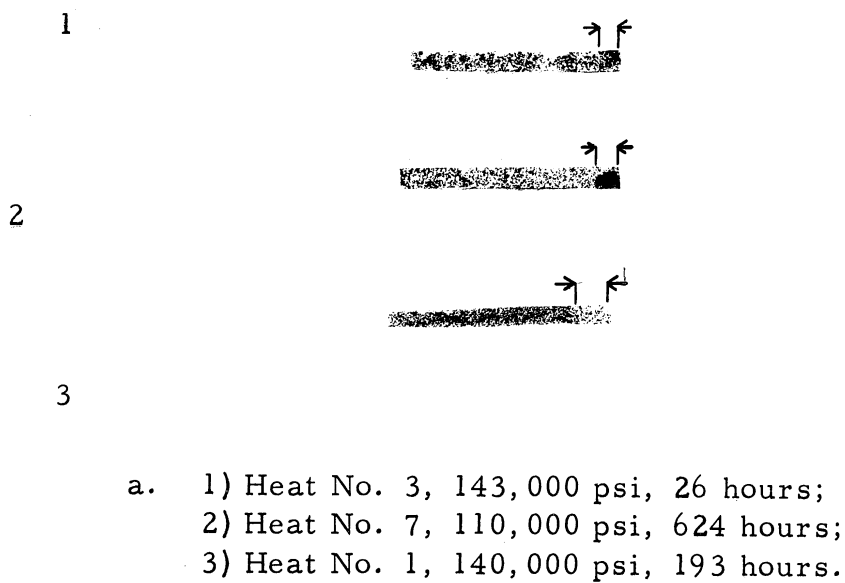
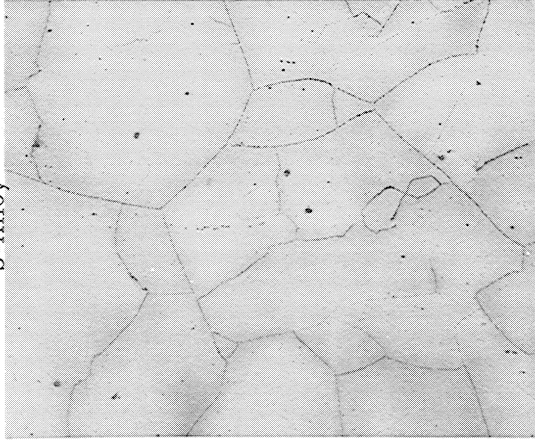


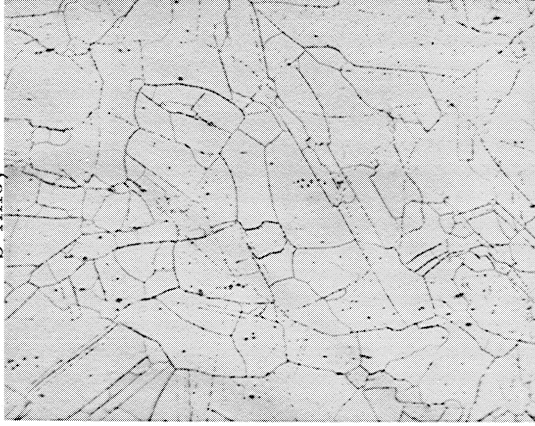
Figure 21. Fracture Surfaces of Smooth and Notched Stress-Rupture Specimens, 3X. Slow Intergranular Crack Propagation Region Indicated by Arrow. a) Smooth, b) Notched.

Low Carbon
S-Alloy



a. Heat No. 1
<math><0.01\% \text{ Mg}</math>

High Carbon
S-Alloy

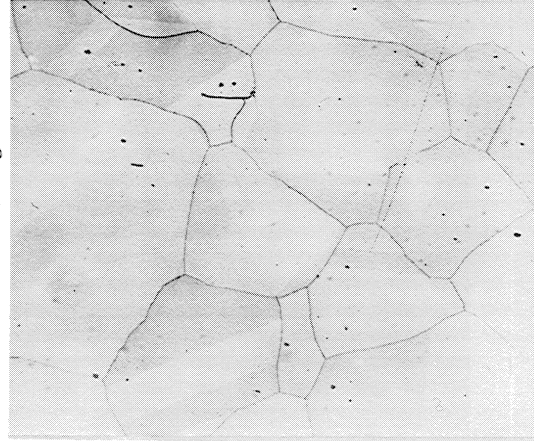


b. Heat No. 2
<math><0.01\% \text{ Mg}</math>

Rend 41



Heat No. 9
<math><0.01\% \text{ Mg}</math>



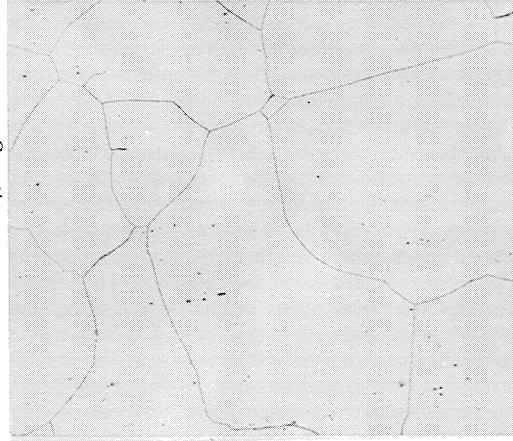
d. Heat No. 3
<math><0.02\% \text{ Mg}</math>



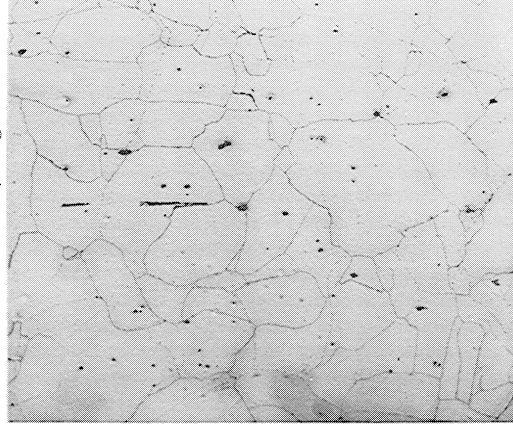
e. Heat No. 4
<math><0.02\% \text{ Mg}</math>



f. Heat No. 10
<math><0.03\% \text{ Mg}</math>



g. Heat No. 7
<math><0.06\% \text{ Mg}</math>



h. Heat No. 8
<math><0.075\% \text{ Mg}</math>



i. Heat No. 12
<math><0.05\% \text{ Mg}</math>

Figure 22. Solution Treated and Aged Microstructures as Represented by Unstressed Section of Hot Tensile Specimens, 250X.

Low Carbon S-Alloy

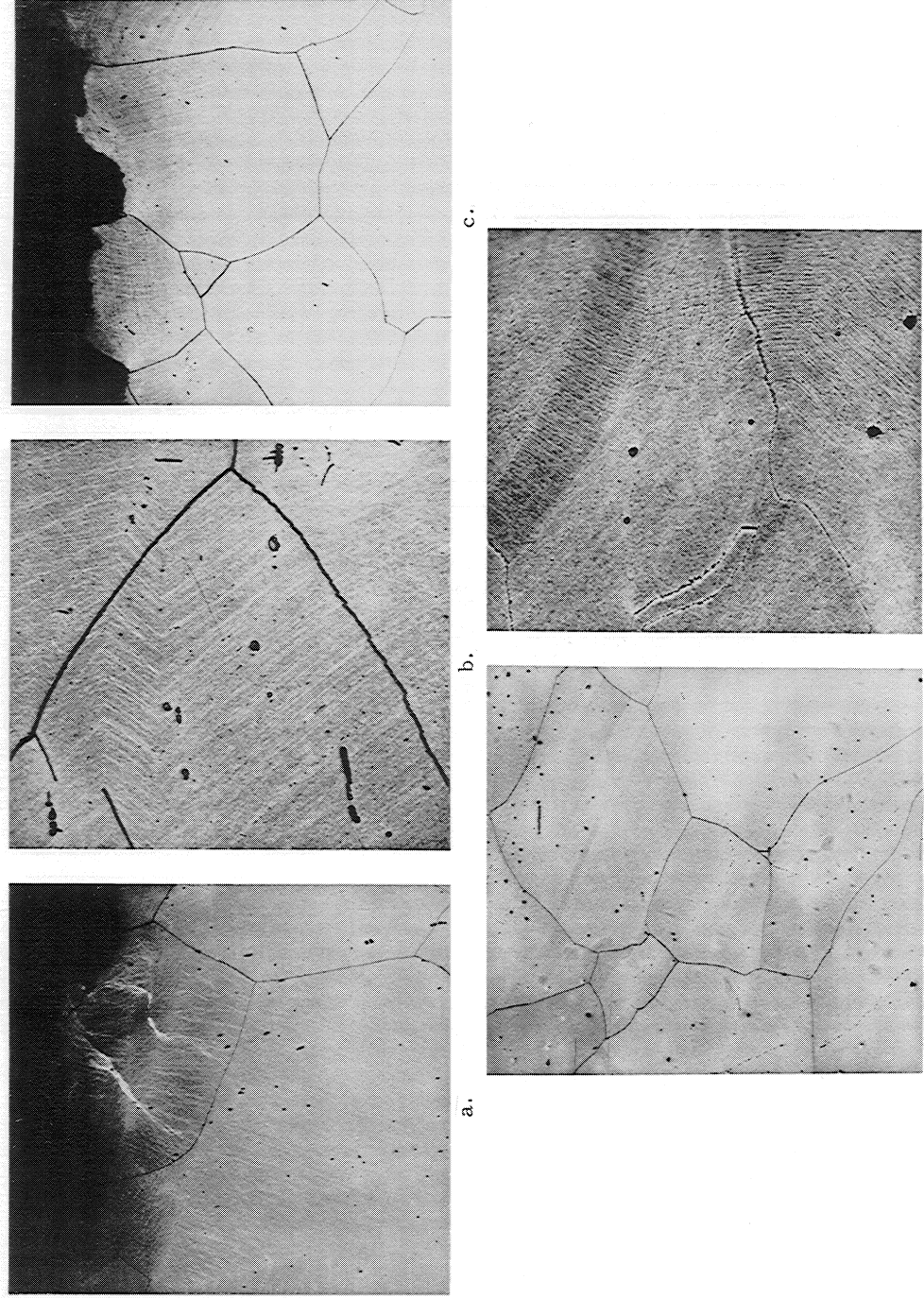
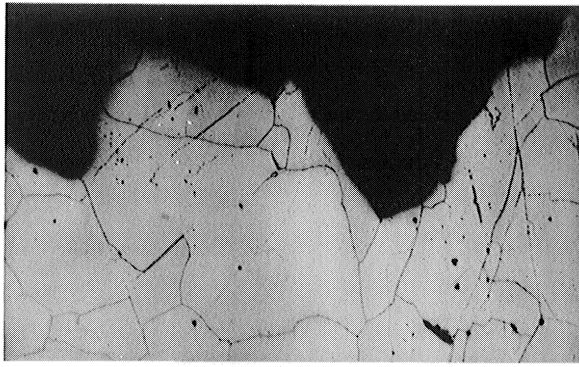
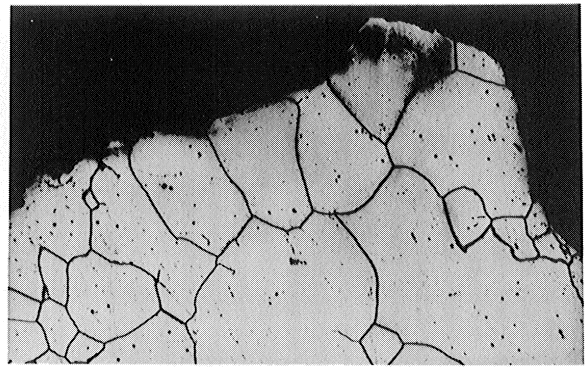


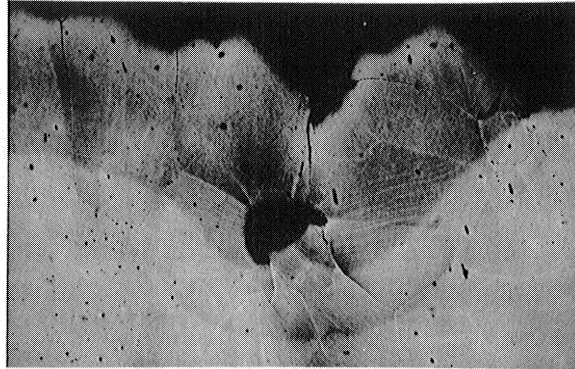
Figure 23. Deformed Areas Near Transgranular Regions of Fracture in Smooth Specimens.
a) Heat No. 3, 115,000 psi, 299 Hr., 250X; b) Same as (a), 1000X;
c) Heat No. 5, 115,000 psi, 423 Hr., 250X; d) Heat No. 7, Tensile, 250X;
e) Same as (d), 1000X.



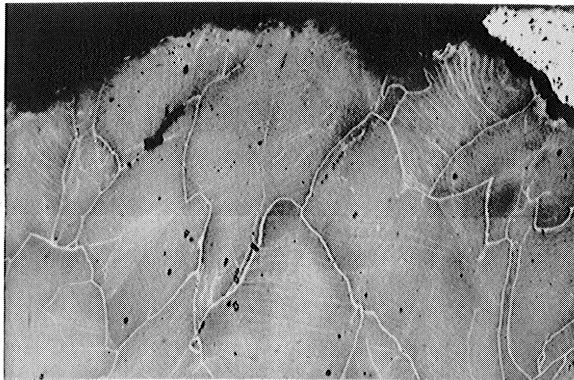
a.



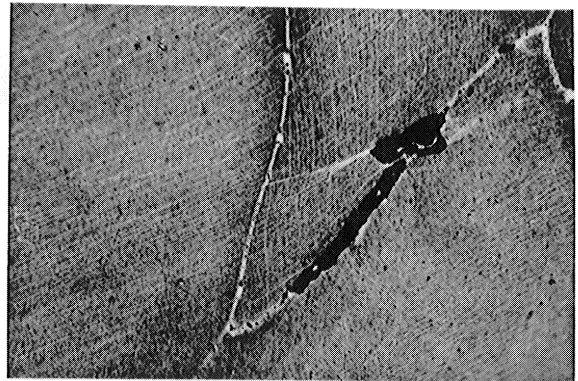
b.



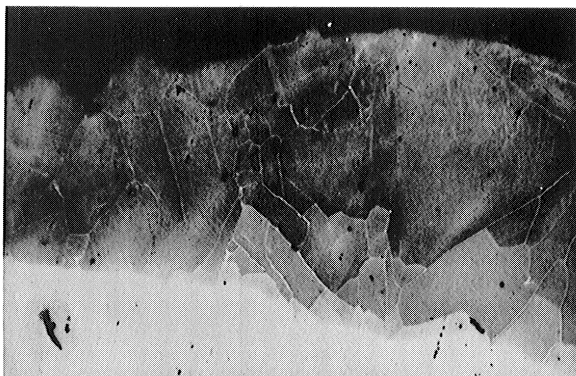
c.



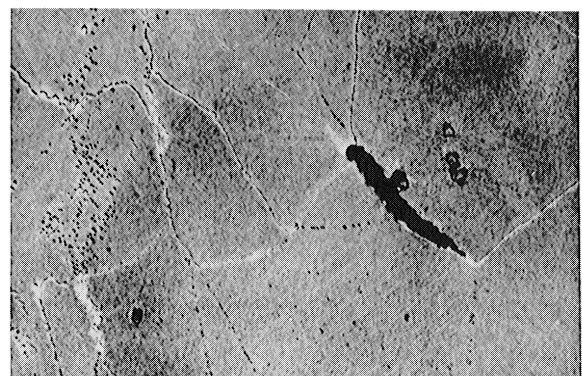
d.



e.

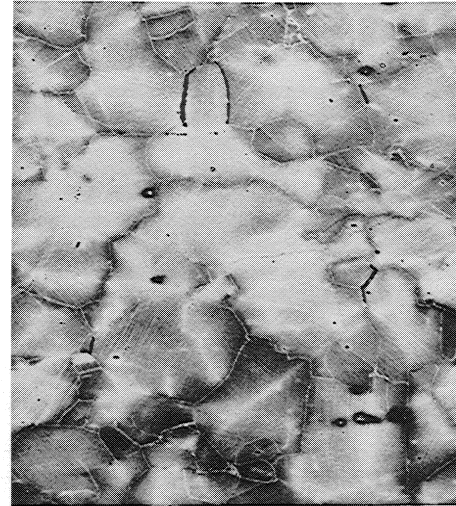


f.

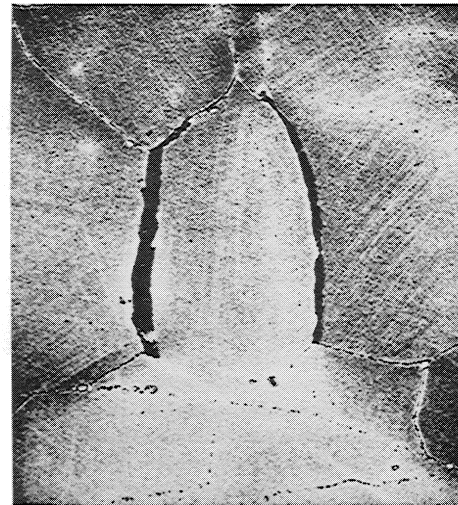


g.

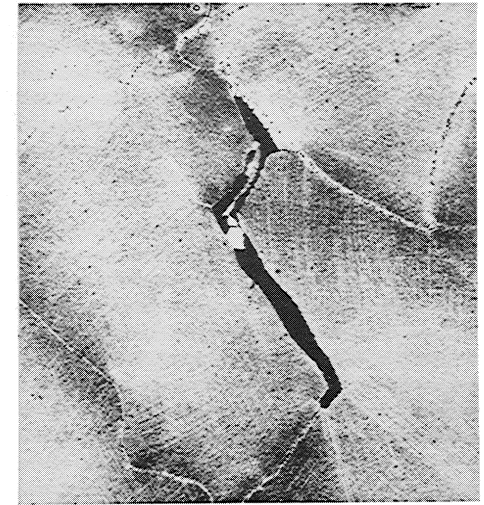
Figure 24. Intergranular Fracture and Cracking in Smooth Specimens of S-Alloy. a) Heat No. 4, 144,000 psi, 248 Hr., 250X; b) Heat No. 7, 130,000 psi, 171 Hr., 250X; c) Heat No. 7, 149,000 psi, 39 Hr., 250X; d) Heat No. 4, Tensile, 250X; e) Same as (d), 1000X; f) Heat No. 4, 162,000 psi, 19 Hr, 250X; g) Same as (f), 1000X.



a. 250X

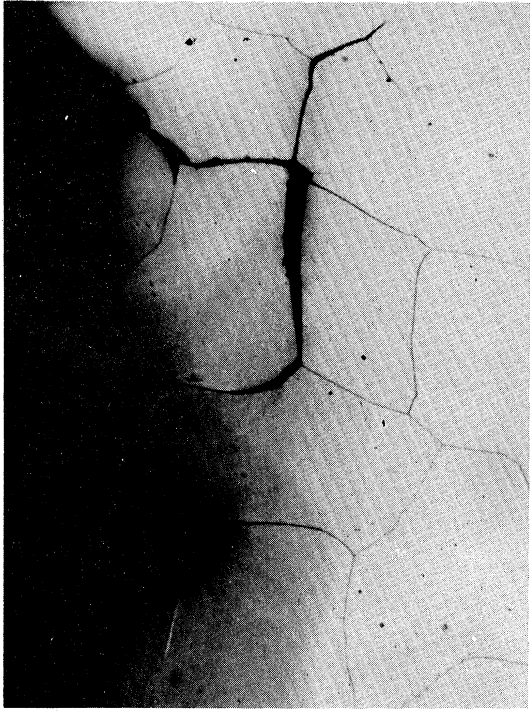


b. 1000X



c. 1000X

Figure 25. An Example of Intergranular Cracking in a Smooth Rupture Specimen. Heat No. 2, 169,000 psi, 13 hr.



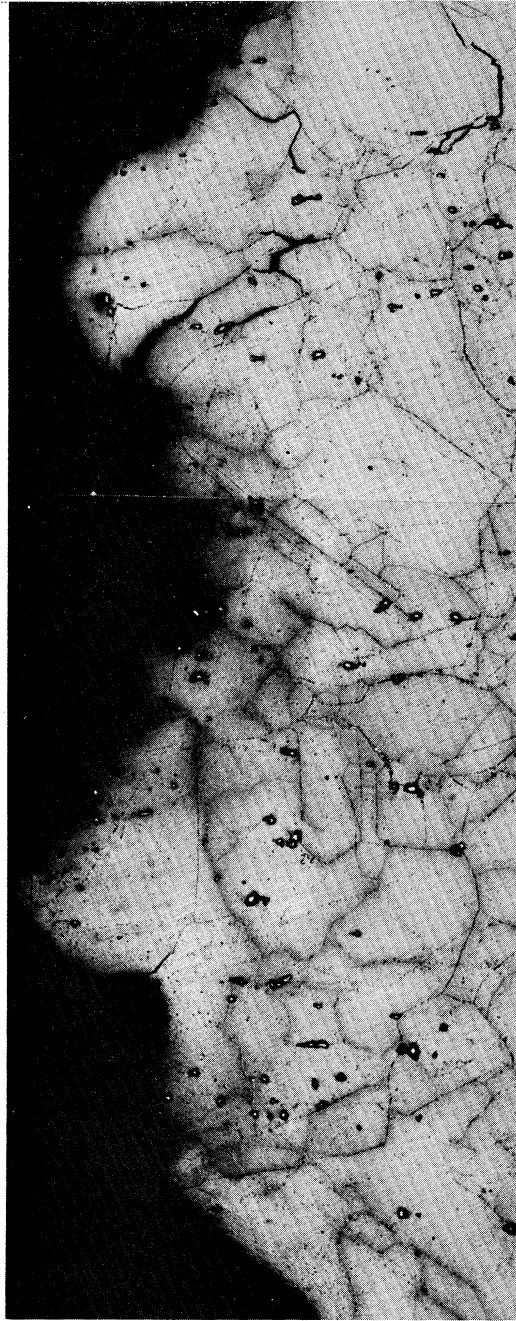
b.



a.



c.



d.

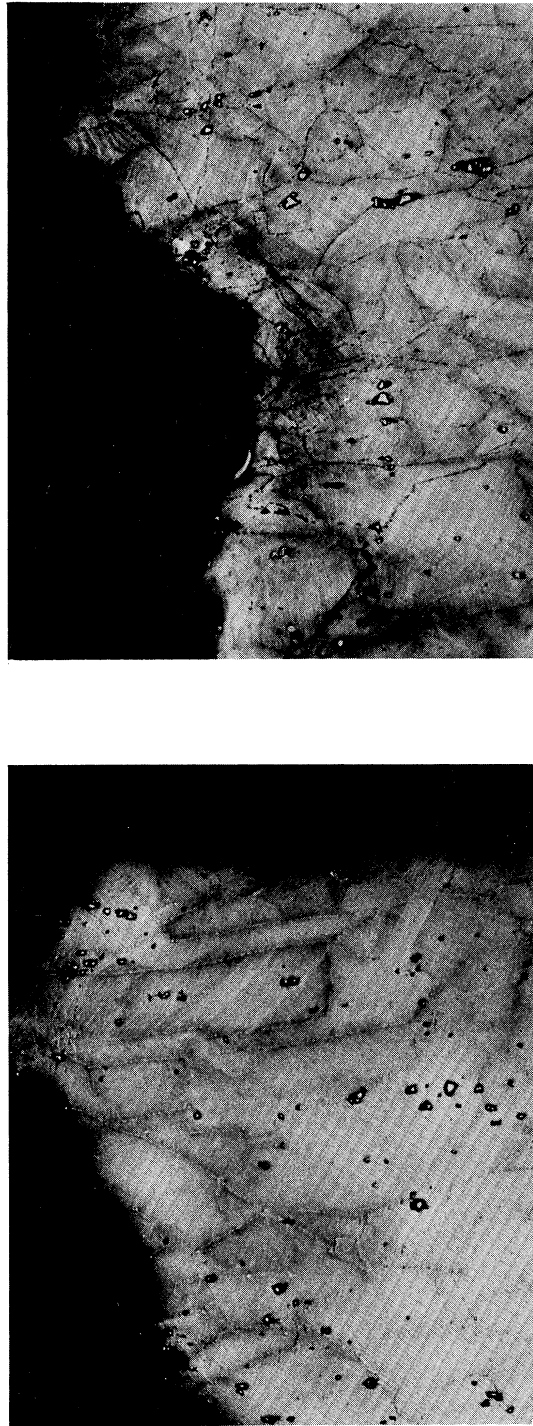
Figure 26. Intergranular Failure Initiation at Edge-Notches. a) Heat No. 5, 70,000 psi, 193 Hr., 250X; b) Heat No. 7, 90,000 psi, 248 Hr., 250X; c) Same as (b), 1000X; d) Heat No. 9, 120,000 psi, 303 Hr., 250X.



a.

b.

c.



d.

e.

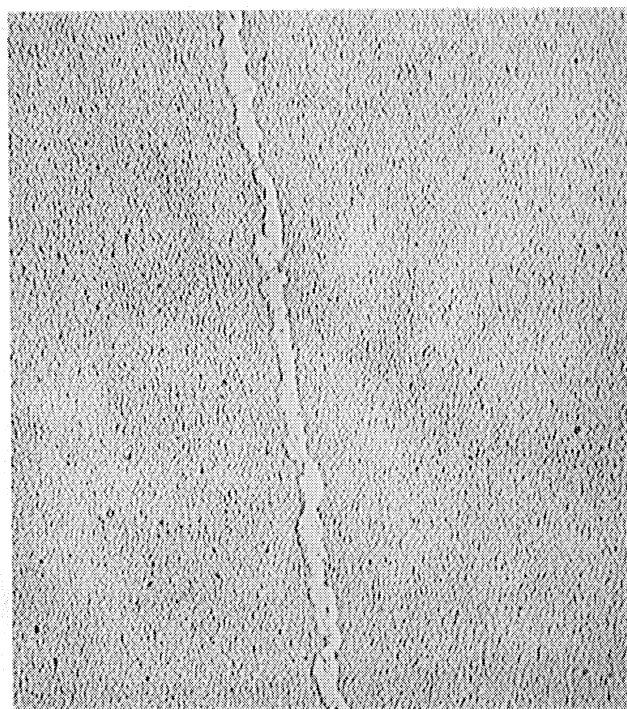
Figure 27. Smooth Specimen Fractures of Rend 41. a) Heat No. 9, Tensile Specimen with Internal Intergranular Cracking, 250X; b) Same as (a), 1000X; c) Heat No. 9, 153,000 psi, 646 Hr., 250X; d) Heat No. 10, 160,000 psi, 659 Hr., Shows Intergranular Crack Initiation at Surface, 250X; e) Heat No. 12, Tensile, 250X.

High C, No Mg S-Alloy

Low C, Low Mg S-Alloy



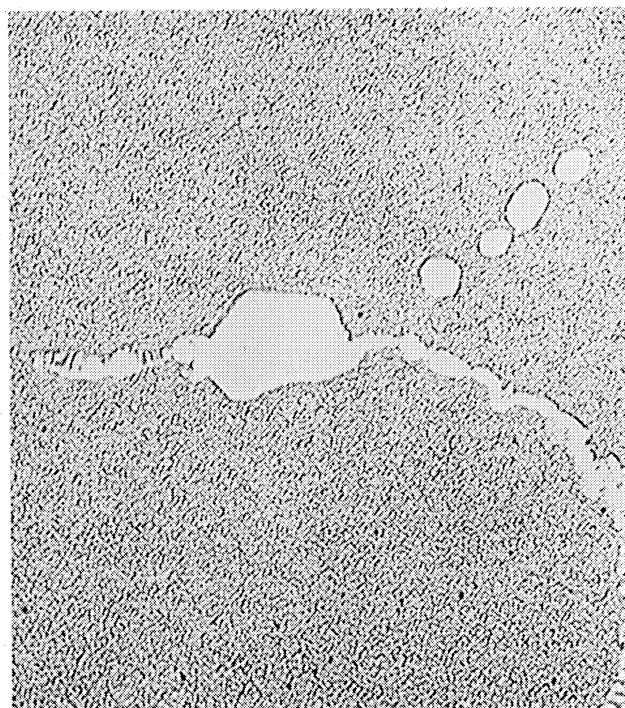
a. Heat No. 2



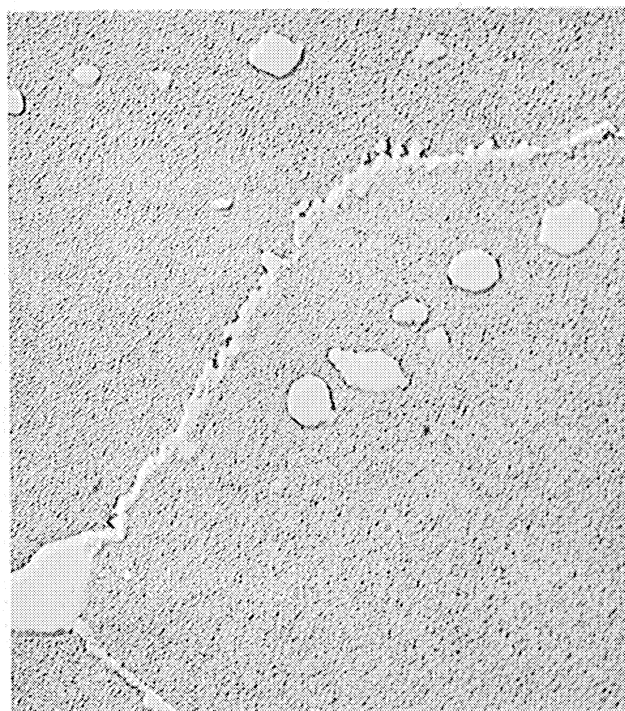
b. Heat No. 3

High C, Low Mg S-Alloy

Low Mg René 41

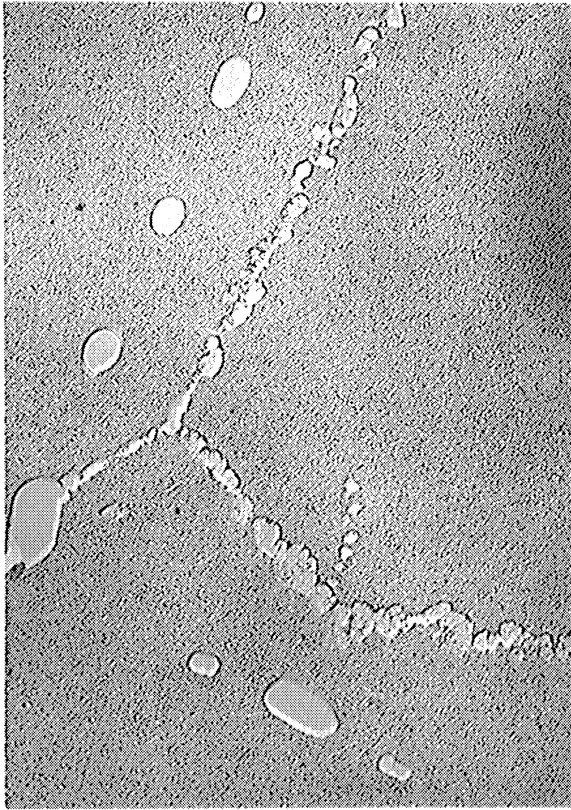


c. Heat No. 4

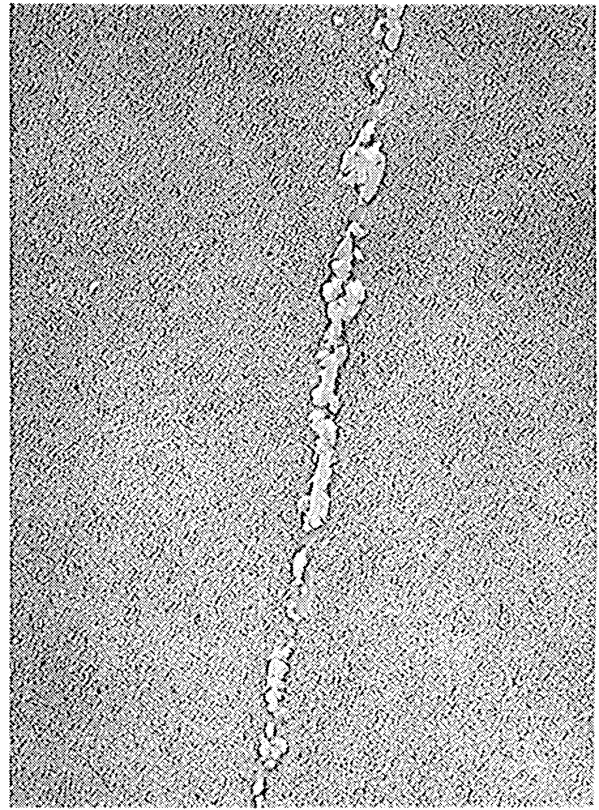


d. Heat No. 10

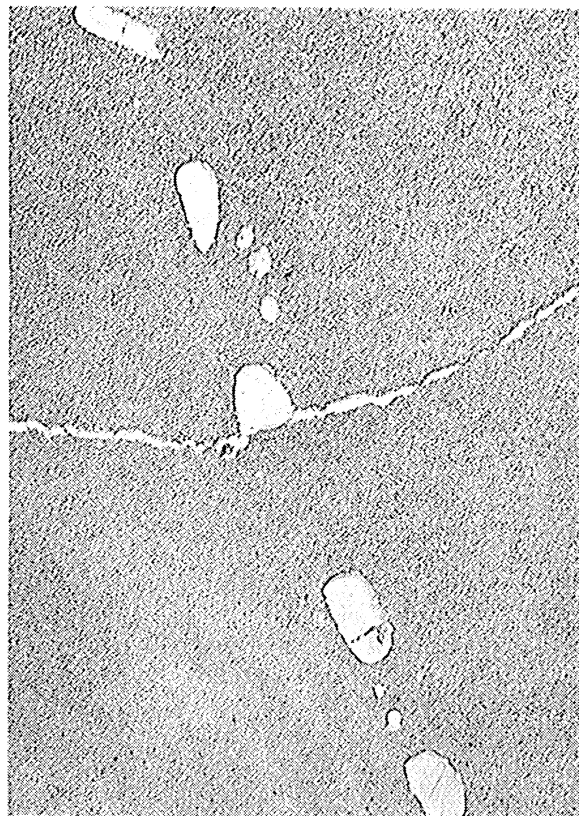
Figure 28. Representative Electron Micrographs of Mechanical Test Specimens, 15,000X.



a. High C, Low Mg S-Alloy



b. Low C, High Mg S-Alloy



c. Low Mg René 41

Figure 29. Electron Micrographs Showing Grain Boundaries and Prior Boundary Carbides. a) Heat No. 4, 144,000 psi, 248 Hr., 10,000X; b) Heat No. 7, 110,000 psi, 624 Hr., 15,000X; c) Heat No. 10, 160,000 psi, 659 Hr., 9000X.

S-Alloy



a.
High C, Low Mg



b.
Low C, Low Mg



c.
Low C, Low Mg

Figure 30. Electron Micrographs of Stringers of a Phase Which Appeared Only in Magnesium-Containing Heats. a) Heat No. 4, Tensile, 30,000X; b) Heat No. 3, Tensile, 28,000X; c) Heat No. 3, Tensile, 41,000X.

APPENDIX A

Quantitative Estimation from Diffraction Patterns

The estimates of the relative quantities of carbide phases presented in Figure 13 were made from the estimated relative integrated intensities of diffraction lines, which are tabulated in Tables IV, V, and VI. Since all of the various factors which effect the line intensities were not known, the estimates involve simplifying assumptions. Two, three, or four lines from the pattern of each compound, as indicated in Table III, were given some weight in the course of these estimates. The most intense line from the pattern of each carbide was given equal weight for the purpose of these estimates. The following simplified estimate from a hypothetical pattern will serve as an example of this:

<u>d</u>	<u>I</u>	<u>Identity of Line</u>
2.38	20	Cr_{23}C_7
2.179	35	$\text{Ti}(\text{C}, \text{N})$
2.12	40	Cr_7C_3
2.04	100	$\text{Cr}_{23}\text{C}_6, \text{Cr}_7\text{C}_3$

The 2.04 line is the most intense line for both Cr_{23}C_6 and Cr_7C_3 . It appears from the relative intergrated line intensities tabulated above, that the following quantitative relationships exist between the carbide phases present:

1. The ratio of ($\text{Cr}_{23}\text{C}_6 + \text{Cr}_7\text{C}_3$) to $\text{Ti}(\text{C}, \text{N})$ is 3 to 1.
2. The ratio of Cr_7C_3 to Cr_{23}C_6 is also 2 to 1.

Therefore, the extracted carbide is composed of 25 per cent $\text{Ti}(\text{C}, \text{N})$, 25 per cent Cr_{23}C_6 and 50 per cent Cr_7C_3 . All of the quantitative estimates were made in the above manner, with some weight being given to the other, more intense lines of each phase as mentioned previously. Obviously, the percentages derived from these estimates are not exact, but estimates of this kind are certainly good enough to indicate which phases are predominant.

